arXiv:1304.7098v1 [hep-ex] 26 Apr 2013

Measurement of the production cross section of jets in association with a Z boson in pp collisions at $\sqrt{s} = 7\,\mathrm{TeV}$ with the ATLAS detector

The ATLAS Collaboration

Abstract

Measurements of the production of jets of particles in association with a Z boson in pp collisions at $\sqrt{s} = 7$ TeV are presented, using data corresponding to an integrated luminosity of 4.6 fb^{-1} collected by the ATLAS experiment at the Large Hadron Collider. Inclusive and differential jet cross sections in Z events, with Z decaying into electron or muon pairs, are measured for jets with transverse momentum $p_\mathrm{T} > 30$ GeV and rapidity $|y| < 4.4$. The results are compared to next-to-leading-order perturbative QCD calculations, and to predictions from different Monte Carlo generators based on leading-order and next-to-leading-order matrix elements supplemented by parton showers.

Measurement of the production cross section of jets in association with a Z boson in pp collisions at $\sqrt{s} = 7\mathrm{TeV}$ with the ATLAS detector

ABSTRACT: Measurements of the production of jets of particles in association with a Z boson in pp collisions at $\sqrt{s} = 7$ TeV are presented, using data corresponding to an integrated luminosity of 4.6 fb^{-1} collected by the ATLAS experiment at the Large Hadron Collider. Inclusive and differential jet cross sections in Z events, with Z decaying into electron or muon pairs, are measured for jets with transverse momentum $p_{\mathrm{T}} > 30$ GeV and rapidity $|y| < 4.4$. The results are compared to next-to-leading-order perturbative QCD calculations, and to predictions from different Monte Carlo generators based on leading-order and next-to-leading-order matrix elements supplemented by parton showers.

Contents

1 Introduction

The production of jets of particles in association with a Z boson[1] at hadron colliders provides an important test of perturbative quantum chromodynamics (pQCD). Such events also constitute a non-negligible background for studies of the Higgs boson candidate [1, 2] and searches for new phenomena. In these searches, the multiplicity and kinematics of jets in Z + jets events are exploited to achieve a separation of signal from background. This procedure often introduces scales larger than the mass of the Z boson, resulting in large logarithmic contributions in the calculation of higher-order QCD corrections to the predicted Z + jets cross section [3, 4]. The measured Z + jets cross section can be compared

---

[1]The notation Z refers to the complete Z/γ^* interference.

directly to fixed-order predictions at next-to-leading-order (NLO) in pQCD [5–7] and to Monte Carlo (MC) generators based on next-to-leading-order or leading-order (LO) matrix elements supplemented by parton showers [8–10]. The simulations based on LO matrix elements are affected by large uncertainties in the factorization and renormalization scales and need to be tuned and validated using data.

Measurements of the Z + jets cross section have been reported for lower jet energies and lower jet multiplicities in proton–antiproton collisions at a center-of-mass energy of $\sqrt{s} = 1.96$ TeV [11–13] and in proton–proton collisions based on a data set of 0.036 fb^{-1} collected at $\sqrt{s} = 7$ TeV [14, 15]. This article extends these measurements, using 4.6 fb^{-1} of proton–proton collision data collected by the ATLAS experiment in 2011 at $\sqrt{s} = 7$ TeV. The large data set allows cross sections to be measured for the production of up to seven jets in association with a Z boson. Differential jet cross sections are accessible for large jet multiplicities and for energy regimes up to 1 TeV, which allows the modelling of the Z + jets process to be probed for typical phase-space regimes expected from new phenomena and from Higgs boson production, for example via vector-boson-fusion (VBF).

Selected events contain a Z boson decaying into a pair of electrons or muons. Associated jets are identified in a rapidity (y^{jet}) range of $|y^{\text{jet}}| < 4.4$ and with transverse momentum ($p_{\text{T}}^{\text{jet}}$) of $p_{\text{T}}^{\text{jet}} > 30$ GeV. The measurements comprise inclusive and exclusive jet multiplicities for different phase-space constraints and differential jet cross sections as a function of the transverse momentum and the rapidity of the four jets with the largest transverse momentum ('leading jets'). Cross sections for events with at least two jets in the final state are measured as a function of the invariant mass (m^{jj}) and the angular separation of the two leading jets. Differential cross sections in events with at least one jet are measured as a function of the scalar p_{T} sum of the jets (S_{T}), of the scalar p_{T} sum of the leptons and jets (H_{T}), and the transverse momentum of the Z boson candidate ($p_{\text{T}}^{\ell\ell}$). The results of the measurements are unfolded for detector effects and quoted at the particle (hadron) level, where they are compared to predictions from fixed-order NLO pQCD programs and from several MC generators.

The paper is organized as follows. The detector and the data sample are described in the next section. Section 3 provides details of the simulations used in the measurements, while section 4 describes the lepton and jet reconstruction and the event selection. The estimation of background contributions is described in section 5 and selected uncorrected distributions are presented in section 6. The procedures used to unfold the measurements for detector effects and to combine electron and muon channels are detailed in section 7. Systematic uncertainties are discussed in section 8. The NLO pQCD predictions are described in section 9. Measured cross sections are presented in section 10 and compared to generator and NLO pQCD predictions. Finally, section 11 provides a summary.

2   Experimental setup

The ATLAS detector [16] at the LHC covers nearly the entire solid angle around the collision point. It consists of an inner tracking detector surrounded by a thin superconducting solenoid, followed by electromagnetic and hadronic calorimeters and a muon spectrometer

incorporating three large superconducting toroid magnets (each with eight coils). The inner detector (ID) is immersed in a 2 T axial magnetic field and provides charged-particle tracking in the pseudorapidity[2] range $|\eta| < 2.5$. The high-granularity silicon pixel detector covers the vertex region and typically provides three measurements per track, the first hit being normally in the innermost layer. It is followed by the silicon microstrip tracker, which provides typically eight measurements (four space-points) per track. These silicon detectors are complemented by the transition radiation tracker, which covers a region up to $|\eta| = 2.0$. The transition radiation tracker also provides electron identification information based on the fraction of hits above a high energy-deposit threshold corresponding to transition radiation. The calorimeter system covers the pseudorapidity range $|\eta| < 4.9$. Within the region $|\eta| < 3.2$, electromagnetic calorimetry is provided by barrel and endcap high-granularity lead/liquid-argon (LAr) calorimeters. An additional thin LAr presampler covers $|\eta| < 1.8$ to correct for energy loss in material upstream of the calorimeters. Hadronic calorimetry is provided by a steel/scintillating-tile calorimeter, segmented radially into three barrel structures within $|\eta| < 1.7$, and two copper/LAr hadronic endcap calorimeters, that cover the region $1.5 < |\eta| < 3.2$. The solid angle coverage is completed in the region of $3.1 < |\eta| < 4.9$ with forward copper/LAr and tungsten/LAr calorimeter modules optimized for electromagnetic and hadronic measurements respectively. The muon spectrometer (MS) comprises separate trigger and high-precision tracking chambers measuring the deflection of muons in a magnetic field generated by superconducting air-core toroids. The precision chamber system covers the region $|\eta| < 2.7$ with three layers of monitored drift tubes, complemented by cathode strip chambers in the forward region, where the background is highest. The muon trigger system covers the range $|\eta| < 2.4$ with resistive plate chambers in the barrel, and thin gap chambers in the endcap regions. A three-level trigger system is used to select interesting events. The Level-1 trigger is implemented in hardware and uses a subset of detector information to reduce the event rate to a design value of at most 75 kHz. This is followed by two software-based trigger levels which together reduce the event rate to about 400 Hz.

The analysis is based on a sample of proton–proton collisions at $\sqrt{s} = 7$ TeV, collected in 2011 during periods of stable beam operation. Di-electron final states are selected with a trigger requiring at least two electrons of $p_\mathrm{T} > 12$ GeV, using an electron identification similar to the one used in offline selection. Di-muon final states are selected with a trigger requiring at least one muon of $p_\mathrm{T} > 18$ GeV, using a higher-level trigger algorithm similar to the one used in the offline selection. The integrated luminosity used in both channels is 4.64 ± 0.08 fb^{-1} [17].

---

[2]ATLAS uses a right-handed coordinate system with its origin at the nominal interaction point (IP) in the centre of the detector and the z-axis along the beam pipe. The x-axis points from the IP to the centre of the LHC ring, and the y-axis points upward. Cylindrical coordinates (r, ϕ) are used in the transverse plane, ϕ being the azimuthal angle around the beam pipe. The pseudorapidity is defined in terms of the polar angle θ as $\eta = -\ln\tan(\theta/2)$.

3 Monte Carlo simulation

Monte Carlo event samples are used to determine background contributions, correct the measurements for detector effects, correct the theory calculations for non-perturbative effects, calculate acceptance corrections, and estimate systematic uncertainties on the final results.

Signal events ($Z(\rightarrow \mu\mu)$ + jets and $Z(\rightarrow ee)$ + jets) are generated using ALPGEN v2.13 [8] interfaced to HERWIG v6.520 [18] for parton shower and fragmentation and to JIMMY v4.31 [19] for modelling interactions of the proton remnants, referred to as 'underlying event' in the following, using the AUET2-CTEQ61L tune [20]. In the following sections, the expression 'ALPGEN' refers to this version unless stated otherwise. Similar samples are produced with ALPGEN v2.14 interfaced to PYTHIA v6.425 [21] using the PERUGIA2011C [22] tune. For both ALPGEN samples, CTEQ61L [23] parton distribution functions (PDFs) are employed. Signal samples are also generated with SHERPA v1.4.1 using the MEnloPS approach [10] and with MC@NLO v4.01 [24], interfaced to HERWIG, both using the CT10 [25] PDF set. The program PHOTOS [26] is used to simulate QED final state radiation (FSR) in the ALPGEN samples. QED-FSR simulation in SHERPA is based on the YFS method [27]. ALPGEN and SHERPA matrix elements are generated for up to five partons. The signal samples do not include Z + jets events produced via VBF. Based on generator-level studies, the expected contribution of these events to the measured cross sections is at the per-mille to per-cent level for the selections and kinematic ranges explored in this paper and always significantly below the statistical and systematic precision of the measurement.

Background samples from W + jets and $Z(\rightarrow \tau\tau)$ + jets final states are generated similarly to the signal samples, using ALPGEN interfaced to HERWIG. The W + jets and Z + jets samples are normalized globally to next-to-next-to-leading-order (NNLO) pQCD inclusive Drell–Yan predictions as determined by the FEWZ [28] program using the MSTW2008NNLO PDF set [29]. The uncertainties of about 5% are taken from an envelope of predictions using different PDF sets and factorization and renormalization scales, as described in ref. [30]. Single-top-quark events are produced with AcerMC [31], interfaced to PYTHIA, using CTEQ61L PDFs. Diboson processes (WW, WZ and ZZ) are simulated with HERWIG using the AUET2-LO* tune [20]. Reference cross sections for single-top-quark and diboson processes are calculated using the MC@NLO generator with the MSTW2008 PDF set [29]. The $t\bar{t}$ samples used for the relative normalization of final states in top-quark pair-production are generated with MC@NLO interfaced to HERWIG and with POWHEG [32, 33] interfaced to PYTHIA, both using the CT10 PDF set.

All samples are processed through the GEANT4-based simulation [34, 35] of the ATLAS detector. The simulation includes the modelling of additional pp interactions in the same and neighbouring bunch crossings (pile-up), with an average of nine interactions per crossing, that matches the distribution of interactions per crossing measured in data.

4   Event selection

Table 1 summarizes the kinematic regions in which Z bosons and jets are selected. They are defined to provide a good experimental coverage for the reconstruction of electrons, muons and jets in the event. Events with less than three tracks associated to the hard scattering vertex, defined as the vertex with the highest p_T sum of its associated tracks, are discarded.

Electrons are reconstructed from clusters of energy in the electromagnetic calorimeter matched to inner detector tracks. The electron candidates must have $p_T > 20$ GeV and $|\eta| < 2.47$, excluding the transition region $1.37 < |\eta| < 1.52$ between barrel and endcap electromagnetic calorimeter sections, and pass the 'medium' identification criteria described in ref. [36], re-optimized for 2011 conditions. No additional isolation requirement is applied, since non-isolated electron candidates are already suppressed by the identification criteria. Muon candidates are identified as tracks in the inner detector matched and combined with track segments in the muon spectrometer [37]. They are required to have $p_T > 20$ GeV and $|\eta| < 2.4$. In order to achieve a sufficient rejection of multi-jet events, muons are required to be isolated: the scalar sum of the transverse momenta of tracks within a cone of $\Delta R \equiv \sqrt{(\Delta\phi)^2 + (\Delta\eta)^2} = 0.2$ around the muon candidate must be less than 10% of the transverse momentum of the muon. All lepton pairs are required to have a separation of $\Delta R^{\ell\ell} > 0.2$. The Z candidates are selected by requiring exactly two oppositely charged leptons of the same flavour. Their invariant mass $(m^{\ell\ell})$ must be within the range 66 GeV $\leq m^{\ell\ell} \leq 116$ GeV. With this selection, 1228767 $Z\,(\to ee)$ and 1678500 $Z\,(\to \mu\mu)$ candidate events are identified.

Jets are reconstructed using the anti-k_t algorithm [38] with a distance parameter $R = 0.4$. The inputs to the jet algorithm are topological clusters of energy in the calorimeter [39]. The energies and directions of reconstructed jets in data and simulated events are corrected for the presence of additional proton–proton interactions, the position of the primary interaction vertex, the measurement biases induced by calorimeter non-compensation, additional dead material, and out-of-cone effects, using detector simulation and a combination of in-situ methods [39, 40]. Jets are required to have a transverse momentum above 30 GeV and a rapidity of $|y^{\mathrm{jet}}| < 4.4$. Jets closer than 0.5 in ΔR to a selected lepton are removed. In order to reject jets from additional proton–proton interactions, the 'jet vertex fraction' is used. This is defined as the p_T sum of the tracks associated to the jet which are consistent with originating from the primary vertex divided by the p_T sum of all tracks associated to the jet. The jet vertex fraction is required to be greater than 0.75 for jets with $|\eta| < 2.4$. The residual impact of additional proton–proton interactions on the distribution of the jet observables has been checked to be correctly simulated such that the unfolded cross sections are expected to be independent of the number of additional interactions. With this definition, 191566 $Z\,(\to ee)$ and 257169 $Z\,(\to \mu\mu)$ candidate events are selected with at least one jet in the final state.

	$Z\,(\to ee)$	$Z\,(\to \mu\mu)$
lepton p_{T}	$p_{\mathrm{T}} > 20$ GeV	$p_{\mathrm{T}} > 20$ GeV
lepton $|\eta|$	$|\eta| < 1.37$ or $1.52 < |\eta| < 2.47$	$|\eta| < 2.4$
lepton charges	opposite charge	
lepton separation $\Delta R^{\ell\ell}$	$\Delta R^{\ell\ell} > 0.2$	
lepton invariant mass $m^{\ell\ell}$	66 GeV $\leq m^{\ell\ell} \leq 116$ GeV	
jet p_{T}	$p_{\mathrm{T}}^{\mathrm{jet}} > 30$ GeV	
jet rapidity y^{jet}	$|y^{\mathrm{jet}}| < 4.4$	
lepton-jet separation $\Delta R^{\ell j}$	$\Delta R^{\ell j} > 0.5$	

Table 1. Summary of $Z\,(\to \ell\ell)$ and jet selection criteria.

5   Background estimation

The selected data sample is expected to contain background events with two isolated leptons ($t\bar{t}$, diboson and $Z\,(\to \tau\tau)$ events), with one isolated lepton ($W \to e\nu$, $W \to \mu\nu$ and single-top-quark production) and without isolated leptons (multi-jet events). The total expected background fraction increases with the jet multiplicity (N_{jet}) from 2% ($N_{\mathrm{jet}} \geq 1$) to 20% ($N_{\mathrm{jet}} \geq 6$). It is dominated by multi-jet processes, $t\bar{t}$ and diboson events for $Z\,(+ \leq 1$ jet$)$ and by $t\bar{t}$ for larger jet multiplicities. The background is estimated using simulated samples, with the exception of the multi-jet and $t\bar{t}$ background contributions, which are derived from data. For these data-driven background estimates, the shape of the background contribution to each of the measured distributions is derived from a dedicated background-enriched sample in data. The background-enriched samples have been selected and normalized as described below.

The multi-jet background contribution in the $Z\,(\to ee)$ + jets channel is estimated using a multi-jet enriched data template with two electron candidates which both pass a 'loose' selection but fail to pass the medium identification requirements [36]. The dedicated trigger used for the selection of this sample requires two clusters of energy in the electromagnetic calorimeter with $p_{\mathrm{T}} > 20$ GeV. This sample is dominated by jets misidentified as electrons in the final state. The normalization of this sample to the multi-jet background expected with medium requirements is extracted from a template fit in the invariant mass distribution for medium electrons (m^{ee}) as follows: A single combined fit is performed of the multi-jet template and the standard simulated signal and non-multi-jet background templates to the measured spectrum of the invariant mass for medium electrons in the extended mass range 50 GeV $< m^{ee} < 150$ GeV in the inclusive selection. Systematic uncertainties are assessed by varying the mass range and the binning in the fit, by using a different generator (SHERPA instead of ALPGEN) for the signal template, by varying the electron energy scale and resolution in the simulation and by allowing for a modification of the shape of the mass distribution in the multi-jet enriched sample. The multi-jet background to the measured inclusive jet multiplicities varies between $(0.65 \pm 0.23)\%$ for $N_{\mathrm{jet}} \geq 1$ and $(1.20 \pm 0.44)\%$ for $N_{\mathrm{jet}} \geq 6$.

In the $Z\,(\to \mu\mu)$ + jets channel, heavy flavour production (with muons originating from

b- and c-quark decays) and decays-in-flight of pions and kaons are the primary source of the multi-jet background, which is highly suppressed by the isolation requirement applied to the muon candidates. The multi-jet template is derived from a data sample where both muons fail the isolation requirement. The normalization factor is obtained by fitting the multi-jet template together with a template composed of the simulated signal and the non-multijet background events that pass the signal selection to the spectrum of the invariant mass of isolated muons ($m^{\mu\mu}$) measured in data in the range 40 GeV $< m^{\mu\mu} < 150$ GeV. In contrast to the $Z(\to ee)$ + jets channel, the creation of the template and the normalization is performed separately for $N_{\text{jet}} \geq 0$, $N_{\text{jet}} \geq 1$ and $N_{\text{jet}} \geq 2$. The normalization factor derived for $N_{\text{jet}} \geq 2$ is used for all higher jet multiplicities. The systematic uncertainty is assessed by replacing the multi-jet template with one formed from muons passing a loose isolation cut but failing the tight cut used to select signal muons. Multi-jet fractions vary between $(0.25 \pm 0.04)\%$ for $N_{\text{jet}} \geq 1$ and $(2.2 \pm 2.2)\%$ for $N_{\text{jet}} \geq 6$.

The $t\bar{t}$ background contributions in the $Z(\to \ell\ell)$ + jets samples are dominated by events where both W bosons decay leptonically. Since the kinematic properties of the jets in the final state are independent of the flavours of the two leptons, final states with one electron and one muon can be used to model the $t\bar{t}$ background contributions to $Z(\to ee)$ and $Z(\to \mu\mu)$ selections. The $t\bar{t}$-enriched sample is selected from data in the $e^{\pm}\mu^{\mp}$ final state with kinematic requirements analogous to the $Z(\to \ell\ell)$ + jets selection. The dedicated trigger used for the selection of this sample requires an electron with $p_{\text{T}} > 10$ GeV and a muon with $p_{\text{T}} > 6$ GeV. For each of the observables, the number of W + jets, Z + jets and diboson events expected from simulation in the $t\bar{t}$-enriched sample is subtracted. The normalization from the $e^{\pm}\mu^{\mp}$ to the e^+e^- and $\mu^+\mu^-$ final states is calculated from $t\bar{t}$ samples generated with MC@NLO+HERWIG and with POWHEG+PYTHIA, separately for each jet multiplicity. Systematic uncertainties on the normalization arise from the choice of the generator, uncertainty on the lepton trigger, reconstruction and identification efficiency (see section 8) and on the electroweak background subtraction. The $t\bar{t}$ fractions vary between $(0.80 \pm 0.05)\%$ for $Z(\to ee)$ + ≥ 1 jet and $(18.6 \pm 7.0)\%$ for $Z(\to ee)$ + ≥ 6 jets and between $(0.74 \pm 0.03)\%$ for $Z(\to \mu\mu)$ + ≥ 1 jet and $(18.1 \pm 5.3)\%$ for $Z(\to \mu\mu)$ + ≥ 6 jets.

6   Detector-level results

Measured and expected distributions of the jet observables have been compared at the reconstruction level, separately in the electron and muon channels. As an example, figure 1 shows the dilepton invariant mass in events with at least one jet in the final state, as well as the inclusive jet multiplicity. For the signal, both ALPGEN and SHERPA expectations are shown. In this figure, $W \to e\nu$, $Z(\to \tau\tau)$ and diboson processes are summarized as 'electroweak' background and $t\bar{t}$ and single-top processes are referred to as 'top' background. For figures 1(a) and 1(b), the selection has exceptionally been extended beyond the fiducial invariant mass range, in order to demonstrate in addition the reasonable agreement between data and expectations for dilepton mass sideband regimes with larger background fractions. Table 2 shows, for the electron and muon channels separately, the observed number of events for the different jet multiplicities in the final state compared to expectations

$Z\,(\to ee)$ channel								
	≥ 0 jets	≥ 1 jet	≥ 2 jets	≥ 3 jets	≥ 4 jets	≥ 5 jets	≥ 6 jets	≥ 7 jets
$Z\,(\to ee)$	1230000	190000	42000	9000	1800	340	60	10
$W \to e\nu$	450	140	36	9	0.5	< 0.5	< 0.5	< 0.5
$Z\,(\to \tau\tau)$	650	110	24	6	1.4	0.2	< 0.1	< 0.1
diboson	1800	1160	500	110	19	3.0	0.3	0.02
$t\bar{t}$, single top	2100	1700	1190	510	160	50	13	4
multi-jet	5000	1200	300	70	16	4	0.8	0.3
total expected	1240000	190000	44000	10000	2000	390	70	14
data (4.6 fb^{-1})	1228767	191566	42358	8941	1941	404	68	17
$Z\,(\to \mu\mu)$ channel								
	≥ 0 jets	≥ 1 jet	≥ 2 jets	≥ 3 jets	≥ 4 jets	≥ 5 jets	≥ 6 jets	≥ 7 jets
$Z\,(\to \mu\mu)$	1700000	260000	57000	12000	2300	400	80	12
$W \to \mu\nu$	120	42	12	3	< 0.5	< 0.5	< 0.5	< 0.5
$Z\,(\to \tau\tau)$	1070	150	36	8	1.6	0.3	0.1	0.1
diboson	2400	1600	680	150	26	4	0.4	0.10
$t\bar{t}$, single top	2700	2100	1500	640	190	50	17	7
multi-jet	3900	700	290	80	20	6	2	0.2
total expected	1700000	260000	59000	13000	2500	500	90	20
data (4.6 fb^{-1})	1678500	257169	56506	12019	2587	552	122	31

Table 2. Numbers of events expected and observed in data that pass the $Z\,(\to ee)$ + jets and $Z\,(\to \mu\mu)$ + jets selections as a function of the inclusive jet multiplicity. The expected numbers are rounded according to the combined statistical and systematic uncertainty. ALPGEN has been used to simulate the signal events.

for signal (ALPGEN) and background processes. The combined statistical and systematic uncertainties on the total expectation increases from 6% to 30% with increasing jet multiplicity. The data are consistent with predictions by the generators ALPGEN and SHERPA, which gives confidence that the simulated samples, which are used in the unfolding, provide a reasonable description of the event kinematics and of the detector response.

7 Correction for detector effects and combination of channels

The cross sections in this article are quoted at the particle level, which corresponds to 'dressed' muons and electrons, calculated using final-state leptons from the Z decay for which collinear radiation in a cone of $\Delta R < 0.1$ is added to the lepton four-momentum. Particle jets are clustered from all final-state particles (decay length $c\tau > 10$ mm) excluding the dressed Z decay products. The phase-space requirements are the same as in the selection at reconstruction level (see table 1).

After subtracting the expected background contributions, the data distributions in each channel are unfolded to the particle level using an iterative technique [41]. Response matrices are calculated for each observable, using Z + jets samples generated with ALPGEN. Before entering the iterative process, the data are corrected for the fraction of reconstructed events in the ALPGEN sample which do not match to a particle-level equivalent. The
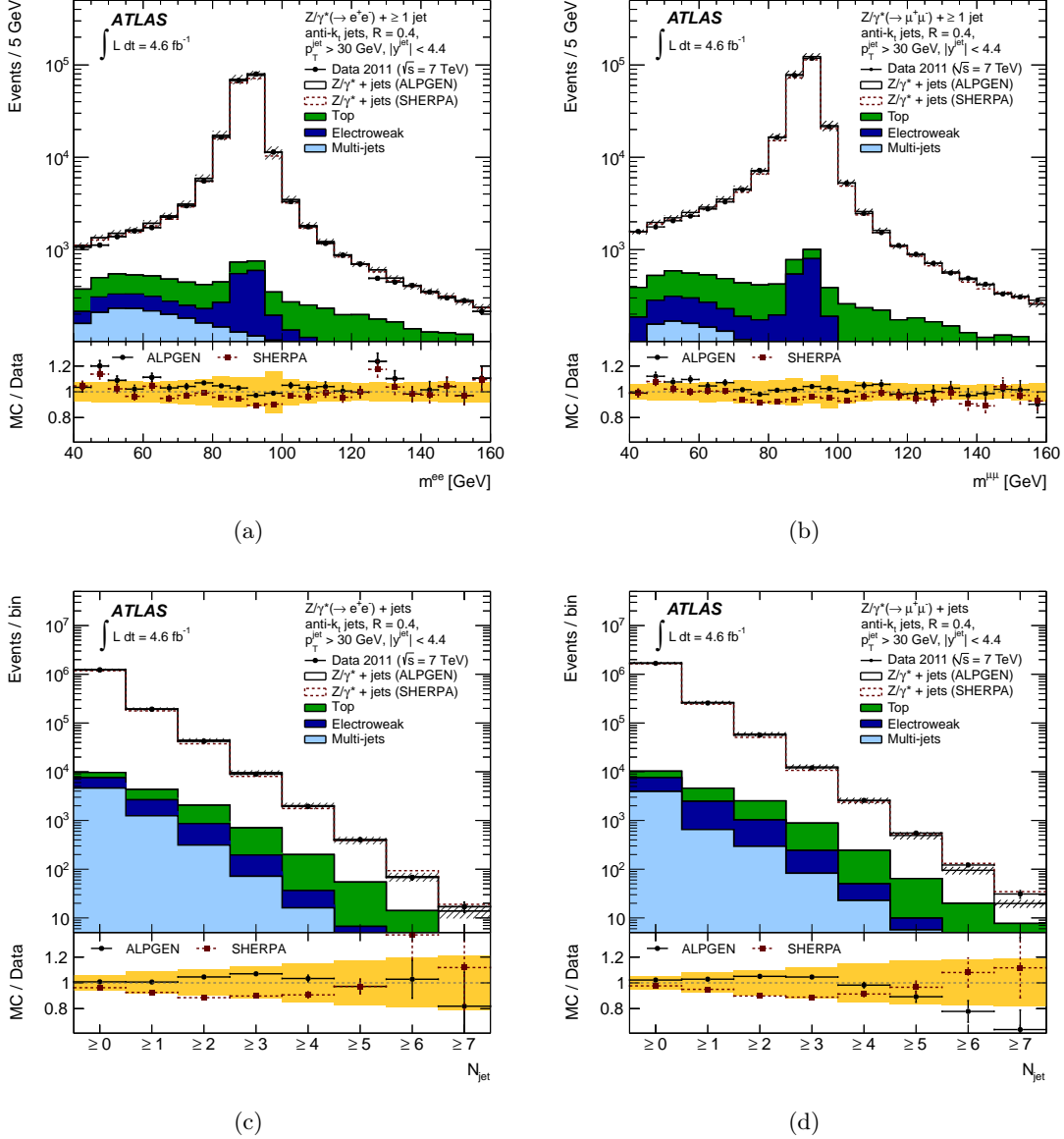
Figure 1. Numbers of events observed in data and predicted in simulation that pass the $Z (\to ee) + \mathrm{jets}$ and $Z (\to \mu\mu) + \mathrm{jets}$ selection as a function of the invariant mass of the Z candidate, (a) m^{ee} and (b) $m^{\mu\mu}$, for events with at least one jet with $p_T^{\mathrm{jet}} > 30$ GeV and $|y^{\mathrm{jet}}| < 4.4$, and as a function of the inclusive jet multiplicity, N_{jet}, in (c) di-electron and (d) di-muon events. The individual contributions of the various backgrounds are also shown, as detailed in the legend. The hatched band corresponds to the combined statistical and systematic uncertainty on the prediction, obtained using ALPGEN to model the $Z + \mathrm{jets}$ process. The error bars on each data point show the statistical uncertainty. The bottom panel shows the corresponding MC/data ratio. The shaded band corresponds to the total systematic uncertainty and the error bars to the statistical uncertainty on the MC/data ratio.

number of iterations, typically two or three, is optimized for each observable using a χ^2 comparison of generated and unfolded reconstructed $Z + \mathrm{jets}$ events from the generators

SHERPA and MC@NLO.

The uncertainties from the limited number of events in data are propagated into the particle-level cross sections using a Monte Carlo method. One thousand pseudo-experimental spectra are generated by fluctuating the content of each bin according to the statistical uncertainty. The unfolding procedure is applied to each pseudo-experiment, and the r.m.s. of the results is taken as the statistical uncertainty. Systematic uncertainties arising from the unfolding procedure are estimated by comparing with an iterative unfolding based on response matrices and corrections derived from SHERPA. The statistical uncertainties of the response matrices are propagated into systematic uncertainties on the unfolded cross sections using pseudo-experiments.

The cross sections measured in the electron and muon channels are extrapolated to a common phase-space region, derived from table 1 by extending the η range of the leptons to $|\eta^{\mathrm{lep}}| < 2.5$, using global acceptance corrections derived from ALPGEN $Z+$jets Monte Carlo samples, reweighted to the CT10 PDF set. The corrections are of the order of 14% and 5% for the electron and muon channel, respectively. Systematic uncertainties are estimated by comparing with corrections obtained using the corresponding SHERPA $Z+$jets sample and the original ALPGEN sample. Total uncertainties on the corrections are calculated as the quadratic sum of the statistical and systematic uncertainties and amount to 0.2–0.3%. The extrapolated cross sections measured in the electron and muon channels are in agreement.

For each observable, the extrapolated cross sections are combined using the averaging procedure introduced in ref. [42], which accounts for systematic uncertainties (bin-to-bin correlated and uncorrelated) proportional to the central values of the respective cross sections. The weights of the individual cross-section measurements (μ_k^i) in channel k (ee or $\mu\mu$) and bin i in the combined cross sections (m^i) are derived by minimizing the following χ^2 function [42]:

$$\chi^2(\mathbf{m}, \mathbf{b}) = \sum_{k,i} \frac{[m^i - \sum_j \gamma_{j,k}^i m^i b_j - \mu_k^i]^2}{(\delta_{\mathrm{stat},k}^i)^2 \mu_k^i (m^i - \sum_j \gamma_{j,k}^i m^i b_j) + (\delta_{\mathrm{uncor},k}^i m^i)^2} + \sum_j b_j^2, \qquad (7.1)$$

where b_j denote the shift introduced by a correlated systematic error source j normalized to its respective standard deviation. The relative statistical and uncorrelated systematic uncertainties on μ_k^i are denoted by $\delta_{\mathrm{stat,k}}^i$ and $\delta_{\mathrm{uncor,k}}^i$ and the variable $\gamma_{j,k}^i$ quantifies the influence of the correlated systematic error source j on the measurement i in the channel k.

The following bin-to-bin correlated systematic sources are taken into account: normalization of the multi-jet background, lepton energy scale and resolution, lepton reconstruction, identification and trigger efficiencies and normalization of $t\bar{t}$, electroweak and single-top background contributions, the latter three treated as correlated between the channels. Bin-to-bin correlated systematic sources which have the same impact in both channels do not enter in the combination procedure. These are the individual components of the jet energy scale, the jet energy resolution, the luminosity, the unfolding procedure, and the extrapolation factor. The uncertainties from these sources on the combined result are taken as the weighted average of the corresponding uncertainties on the electron and muon measurements.

8   Systematic uncertainties

The kinematic ranges and the binning are chosen such that the statistical uncertainty of the measurement is comparable to or smaller than the systematic uncertainty. The relative systematic uncertainties on the cross sections measured in each channel are derived for each observable by propagating systematic shifts from a set of independent sources through the response matrices and the subtracted background contributions into the unfolded data. The resulting systematic uncertainties for each source in each channel are symmetrized in order to mitigate the impact of statistical fluctuations and are combined in the averaging procedure.

The uncertainty on the jet energy scale (JES), determined from the combination of methods based on MC and in-situ techniques used to determine the scale, constitutes the dominant component of the total systematic uncertainty. It is propagated through the analysis using 14 independent components fully correlated in $p_{\mathrm{T}}^{\mathrm{jet}}$ [39, 40]. They account for uncertainties on the different in-situ measurements which enter the jet calibration, on the jet flavour and on the impact of pile-up and close-by jets. The uncertainty on the jet energy resolution, derived from a comparison of the resolution obtained in data and in simulated dijet events, is propagated into the final cross section by varying the energy resolution of the simulated jets. Uncertainties on the normalization of the background expectations, for simulated and data-driven background contributions respectively, are treated as correlated between bins and are propagated to the measured cross sections by unfolding the data distributions after the subtraction of the systematically shifted background. The statistical uncertainties of the background contributions are added quadratically to the statistical uncertainties of the data. The uncertainty from the unfolding process is derived from the different components discussed in section 7, which are considered to be uncorrelated. Systematic uncertainties on electron and muon trigger efficiencies, energy scale, resolution, reconstruction and identification efficiencies are derived from the comparison of tag-and-probe results in data and simulated events [36, 37].

Table 3 summarizes the systematic uncertainties on the Z + jets cross sections as a function of the inclusive jet multiplicity and of $p_{\mathrm{T}}^{\mathrm{jet}}$ of the leading jet separately for the electron and muon channels. The uncertainty on the integrated luminosity of 1.8% translates into comparable uncertainties on the measured cross sections. The total uncertainties on the inclusive jet cross sections range from 8% for $N_{\mathrm{jet}} \geq 1$ to 16–17% for $N_{\mathrm{jet}} \geq 4$, dominated by the JES uncertainty.

The uncertainty on cross-section ratios, $R_{\geq(n+1)/\geq n}$ [3] , for successive jet multiplicities n is significantly reduced due to the strong correlations between the lepton and jet reconstruction and calibration uncertainties in neighbouring jet bins and amounts to a total of 3–4% for $R_{\geq 2/\geq 1}$ and higher multiplicities, which are of interest in this article, dominated by the residual JES uncertainty. The large JES uncertainties in the forward region propagate into uncertainties on the unfolded cross sections at the level of 20% (30%) for jet rapidities of $|y^{\mathrm{jet}}| = 3.0$ (4.0). This is reflected in large jet energy scale uncertainties on the cross section

---

[3]For simplicity, n is used in the subscript instead of N_{jet}

$Z(\to ee)$	≥ 1 jet	≥ 2 jets	≥ 3 jets	≥ 4 jets	$p_{\mathrm{T}}^{\mathrm{jet}}$ in [30–500 GeV]
electron reconstruction	2.8%	2.8%	2.8%	2.8%	2.6–2.9%
jet energy scale, resol.	7.4%	10.1%	13%	17%	4.3–9.0%
backgrounds	0.26%	0.34%	0.44%	0.50%	0.2–3.2%
unfolding	0.22%	0.94%	1.2%	1.9%	1.4–6.8%
total	7.9%	10.5%	13%	17%	5.5–12.0%
$Z(\to \mu\mu)$	≥ 1 jet	≥ 2 jets	≥ 3 jets	≥ 4 jets	$p_{\mathrm{T}}^{\mathrm{jet}}$ in [30–500 GeV]
muon reconstruction	0.86%	0.87%	0.87%	0.88%	0.8–1.0%
jet energy scale, resol.	7.5%	9.9%	13%	16%	3.2–8.7%
backgrounds	0.093%	0.20%	0.41%	0.66%	0.1–1.9%
unfolding	0.30%	0.68%	0.52%	1.3%	0.5–6.2%
total	7.6%	10.0%	13%	16%	4.4–10.2%

Table 3. Systematic uncertainties on the cross sections for $Z(\to ee)$ + jets and $Z(\to \mu\mu)$ + jets as a function of the inclusive jet multiplicity and as a function of the transverse momentum, $p_{\mathrm{T}}^{\mathrm{jet}}$, of the leading jet for events with at least one jet with $p_{\mathrm{T}}^{\mathrm{jet}} > 30$ GeV and $|y^{\mathrm{jet}}| < 4.4$. The rows labelled 'electron reconstruction' and 'muon reconstruction' include uncertainties on trigger, reconstruction and identification, energy scale and resolution.

for events with large rapidity distance ($|\Delta y^{jj}|$) between the leading jets, which combine with the unfolding uncertainties to total uncertainties of 20% (50%) for $|\Delta y^{jj}| = 3.0$ (4.0).

9   Theoretical predictions

Fixed-order calculations at NLO pQCD for the production of $Z(+ \geq 1$ jet$)$ up to $Z(+ \geq 4$ jets$)$ are computed using the BLACKHAT+SHERPA program [5–7]. CT10 PDFs [25] are employed and renormalization and factorization scales are set to $H_{\mathrm{T}}/2$, where H_{T} is defined event-by-event as the scalar sum of the p_{T} of all stable particles/partons. The anti-k_t algorithm with $R = 0.4$ is used to reconstruct jets at the parton level. Systematic uncertainties on the predictions related to PDF uncertainties are computed from the 52 CT10 eigenvectors at 68% confidence level [25]. The uncertainties on the cross sections increase from 1% for ($N_{\mathrm{jet}} \geq 1$) to 3% for ($N_{\mathrm{jet}} \geq 4$) and from 1% to 5% with $p_{\mathrm{T}}^{\mathrm{jet}}$ of the leading jet between 30 GeV and 500 GeV. Additional changes in the PDFs due to the variation of the input value for the strong coupling constant α_{s} at the Z-boson mass scale by ± 0.001 around its nominal value $\alpha_{\mathrm{s}}(m_{\mathrm{Z}}) = 0.118$ introduce uncertainties on the predicted cross sections in the range of 1% to 3% for $Z(+(1-4)$ jets$)$. These are added in quadrature to the PDF uncertainties. Scale uncertainties are estimated by variations of the renormalization and factorization scales to one half and two times the nominal scale. The scale uncertainties for different parton multiplicities are assumed to be uncorrelated. For inclusive calculations, the scale variations translate into variations of the cross section by 4% to 13% as N_{jet} increases and by 2% to 18% with increasing $p_{\mathrm{T}}^{\mathrm{jet}}$ of the leading jet. For exclusive final states, the scale uncertainties are calculated using the prescription of ref. [43]. For comparison, the theory/data ratios presented in section 10 also show the scale uncertainty resulting from a

simple variation of the renormalization and factorization scales by a factor of two, assuming the uncertainties to be correlated for different parton multiplicities. The scale uncertainties constitute the dominant uncertainties in most kinematic regions.

The NLO fixed-order calculations at the parton level are corrected to the particle level for the underlying event and for effects of fragmentation and of QED final-state radiation (QED-FSR). Parton-to-hadron correction factors (δ^{had}) approximately account for non-perturbative contributions from the underlying event and fragmentation into particles. For each observable, the correction factor is estimated using simulated Z + jets samples, produced with ALPGEN with the HERWIG cluster fragmentation in which JIMMY models the underlying event using the AUET2-CTEQ61L [20] tune. It is calculated as the bin-by-bin ratio of the nominal distribution at the particle level to the one obtained by turning off both the interactions between proton remnants and the fragmentation in the simulated samples. The non-perturbative corrections are also computed using ALPGEN samples, this time interfaced to PYTHIA, where the correction corresponds to the combined effect of string fragmentation and of the underlying event predicted by the PERUGIA2011C [22] tune. The difference is taken as a systematic uncertainty. The combined nominal correction is 7% in the low $p_{\mathrm{T}}^{\mathrm{jet}}$ region and decreases with increasing $p_{\mathrm{T}}^{\mathrm{jet}}$ towards zero. The correction factors for the inclusive N_{jet} distributions are about 3–4%. Nonperturbative corrections for quantities calculated with several jets include implicitly the corrections for all jets. The statistical and the symmetrized systematic uncertainties on δ^{had} are added in quadrature to the total uncertainty from the BLACKHAT+SHERPA calculation.

The QED-FSR correction factors (δ^{QED}) are determined using Z + jets samples produced with the ALPGEN generator, interfaced to PHOTOS [26], by calculating the expected cross sections both with the lepton four-momentum before final-state photon radiation ('Born level'), and with dressed leptons. The correction factors are about 2% for the electron and muon channels. They do not show a significant N_{jet} dependence and are stable with respect to the jet rapidity and for large jet transverse momentum. Systematic uncertainties are derived by comparing with δ^{QED} obtained using a Z + jets sample produced with the SHERPA generator [9] which generates QED-FSR using the YSF method [27]. The differences between the two predictions are usually at the per-mille level.

10 Results and discussion

For each observable, the spectrum measured in data is unfolded to the particle level. After extrapolation and combination of electron and muon channels, the results are compared with calculations from BLACKHAT+SHERPA, corrected to the particle level, and with predictions by ALPGEN, SHERPA and MC@NLO. Both ALPGEN and SHERPA employ matrix elements for up to five partons. Higher multiplicities are generated by the parton shower. In contrast, MC@NLO generates the Drell–Yan process at NLO precision, which includes the real emission of one additional parton. All higher parton multiplicities are generated by the parton shower. Inclusive and differential cross sections for $Z\,(\rightarrow \ell\ell) + \geq n\,$jets are compared with BLACKHAT+SHERPA fixed-order pQCD calculations for $Z + \geq n\,$partons, which provide a NLO estimate for the respective parton multi-

plicity, including the real emission of one additional parton. Measured cross sections as a function of the jet multiplicity and their ratios are detailed in table 4. Tabulated values of all observed results are available in the Durham HEP database [44].

10.1 Jet multiplicities

Figure 2(a) presents the absolute cross sections for inclusive jet multiplicities for up to seven hadronic jets in the final state. The ratios $R_{\geq(n+1)/\geq n}$ of cross sections for two successive multiplicities, presented in figure 2(b), provide a more precise measurement of the QCD process, due to the cancellation of part of the systematic uncertainty. The data are consistent with BLACKHAT+SHERPA calculations and with predictions of the generators ALPGEN and SHERPA. The MC@NLO parton shower underestimates the observed rate for additional jet emission by a factor of two, which leads to large offsets to the data for higher jet multiplicities. For this reason, in subsequent figures the MC@NLO predictions are only shown for $Z\,(\to \ell\ell) + \geq 1$ jet selections, where the parton corresponding to the NLO real emission can be expected to yield a reasonable description of the kinematics.

Exclusive jet multiplicities at the LHC are expected to be described by means of two benchmark patterns, 'staircase scaling' with $R_{(n+1)/n}$ constant and 'Poisson scaling' with $R_{(n+1)/n}$ inversely proportional to n [3, 45], which provide limiting cases for certain kinematic conditions. While for high multiplicities a flat exclusive jet multiplicity ratio is derived from the non-abelian nature of QCD FSR, at low multiplicity the jet multiplicity ratio is flat due to the combined effect of a Poisson-distributed multiplicity distribution and parton density suppression [3]. The emission of the first parton should be suppressed more strongly than the subsequent parton emissions. The underlying Poisson scaling is expected to emerge after introducing large scale differences between the core process ($Z\,(+1$ jet)) and the $p_{\mathrm{T}}^{\mathrm{jet}}$ of the second leading jet. Two selections are chosen to test the two benchmark scenarios: (a) the standard Z + jets selection and (b) events where the leading jet has a transverse momentum in excess of 150 GeV.

Figure 3(a) presents the ratios $R_{(n+1)/n}$ of cross sections for two successive exclusive multiplicities for the standard Z + jets selection. The comparitatively large scale uncertainties on the pQCD predictions result from the prescription of ref. [43], assuming the scale variations to be uncorrelated across the jet multiplicities. For comparison, the total uncertainty calculated using a naive scale variation, and a reduced uncertainty that does not include any scale uncertainty are also shown. The data are consistent with the central values of the BLACKHAT+SHERPA calculations and with predictions by the generators ALPGEN and SHERPA. The cross-section ratios show an approximately linear dependence on the jet multiplicity with a small slope. A linear fit $R_{(n+1)/n} = R_0 + \frac{\mathrm{d}R}{\mathrm{d}n} \cdot n$ of the observed multiplicity ratio starting with $R_{2/1}$ yields $R_0 = 0.232 \pm 0.009$ and $\mathrm{d}R/\mathrm{d}n = -0.011 \pm 0.003$. The uncertainties include a systematic contribution, derived from a series of fits to systematic variations of the multiplicity ratio. The flat staircase pattern provides an acceptable approximation of the observed scaling behaviour for the standard Z + jets selection. The observation is consistent with results presented in [15] on the smaller data set collected in 2010.
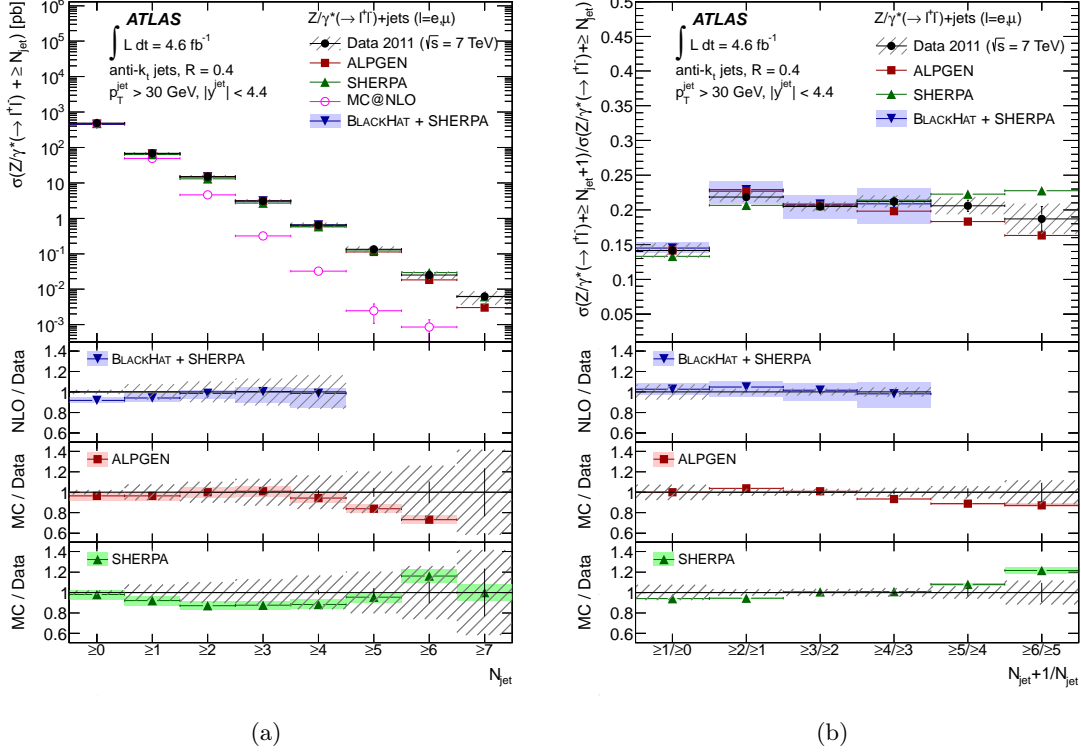
Figure 2. (a) Measured cross section for $Z\,(\to \ell\ell)$ + jets as a function of the inclusive jet multiplicity, N_{jet}, and (b) ratio of cross sections for successive inclusive jet multiplicities. The data are compared to NLO pQCD predictions from BLACKHAT+SHERPA corrected to the particle level, and the ALPGEN, SHERPA and MC@NLO event generators (see legend for details). The error bars indicate the statistical uncertainty on the data, and the hatched (shaded) bands the statistical and systematic uncertainties on data (prediction) added in quadrature.

Figure 3(b) presents the exclusive jet multiplicity ratio for events where the leading jet has a transverse momentum in excess of 150 GeV. The observed ratio $R_{(n+1)/n}$ is now steeply increasing towards low jet multiplicities, a pattern described by the central values of the BLACKHAT+SHERPA calculations, by the generator ALPGEN and approximately also by SHERPA. The observed cross-section ratios have been fitted with a pattern expected from a Poisson-distributed jet multiplicity with the expectation value $\bar{n}$, $R_{(n+1)/n} = \frac{\bar{n}}{n}$. The Poisson scaling provides a good overall description of the jet multiplicity observed in data for the selected kinematic regime, with $\bar{n} = 1.02 \pm 0.04$, where the uncertainty includes statistical and systematic components.

The scaling pattern is also investigated for a preselection typically employed in the selection of particles produced via vector boson fusion (VBF). Figure 4 presents the absolute cross section as a function of the exclusive jet multiplicity and $R_{(n+1)/n}$ after requiring two jets with $m^{jj} > 350$ GeV and $|\Delta y^{jj}| > 3.0$, in the following referred to as 'VBF preselection'. The data are consistent with the BLACKHAT+SHERPA prediction. SHERPA describes the multiplicity well whereas ALPGEN overestimates $R_{3/2}$.
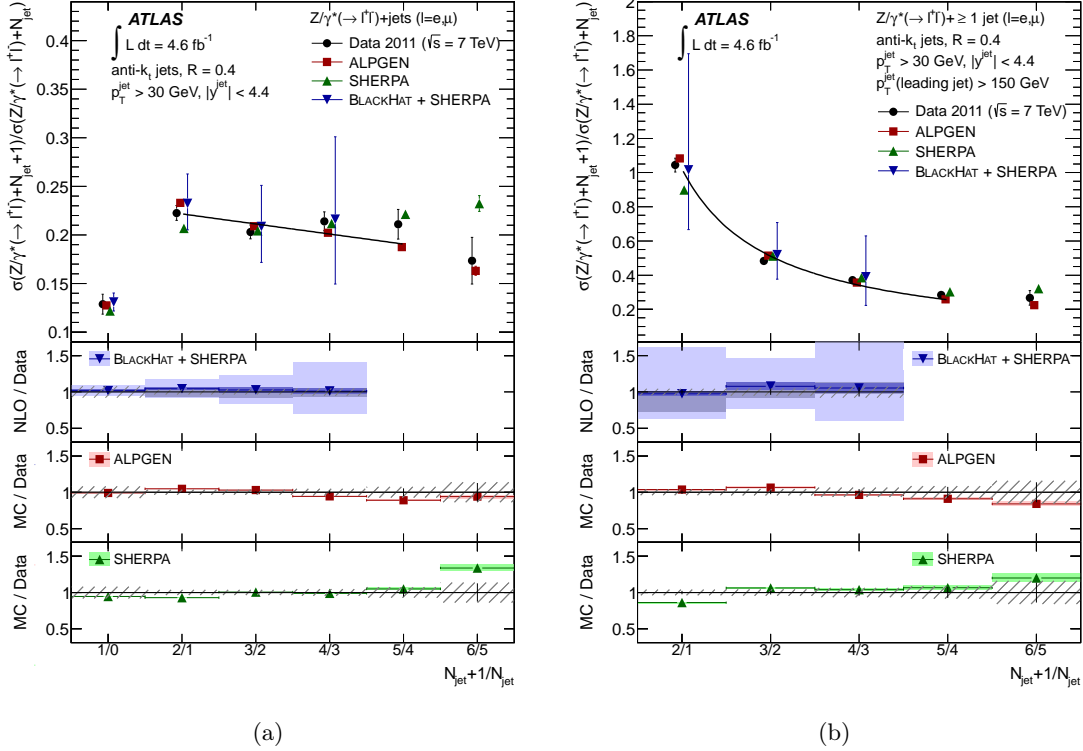
Figure 3. (a) Ratio of cross sections for successive exclusive jet multiplicities, N_{jet}, in events selected with the standard selection and (b) in events with at least one jet with $p_T^{jet} > 150$ GeV and $|y^{jet}| < 4.4$. The data are compared to NLO pQCD predictions from BLACKHAT+SHERPA corrected to the particle level, and the ALPGEN, SHERPA and MC@NLO event generators (see legend for details). The error bars indicate the statistical uncertainty on the data, and the hatched (shaded) bands the statistical and systematic uncertainties on data (prediction) added in quadrature. The shaded bands on the theory calculations show the systematic uncertainty excluding the scale uncertainty (dark shaded) and the total systematic uncertainties using the naive approach (medium shaded) and the nominal approach (light shaded) to derive the scale uncertainty (see section 9). The figures include (a) a linear fit $R_{(n+1)/n} = R_o + \frac{dR}{dn} \cdot n$ in the range $R_{2/1} < R_{(n+1)/n} < R_{5/4}$ and (b) a Poisson fit $R_{(n+1)/n} = \frac{\bar{n}}{n}$ to the data points, with the free parameters R_o, $\frac{dR}{dn}$ and $\bar{n}$.

10.2 Jet transverse momentum

Differential cross sections with respect to the jet transverse momentum, p_T^{jet}, provide a test of pQCD over a large kinematic range. In particular, when p_T^{jet} exceeds the scale given by the gauge boson mass, NLO/LO K-factors can be large due to the presence of QCD corrections of the order of $\alpha_s \ln^2(p_T^{jet}/m_Z)$ [4]. In addition, higher-order electroweak corrections are expected to reduce the cross section with increasing transverse momentum of the Z boson candidate, by 5–20% for 100 GeV $< p_T^{\ell\ell} < 500$ GeV [46].

Figures 5 and 6 show the cross section as a function of p_T^{jet} of the first, the second, the third and the fourth leading jet (in descending order of p_T^{jet}) for events with at least one, two, three and four jets in the final state, respectively. The cross sections are normalized to

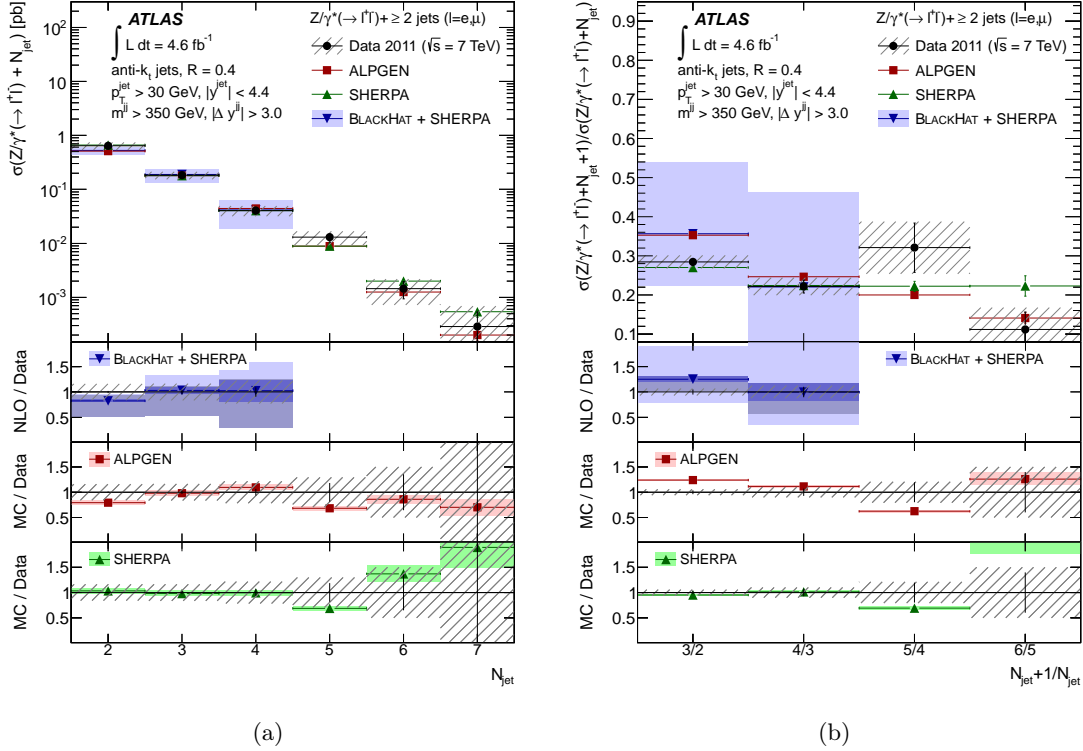**Figure 4**. (a) Measured cross section for $Z(\to \ell\ell)+$ jets as a function of the exclusive jet multiplicity, N_{jet}, and (b) ratio of the cross sections for two successive multiplicities, in events passing the VBF preselection (at least two jets with $p_T^{\text{jet}} > 30$ GeV and $|y^{\text{jet}}| < 4.4$ and $m^{jj} > 350$ GeV and $|\Delta y^{jj}| > 3.0$ for the two leading jets). The other details are as in Figure 3.

the inclusive $Z(\to \ell\ell)$ cross section, which reduces the systematic uncertainties connected to lepton identification and integrated luminosity. The fixed-order NLO predictions by BLACKHAT+SHERPA are consistent with the data for all jet multiplicities.

For the leading jet, the precision of the measurement exceeds the precision of the theory prediction. While ALPGEN predictions for the p_T^{jet} spectrum of the second to fourth leading jet are consistent with the data, the p_T^{jet} spectrum of the leading jet is predicted to be too hard for larger values of p_T^{jet}. SHERPA is characterized by offsets to the data at the level of 5–15%, consistent with the observations presented in figure 2(a) for the inclusive jet cross section. MC@NLO predicts a too soft p_T^{jet} spectrum, resulting in a discrepancy with the data by one order of magnitude for large p_T^{jet}. This is attributed to the fact that the fraction of events with a second resolved jet, which in MC@NLO is modelled via the parton shower, increases considerably with p_T^{jet} of the leading jet (see figures 3(a) and 3(b) for small and larger p_T^{jet} (leading jet)). A too soft p_T^{jet} spectrum of the parton shower will hence result in an increasing discrepancy between the MC@NLO prediction and the data.

Figure 7(a) shows the cross section as a function of p_T^{jet} of the leading jet, normalized to the inclusive $Z(\to \ell\ell)$ cross section, when a veto on a second jet is applied. A better
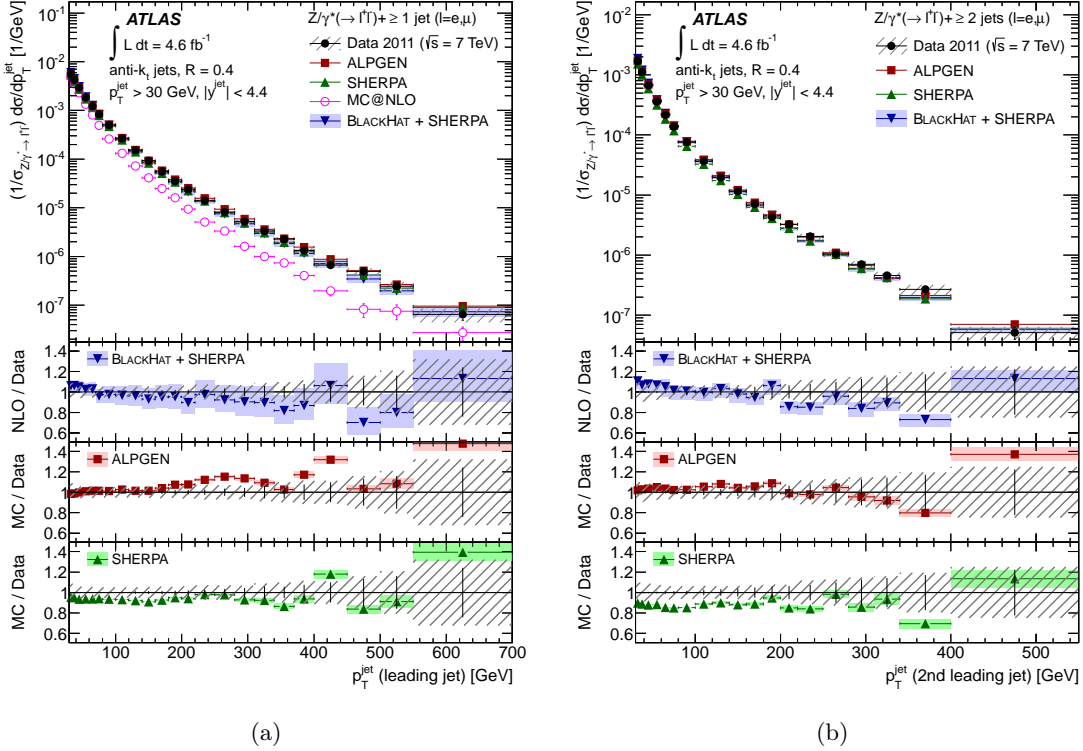
– 17 –

Figure 5. (a) Measured cross section for $Z(\to \ell\ell)$ + jets as a function of the transverse momentum, p_T^{jet}, of the leading jet for events with at least one jet with $p_T^{\text{jet}} > 30$ GeV and $|y^{\text{jet}}| < 4.4$ in the final state and (b) as a function of p_T^{jet} of the second leading jet for events with at least two jets. The cross sections are normalized to the inclusive $Z(\to \ell\ell)$ cross section. The other details are as in Figure 2.

agreement between the predicted and observed cross-sections is observed. For events with at least two jets, figure 7(b) shows cross section as a function of the p_T^{jet} ratio of the two leading jets, normalized to the inclusive $Z(\to \ell\ell)$ cross section. ALPGEN overestimates the cross section for events with a p_T^{jet} ratio of the leading jets in the range of 0.1–0.2. SHERPA underestimates the cross section as a function of the p_T^{jet} ratio by $\approx 15\%$, consistent with the results presented in figure 2(a).

In a complementary approach, the cross section is measured as a function of the p_T of the recoiling Z boson, reconstructed from the momenta of the two leptons. The results are presented in figure 8 for both the inclusive and the exclusive $Z(+1$ jet$)$ selection, normalized to the inclusive $Z(\to \ell\ell)$ cross section. Both ALPGEN and SHERPA predict a too hard $p_T^{\ell\ell}$ spectrum, in particular in the inclusive case. The discrepancy with the data is comparable to the expected higher-order electroweak corrections [46] although higher-order QCD corrections could equally account for this. The BLACKHAT+SHERPA $Z(+ \geq 1$ jet$)$ fixed-order calculation for the inclusive final state is too soft whereas for the exclusive final state the central predictions are closer to the observed spectrum. This result is attributed to missing higher jet multiplicities in the fixed-order calculation and will be discussed in more
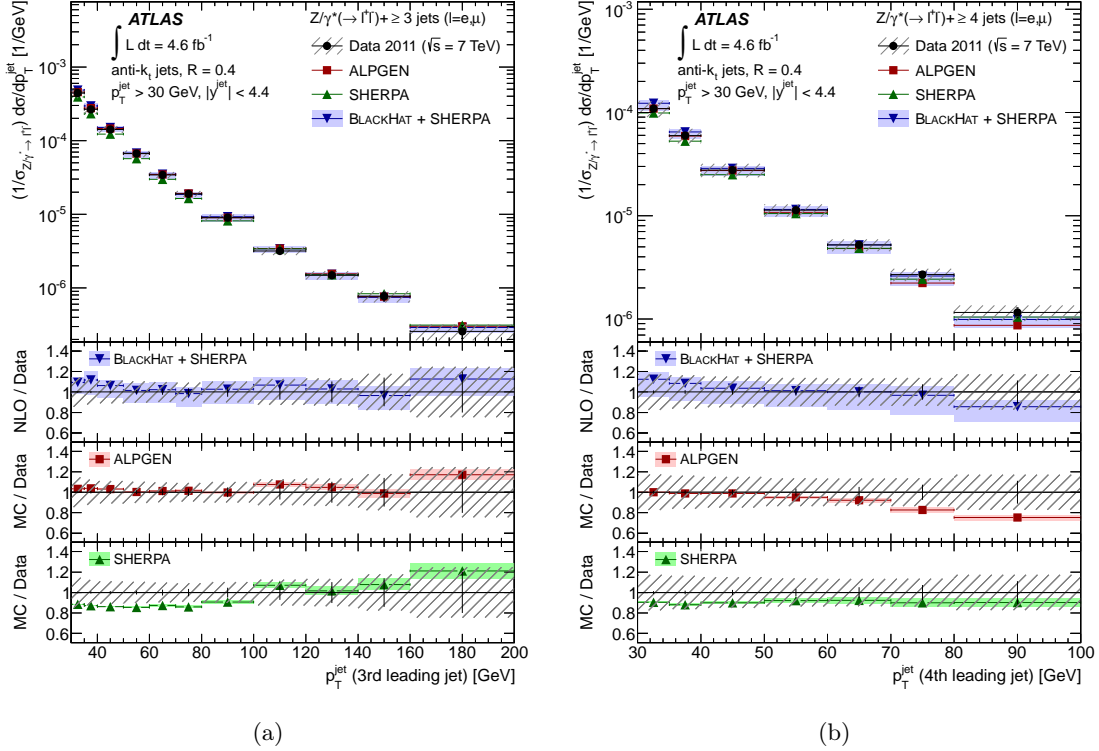
Figure 6. (a) Measured cross section for $Z\,(\to \ell\ell)$ + jets as a function of the transverse momentum, p_T^{jet}, of the third leading jet for events with at least three jets with $p_T^{\text{jet}} > 30$ GeV and $|y^{\text{jet}}| < 4.4$ in the final state and (b) as a function of p_T^{jet} of the fourth leading jet for events with at least four jets. The cross sections are normalized to the inclusive $Z\,(\to \ell\ell)$ cross section. The other details are as in Figure 2.

detail in section 10.5. The comparison with BLACKHAT+SHERPA yields no indication for missing higher-order electroweak corrections in the large-$p_T^{\ell\ell}$ region. Consistent with the results presented for the p_T^{jet} spectrum of the leading jet, MC@NLO describes the exclusive $Z\,(+1 \text{ jet})$ final state better than the corresponding inclusive final state.

10.3 Angular distributions

Figures 9 and 10 show the rapidity spectrum of the four leading jets, normalized to the inclusive $Z\,(\to \ell\ell)$ cross section. Both BLACKHAT+SHERPA and SHERPA predict rapidity spectra for the leading jet that are somewhat wider than observed in the data. ALPGEN predictions are compatible with the measurements.

Figure 11 presents the separation in rapidity, $|\Delta y^{jj}|$, and the invariant mass, m^{jj}, of the two leading jets, normalized to the inclusive $Z\,(\to \ell\ell)$ cross section. The predictions by BLACKHAT+SHERPA and ALPGEN are consistent with the data. SHERPA overestimates the cross section for large $|\Delta y^{jj}|$, consistent with the too wide rapidity spectra.

Differential jet cross sections as a function of angular distances ($\Delta\phi^{jj}$ and ΔR^{jj}) between the two leading jets are presented in figures 12(a) and 12(b), respectively, normal-
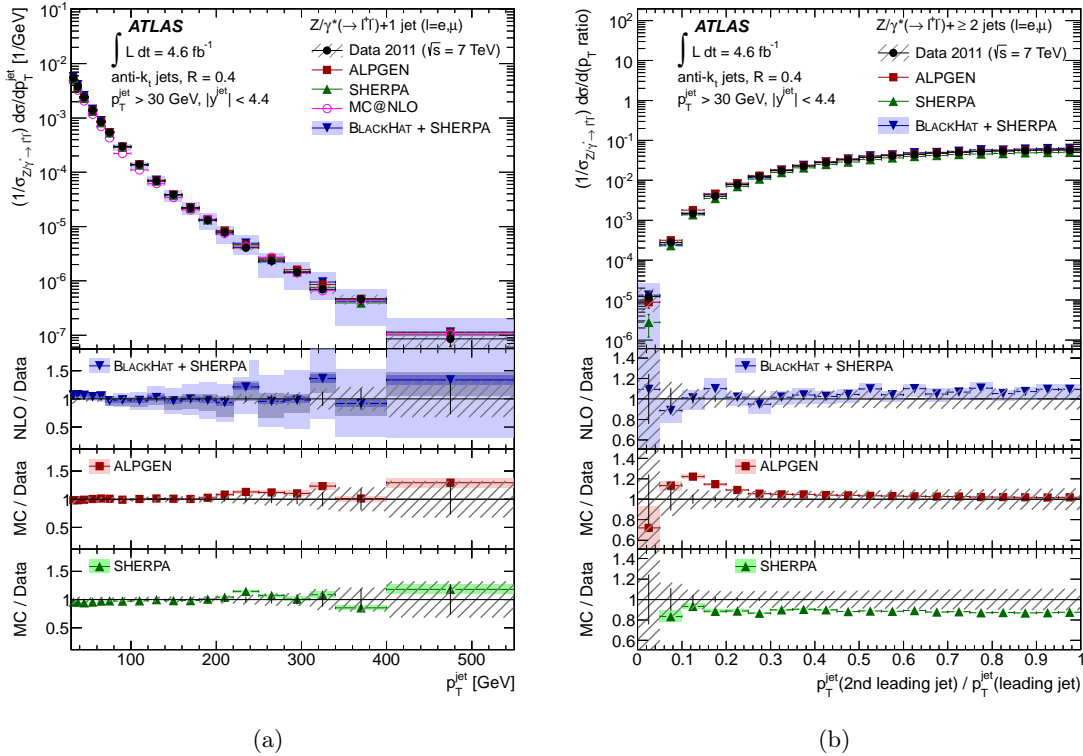
Figure 7. (a) Measured cross section for $Z(\to \ell\ell)$ + jets as a function of the jet transverse momentum, p_T^{jet}, for events with exactly one jet with $p_T^{\text{jet}} > 30$ GeV and $|y^{\text{jet}}| < 4.4$ in the final state and (b) as a function of the ratio of p_T^{jet} of the second leading jet to p_T^{jet} of the leading jet for events with at least two jets. The cross sections are normalized to the inclusive $Z(\to \ell\ell)$ cross section. The other details are as in Figure 3.

ized to the inclusive $Z(\to \ell\ell)$ cross section. The azimuthal distance is well modelled by ALPGEN and by BLACKHAT+SHERPA. The tendencies observed in the modelling of the distance in ϕ and in rapidity are reflected in the measurement of the ΔR spectrum of the leading jets. SHERPA models a too flat spectrum for both $\Delta\phi$ and ΔR. The offset of 15% of the SHERPA prediction from the observed cross section in the bulk of the data in figures 11 and 12 is consistent with the results presented in figure 2(a) for the inclusive $Z(\to \ell\ell)$ + ≥ 2 jets cross section.

10.4 Distributions after VBF preselection

A veto on a third jet is used to reject Z + jets background in selections of Higgs boson candidates produced by VBF. Figure 13 shows the transverse momentum and rapidity distributions of the third jet after the VBF preselection, as defined in section 10.1, normalized to the inclusive $Z(\to \ell\ell)$ cross section. The predictions by BLACKHAT+SHERPA, ALPGEN and SHERPA are consistent with the measurements. Figure 14 shows the fraction of events which have fulfilled the requirements of a VBF preselection that pass in addition a veto on a third jet in the central region ($|\eta| < 2.4$) as a function of the minimum trans-
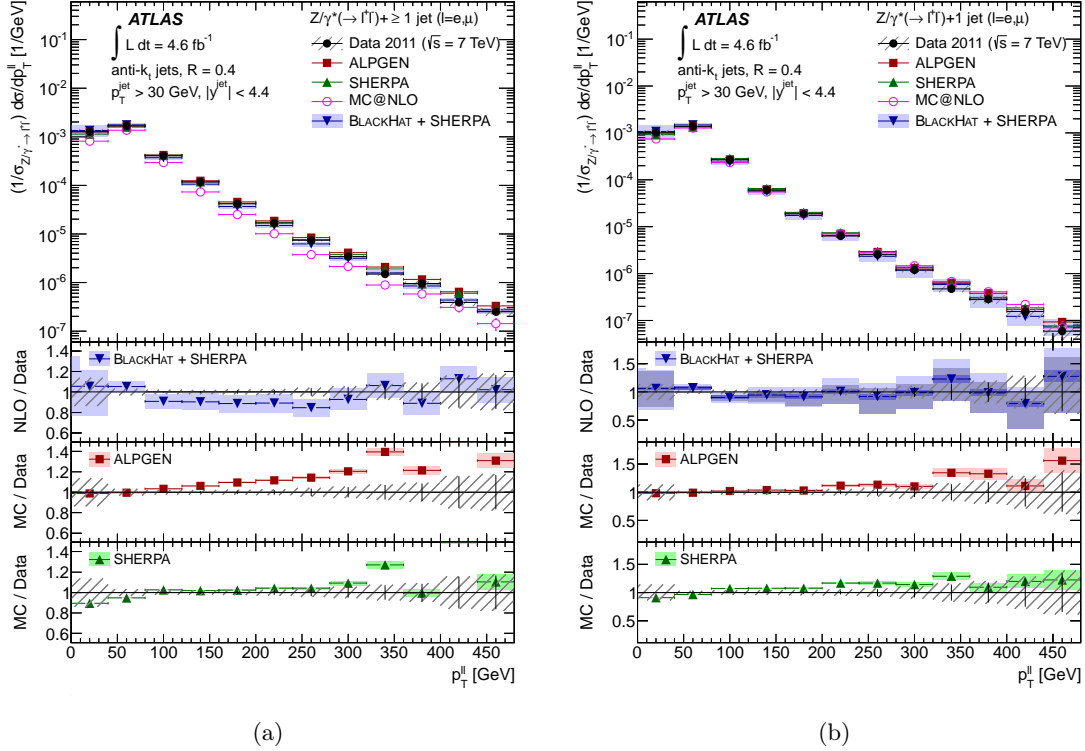
Figure 8. (a) Measured cross section for $Z (\rightarrow \ell\ell) +$ jets as a function of the transverse momentum of the Z candidate, $p_T^{\ell\ell}$, in events with at least one jet with $p_T^{jet} > 30$ GeV and $|y^{jet}| < 4.4$ in the final state and (b) as a function of $p_T^{\ell\ell}$ in events with exactly one jet. The cross sections are normalized to the inclusive $Z (\rightarrow \ell\ell)$ cross section. The other details are as in Figure 3.

verse momentum of the veto jet, referred to as 'jet veto efficiency' in the following. The results are shown at detector level, separately for the $Z \rightarrow ee$ and the $Z \rightarrow \mu\mu$ channel. The overestimate of $R_{3/2}$ in ALPGEN (see figure 4) leads to an underestimate of the veto efficiency, particularly for the low-p_T^{jet} regime. SHERPA predicts the veto efficiencies better.

10.5 Inclusive quantities

Quantities based on inclusive p_T sums of final-state objects, such as H_T or S_T, are often employed in searches in order to enrich final states resulting from the decay of heavy particles. Reference [47] reports a discrepancy between fixed-order pQCD calculations and data for moderate energy regimes in $W +$ jets events which can be mitigated by including higher jet multiplicities in the theoretical calculations by means of 'exclusive sums' [48].

Differential cross sections of $Z (+ \geq 1 \text{ jet})$ events as a function of H_T and S_T, normalized to the inclusive $Z (\rightarrow \ell\ell)$ cross section, are presented in figure 15. ALPGEN predicts slightly too hard spectra for both variables in line with the too hard spectrum for p_T^{jet}. SHERPA predictions show an offset of 10–15% to the data. The softer spectra from BLACKHAT+SHERPA, based on a $Z (+ \geq 1 \text{ jet})$ fixed-order NLO calculation, deviate
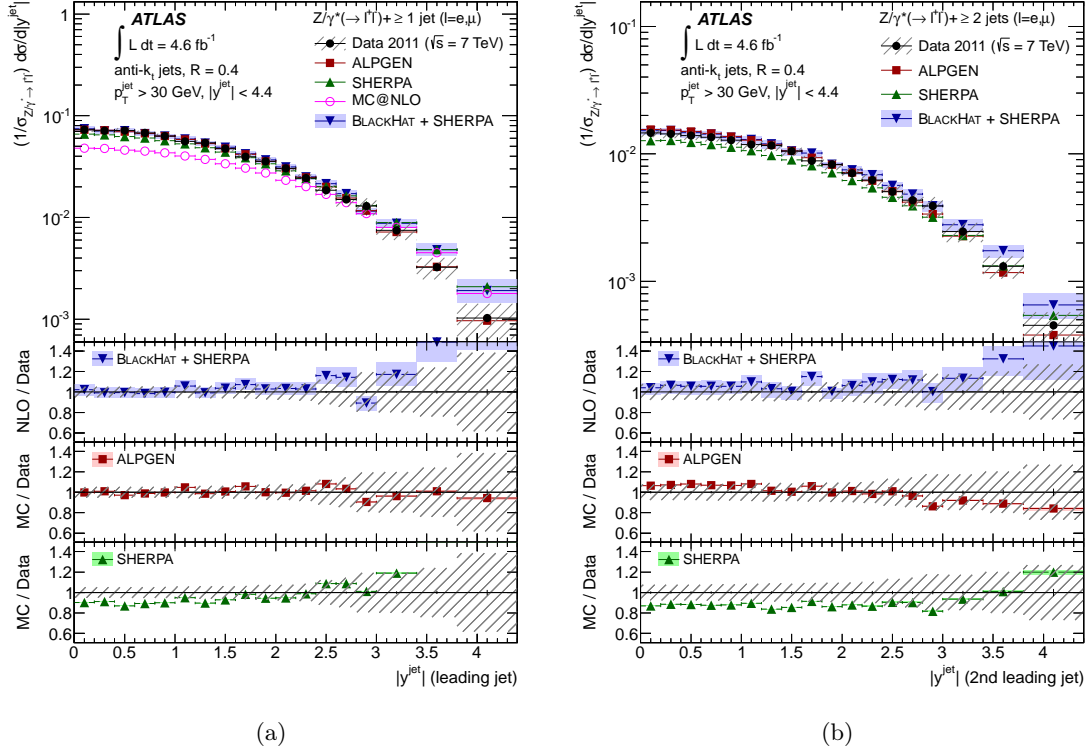
Figure 9. (a) Measured cross section for $Z(\to \ell\ell)$ + jets as a function of the absolute value of the rapidity, $|y^{\text{jet}}|$, of the leading jet for events with at least one jet with $p_T^{\text{jet}} > 30$ GeV and $|y^{\text{jet}}| < 4.4$ in the final state and (b) as a function of $|y^{\text{jet}}|$ of the second leading jet for events with at least two jets. The cross sections are normalized to the inclusive $Z(\to \ell\ell)$ cross section. The other details are as in Figure 2.

increasingly from the data for larger values of H_T and S_T, which confirms and extends the results in reference [47] to a higher energy regime. The discrepancy is attributed to missing higher jet multiplicities in the fixed-order calculation. This interpretation is investigated further in what follows.

Figure 16(a) shows, at reconstruction level, the average jet multiplicity as a function of H_T for the $Z \to ee$ channel. Compatible results have been obtained in the muon channel. Predictions by ALPGEN and SHERPA are consistent with the data. For values of $H_T \approx 350$ GeV, where data and NLO calculation start to deviate significantly, the average jet multiplicity exceeds two. A similar measurement is performed as a function of the $p_T^{\ell\ell}$ in the $Z \to \mu\mu$ channel and shown in figure 16(b). Compatible results have been obtained in the electron channel. For values of $p_T^{\ell\ell} \approx 200$ GeV, where the NLO predictions underestimate the measured cross section (see figure 8), on average two jets are resolved, typically one hard jet that carries most of the Z recoil, accompanied by a soft jet. In both cases, the kinematic regions where the NLO fixed-order calculations perform poorly are characterized by average jet multiplicities in excess of the fixed order used in the NLO calculation.

Figures 17(a) and 17(b) replace the fixed-order BLACKHAT+SHERPA estimate for H_T
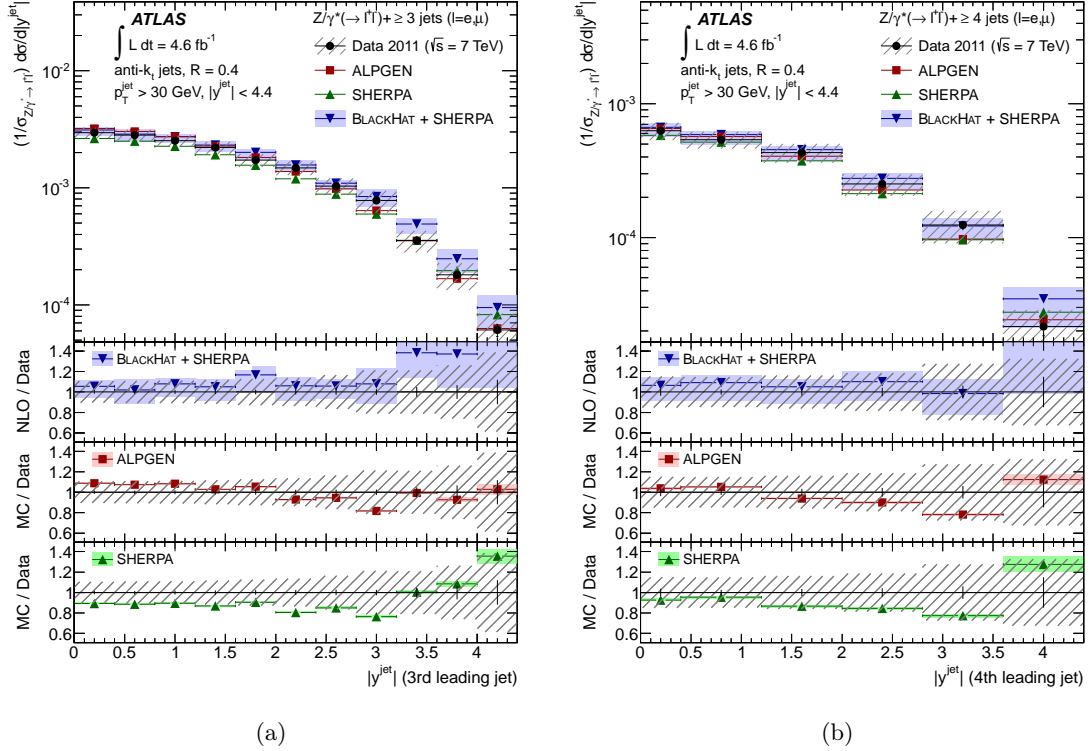
Figure 10. (a) Measured cross section for $Z\,(\to \ell\ell)$ + jets as a function of the absolute value of the rapidity, $|y^{\text{jet}}|$, of the third jet for events with at least three jets with $p_{\text{T}}^{\text{jet}} > 30$ GeV and $|y^{\text{jet}}| < 4.4$ in the final state and (b) as a function of $|y^{\text{jet}}|$ of the fourth jet for events with at least four jets. The cross sections are normalized to the inclusive $Z\,(\to \ell\ell)$ cross section. The other details are as in Figure 2.

and $p_{\text{T}}^{\ell\ell}$ in figures 15 and 8 with the 'exclusive sum' of the cross sections for the first two jets: $(Z\,(+1\text{ jet})) + (Z\,(+ \geq 2\text{ jets}))$. The exclusive sum is consistent with the observed H_{T} and $p_{\text{T}}^{\ell\ell}$ spectra in the phase space considered. These results support the interpretation of the poor performance of the fixed-order calculation for inclusive quantities like H_{T}, S_{T} and $p_{\text{T}}^{\ell\ell}$ as a sign of missing higher jet multiplicities. Agreement with the data can be restored by adding explicitly higher jet multiplicities via exclusive sums.

11 Conclusions

Cross sections for jets produced in association with a Z boson have been measured in proton–proton collisions at $\sqrt{s} = 7$ TeV with 4.6 fb^{-1} of data observed with the ATLAS detector at the LHC, using electron and muon decay modes of the Z boson. The data have been unfolded to the particle level and compared with predictions from the SHERPA generator, from MC@NLO interfaced with HERWIG, from the ALPGEN generator, interfaced with HERWIG, and with fixed-order calculations from BLACKHAT+SHERPA. The cross sections are quoted with respect to a phase-space region defined by Z candidates
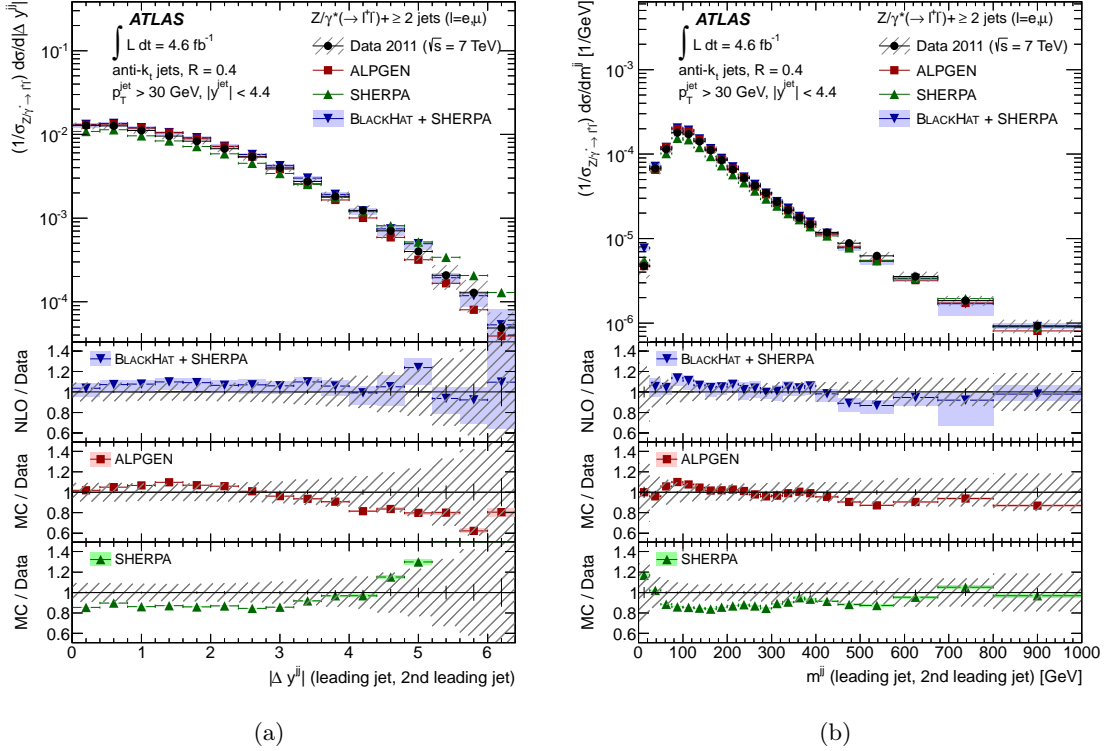
Figure 11. (a) Measured cross section for $Z(\to \ell\ell)$ + jets as a function of the separation in rapidity, $|\Delta y^{jj}|$, between the two leading jets and (b) as a function of the invariant mass of the two leading jets, m^{jj}, for events with at least two jets with $p_T^{\text{jet}} > 30$ GeV and $|y^{\text{jet}}| < 4.4$ in the final state. The cross sections are normalized to the inclusive $Z(\to \ell\ell)$ cross section. The other details are as in Figure 2.

constructed from opposite-sign leptons with $p_T > 20$ GeV, $|\eta| < 2.5$, $\Delta R^{\ell\ell} > 0.2$ and 66 GeV $\leq m^{\ell\ell} \leq 116$ GeV and for jets with $p_T^{\text{jet}} > 30$ GeV, $|y^{\text{jet}}| < 4.4$ and $\Delta R^{\ell j} > 0.5$.

Cross sections as a function of the inclusive and exclusive jet multiplicities and their ratios have been compared, as well as differential cross sections as a function of transverse momenta and rapidity of the jets, angular separation between the leading jets and the inclusive variables H_T and S_T. Compared with previous publications, the sensitivity has been extended to regimes with larger jet multiplicities and larger jet transverse momenta. In addition, the sample has been compared to theory in specific kinematic regions governed by large logarithmic corrections.

In general, the predictions of the matrix element plus parton shower generators and the fixed-order calculations are consistent with the measured values over a large kinematic range. MC@NLO fails to model not only higher jet multiplicities but also the transverse momentum of the leading jet. The transition from staircase to Poisson scaling of the exclusive jet multiplicity ratio, expected from theory when introducing a large scale difference, is observed in the data.

In events where two jets have passed a VBF preselection, the cross sections for higher
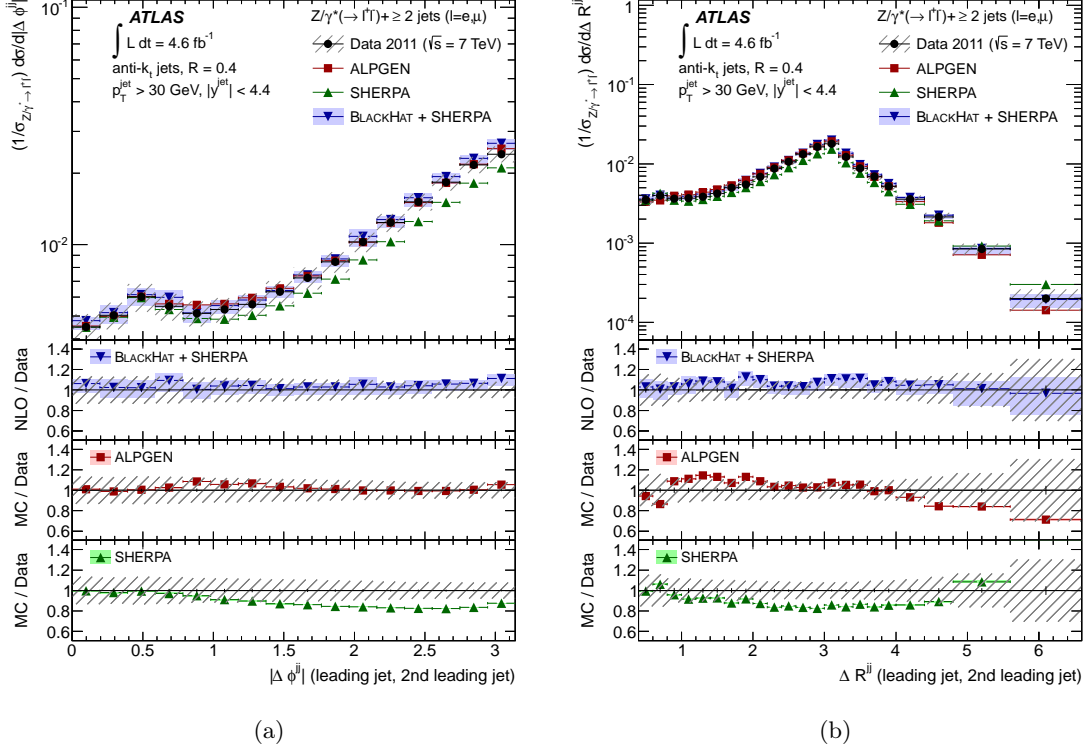
Figure 12. (a) Measured cross section for $Z\,(\rightarrow \ell\ell)$ + jets as a function of the distance in ϕ between the two leading jets, $\Delta\phi^{jj}$, and (b) as a function of the distance ΔR^{jj} between the two leading jets, for events with at least two jets with $p_T^{jet} > 30$ GeV and $|y^{jet}| < 4.4$ in the final state. The cross sections are normalized to the inclusive $Z\,(\rightarrow \ell\ell)$ cross section. The other details are as in Figure 2.

jet multiplicities are overestimated by ALPGEN. This leads to a small underestimation of the probability for Z + jets events to survive a veto on a soft third jet.

ALPGEN predicts a too hard spectrum of the transverse momentum of the leading jet, of $p_T^{\ell\ell}$, H_T and S_T in a regime where large corrections from higher-order electroweak and higher-order QCD processes are expected. The jet rapidity distribution is predicted to be too wide in BLACKHAT+SHERPA and in SHERPA. BLACKHAT+SHERPA underestimates the cross section for large $p_T^{\ell\ell}$ where more than one jet can be resolved. The H_T or S_T spectra predicted by BLACKHAT+SHERPA fixed order NLO calculations deviate by several standard deviations from the measured spectra in the hard H_T and S_T regime characterized by large average jet multiplicities. The observed spectra of H_T and $p_T^{\ell\ell}$ can be described by an exclusive sum of BLACKHAT+SHERPA fixed-order calculations for Z (+1 parton) and Z (+ $\geq$ 2 partons).
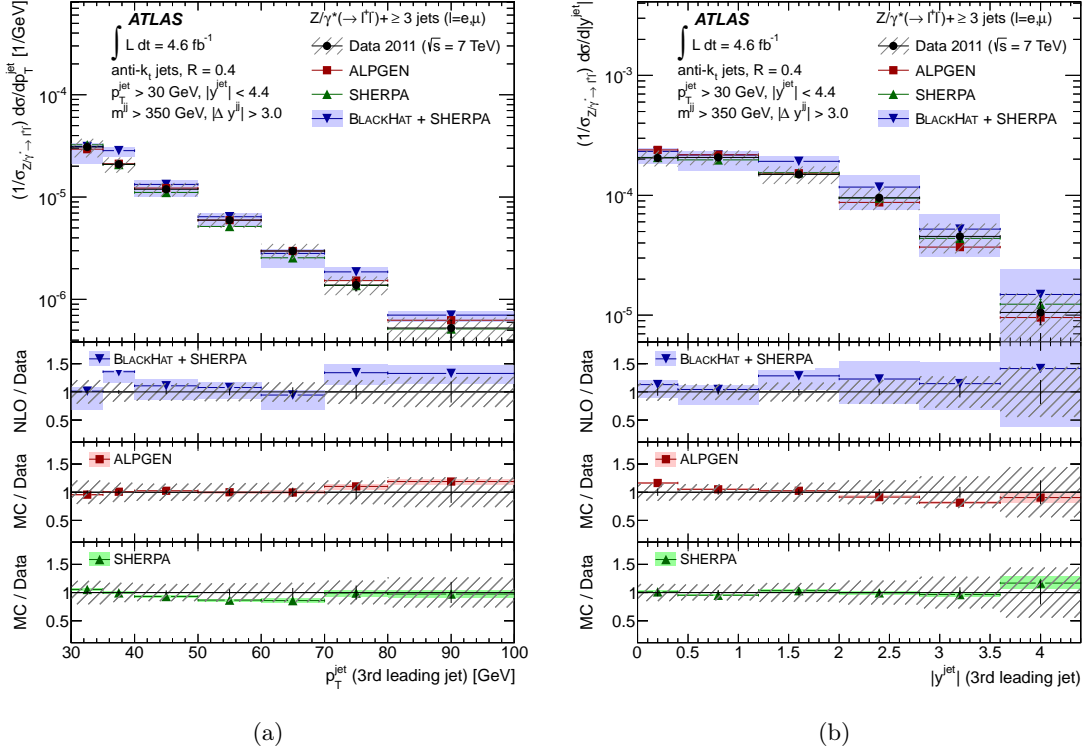
Figure 13. (a) Measured cross section for $Z(\to \ell\ell)$ + jets as a function of the transverse momentum, p_T^{jet}, of the third jet and (b) as a function of the absolute value of the rapidity, $|y^{\text{jet}}|$, of the third jet, in events passing the VBF preselection (at least two jets with $p_T^{\text{jet}} > 30$ GeV and $|y^{\text{jet}}| < 4.4$ and $m^{jj} > 350$ GeV and $|\Delta y^{jj}| > 3.0$ for the two leading jets). The cross sections are normalized to the inclusive $Z(\to \ell\ell)$ cross section. The other details are as in Figure 2.

12   Acknowledgements

Figure 14. Fraction of events that pass a veto on a central ($|\eta| < 2.4$) third jet after VBF preselection (at least two jets with $p_T^{\mathrm{jet}} > 30$ GeV and $|y^{\mathrm{jet}}| < 4.4$, $m^{jj} > 350$ GeV and $|\Delta y^{jj}| > 3.0$ for the two leading jets) as a function of the third jet p_T^{jet} threshold, min p_T^{jet}, (a) in the electron channel and (b) in the muon channel, measured in data and predicted by the generators ALPGEN and SHERPA (see legend for details). The data points indicate the measured distribution after subtraction of electroweak and multi-jet background. The hatched bands correspond to the combined statistical and systematic uncertainty on the Z + jets prediction, using ALPGEN to derive the systematic uncertainties. The error bars on each data point show the combined statistical and systematic uncertainty on the data. The bottom panel shows the MC/data ratio. The shaded band corresponds to the total systematic uncertainty and the error bars to the statistical uncertainty on the MC/data ratio.

Figure 15. (a) Measured cross section for $Z(\to \ell\ell) + \text{jets}$ as a function of the scalar p_T sum of the leptons and the jets, H_T, and (b) as a function of the scalar p_T sum of the jets, S_T, in events with at least one jet with $p_T^{\text{jet}} > 30$ GeV and $|y^{\text{jet}}| < 4.4$ in the final state. The cross sections are normalized to the inclusive $Z(\to \ell\ell)$ cross section. The other details are as in Figure 2.
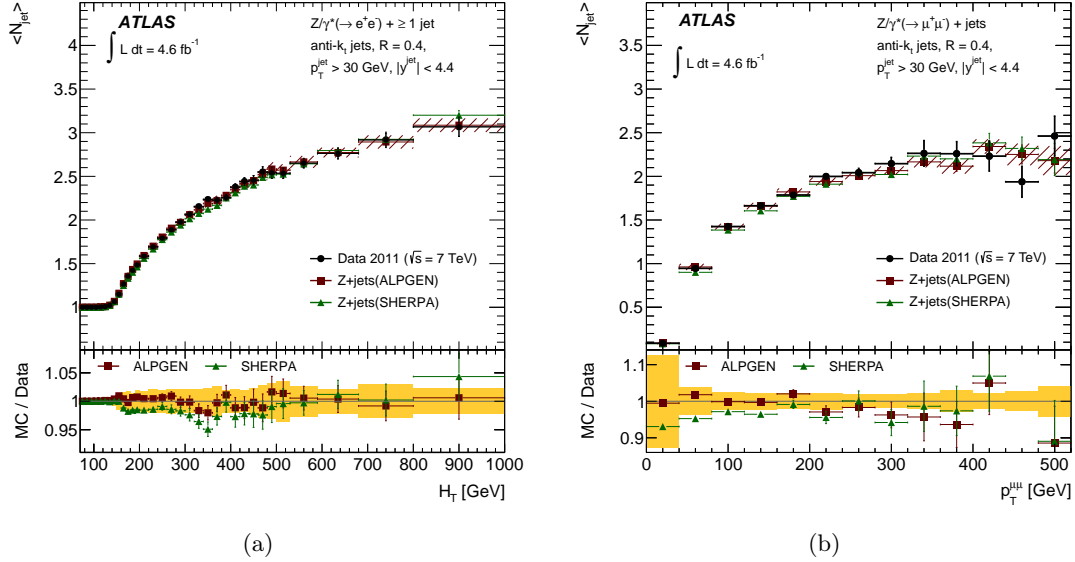
Figure 16. (a) Average number of jets, $<N_{\mathrm{jet}}>$, in $Z\,(\to ee)$ + jets events as a function of the scalar p_{T} sum of the leptons and the jets, H_{T}, and (b) average number of jets in $Z\,(\to \mu\mu)$ + jets events as a function of the transverse momentum of the Z boson candidate, $p_{\mathrm{T}}^{\ell\ell}$, measured in data and predicted by the generators ALPGEN and SHERPA (see legend for details). The data points indicate the measured distribution after subtraction of electroweak and multi-jet background. The hatched band corresponds to the combined statistical and systematic uncertainty on the Z + jets prediction, modelled with ALPGEN. The error bars on each data point show the combined statistical and systematic uncertainty on the data. The bottom panel shows the MC/data ratio. The shaded band corresponds to the total systematic uncertainty and the error bars to the statistical uncertainty on the MC/data ratio.

(a) (b)
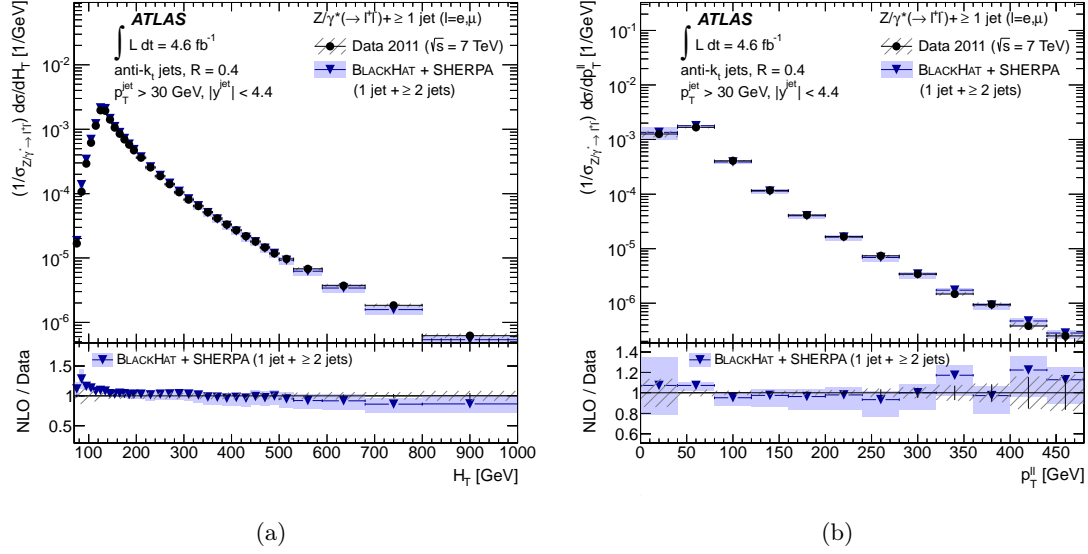
Figure 17. (a) Measured cross section for $Z\,(\to \ell\ell)$ + jets as a function of the scalar p_{T} sum of the leptons and the jets, H_{T}, and (b) as a function of the transverse momentum of the Z candidate, $p_{\mathrm{T}}^{\ell\ell}$, in events with at least one jet with $p_{\mathrm{T}}^{\mathrm{jet}} > 30$ GeV and $|y^{\mathrm{jet}}| < 4.4$ in the final state. The cross sections are normalized to the inclusive $Z\,(\to \ell\ell)$ cross section. The unfolded data are compared to NLO pQCD predictions from BLACKHAT+SHERPA, obtained by adding the exclusive $Z\,(\to \ell\ell)$ + 1 jet and the inclusive $Z\,(\to \ell\ell)$ + ≥ 2 jets calculations and corrected to the particle level. The error bars indicate the statistical uncertainty on the data, and the hatched (shaded) bands the statistical and systematic uncertainties on data (prediction) added in quadrature.

Incl. jet multiplicity	Data cross-section (pb)	δ^{had}	δ^{QED}
≥ 1 jets	$[\,6.88\pm 0.01\,\text{(stat)}\pm 0.52\,\text{(syst)}\pm 0.13\,\text{(lumi)}\,]\times 10^{1}$	1.027 ± 0.015	0.976 ± 0.005
≥ 2 jets	$[\,1.51\pm 0.01\,\text{(stat)}\pm 0.15\,\text{(syst)}\pm 0.03\,\text{(lumi)}\,]\times 10^{1}$	1.036 ± 0.017	0.979 ± 0.005
≥ 3 jets	$3.09\pm 0.03\,\text{(stat)}\pm 0.40\,\text{(syst)}\pm 0.06\,\text{(lumi)}$	1.031 ± 0.033	0.980 ± 0.005
≥ 4 jets	$[\,6.55\pm 0.13\,\text{(stat)}\pm 1.06\,\text{(syst)}\pm 0.12\,\text{(lumi)}\,]\times 10^{-1}$	1.043 ± 0.023	0.982 ± 0.004
≥ 5 jets	$[\,1.35\pm 0.06\,\text{(stat)}\pm 0.27\,\text{(syst)}\pm 0.02\,\text{(lumi)}\,]\times 10^{-1}$		
≥ 6 jets	$[\,2.53\pm 0.27\,\text{(stat)}\pm 0.60\,\text{(syst)}\pm 0.05\,\text{(lumi)}\,]\times 10^{-2}$		
≥ 7 jets	$[\,6.23\pm 1.46\,\text{(stat)}\pm 2.14\,\text{(syst)}\pm 0.11\,\text{(lumi)}\,]\times 10^{-3}$		

Incl. jet multiplicity ratio	Data cross-section ratio	δ^{had}	δ^{QED}
≥ 1 jets $/ \geq 0$ jets	$[\,1.42\pm 0.00\,\text{(stat)}\pm 0.11\,\text{(syst)}\,]\times 10^{-1}$	1.036 ± 0.015	0.995 ± 0.010
≥ 2 jets $/ \geq 1$ jets	$[\,2.18\pm 0.01\,\text{(stat)}\pm 0.07\,\text{(syst)}\,]\times 10^{-1}$	1.009 ± 0.002	1.003 ± 0.010
≥ 3 jets $/ \geq 2$ jets	$[\,2.05\pm 0.02\,\text{(stat)}\pm 0.07\,\text{(syst)}\,]\times 10^{-1}$	0.995 ± 0.016	1.001 ± 0.010
≥ 4 jets $/ \geq 3$ jets	$[\,2.12\pm 0.04\,\text{(stat)}\pm 0.08\,\text{(syst)}\,]\times 10^{-1}$	1.011 ± 0.010	1.001 ± 0.009
≥ 5 jets $/ \geq 4$ jets	$[\,2.06\pm 0.08\,\text{(stat)}\pm 0.10\,\text{(syst)}\,]\times 10^{-1}$		
≥ 6 jets $/ \geq 5$ jets	$[\,1.87\pm 0.18\,\text{(stat)}\pm 0.13\,\text{(syst)}\,]\times 10^{-1}$		
≥ 7 jets $/ \geq 6$ jets	$[\,2.46\pm 0.49\,\text{(stat)}\pm 0.39\,\text{(syst)}\,]\times 10^{-1}$		

Excl. jet multiplicity ratio	Data cross-section ratio	δ^{had}	δ^{QED}
1 jet / 0 jet	$[\,1.29\pm 0.00\,\text{(stat)}\pm 0.10\,\text{(syst)}\,]\times 10^{-1}$	1.032 ± 0.013	0.994 ± 0.010
2 jets / 1 jet	$[\,2.23\pm 0.01\,\text{(stat)}\pm 0.08\,\text{(syst)}\,]\times 10^{-1}$	1.013 ± 0.010	1.003 ± 0.010
3 jets / 2 jets	$[\,2.03\pm 0.02\,\text{(stat)}\pm 0.07\,\text{(syst)}\,]\times 10^{-1}$	0.990 ± 0.032	1.001 ± 0.010
4 jets / 3 jets	$[\,2.14\pm 0.05\,\text{(stat)}\pm 0.08\,\text{(syst)}\,]\times 10^{-1}$	1.022 ± 0.028	1.001 ± 0.009
5 jets / 4 jets	$[\,2.11\pm 0.11\,\text{(stat)}\pm 0.10\,\text{(syst)}\,]\times 10^{-1}$		
6 jets / 5 jets	$[\,1.74\pm 0.22\,\text{(stat)}\pm 0.10\,\text{(syst)}\,]\times 10^{-1}$		
7 jets / 6 jets	$[\,2.60\pm 0.79\,\text{(stat)}\pm 0.45\,\text{(syst)}\,]\times 10^{-1}$		

Excl. jet multiplicity ratio $p_{\mathrm{T}}^{\mathrm{jet}}$ (1st jet) > 150 GeV	Data cross-section ratio	δ^{had}	δ^{QED}
2 jets / 1 jet	$1.04\pm 0.03\,\text{(stat)}\pm 0.03\,\text{(syst)}$	1.004 ± 0.002	1.000 ± 0.009
3 jets / 2 jets	$[\,4.82\pm 0.13\,\text{(stat)}\pm 0.16\,\text{(syst)}\,]\times 10^{-1}$	0.989 ± 0.037	1.002 ± 0.006
4 jets / 3 jets	$[\,3.71\pm 0.17\,\text{(stat)}\pm 0.16\,\text{(syst)}\,]\times 10^{-1}$	1.025 ± 0.040	0.996 ± 0.006
5 jets / 4 jets	$[\,2.85\pm 0.21\,\text{(stat)}\pm 0.12\,\text{(syst)}\,]\times 10^{-1}$		
6 jets / 5 jets	$[\,2.67\pm 0.37\,\text{(stat)}\pm 0.21\,\text{(syst)}\,]\times 10^{-1}$		
7 jets / 6 jets	$[\,2.57\pm 0.78\,\text{(stat)}\pm 0.51\,\text{(syst)}\,]\times 10^{-1}$		

Table 4. Combined inclusive $Z\,(\to \ell\ell)+$ jets cross sections per lepton flavour and their ratios and exclusive cross-section ratios for various preselections measured in data together with the corresponding non-perturbative corrections δ^{had} and δ^{QED}. The cross sections are quoted with respect to a phase-space region defined by Z candidates constructed from opposite-sign leptons with $p_{\mathrm{T}} > 20$ GeV, $|\eta| < 2.5$, $\Delta R^{\ell\ell} > 0.2$ and 66 GeV $\leq m^{\ell\ell} \leq 116$ GeV and for jets with $p_{\mathrm{T}}^{\mathrm{jet}} > 30$ GeV, $|y^{\mathrm{jet}}| < 4.4$ and $\Delta R^{\ell j} > 0.5$.

References

[1] ATLAS Collaboration, *Observation of a New Particle in the Search for the Standard Model Higgs Boson with the ATLAS Detector at the LHC*, Phys. Lett. **B 716** (2012) 001, arXiv:1207.7214 [hep-ex].

[2] CMS Collaboration, *Observation of a new boson at a mass of 125 GeV with the CMS experiment at the LHC*, Phys. Lett. **B 716** (2012) 030, arXiv:1207.7235 [hep-ex].

[3] E. Gerwick, T. Plehn, S. Schumann and P. Schichtel, *Scaling Patterns for QCD Jets*, JHEP **1210** (2012) 162, arXiv:1208.3676 [hep-ph].

[4] M. Rubin, G. P. Salam and S. Sapeta, *Giant QCD K-factors beyond NLO*, JHEP **1009** (2010) 084, arXiv:1006.2144 [hep-ph].

[5] C. F. Berger *et al.*, *An Automated Implementation of On-Shell Methods for One-Loop Amplitudes*, Phys. Rev. **D 78** (2008) 036003, arXiv:0803.4180 [hep-ph].

[6] C. F. Berger *et al.*, *Next-to-Leading Order QCD Predictions for Z, γ^* +3-Jet Distributions at the Tevatron*, Phys. Rev. **D 82** (2010) 074002, arXiv:1004.1659 [hep-ph].

[7] H. Ita *et al.*, *Precise Predictions for $Z + 4$ Jets at Hadron Colliders*, Phys. Rev. **D 85** (2012) 031501, arXiv:1108.2229 [hep-ph].

[8] M. Mangano *et al.*, *ALPGEN, a Generator for Hard Multiparton Processes in Hadronic Collisions*, JHEP **0307** (2003) 001, arXiv:hep-ph/0206293.

[9] T. Gleisberg *et al.*, *Event Generation with SHERPA 1.1*, JHEP **0902** (2009) 007, arXiv:0811.4622 [hep-ph].

[10] S. Hoeche, F. Krauss, M. Schönherr, F. Siegert, *QCD matrix elements + parton showers: The NLO case*, JHEP **1304** (2013) 027, arXiv:1207.5030[hep-ph].

[11] CDF Collaboration, T. Aaltonen *et al.*, *Measurement of Inclusive Jet Cross Sections in $Z/\gamma^*(\to e^+e^-)$ + jets Production in pp Collisions at $\sqrt{s} = 1.96$ TeV*, Phys. Rev. Lett. **100** (2008) 102001, arXiv:0711.3717 [hep-ex].

[12] D0 Collaboration, V. M. Abazov *et al.*, *Measurement of Z/γ^* +jet+X angular distributions in $p\bar{p}$ collisions at $\sqrt{s} = 1.96$ TeV*, Phys. Lett. **B 682** (2010) 370, arXiv:0907.4286 [hep-ex].

[13] D0 Collaboration, V. M. Abazov *et al.*, *Measurement of differential Z/γ^* +jet+X cross sections in $p\bar{p}$ collisions at $\sqrt{s} = 1.96$ TeV*, Phys. Lett. **B 669** (2008) 278, arXiv:0808.1296 [hep-ex].

[14] ATLAS Collaboration, *Measurement of the production cross section for Z/γ^* in association with jets in pp collisions at $\sqrt{s} = 7$ TeV with the ATLAS detector*, Phys. Rev. **D 85** (2012) 032009, arXiv:1111.2690 [hep-ex].

[15] CMS Collaboration, *Jet Production Rates in Association with W and Z Bosons in pp Collisions at $\sqrt{s} = 7$ TeV*, JHEP **1201** (2012) 010, arXiv:1110.3226 [hep-ex].

[16] ATLAS Collaboration, *The ATLAS Experiment at the CERN Large Hadron Collider*, JINST **3** (2008) S08003.

[17] ATLAS Collaboration, *Improved luminosity determination in pp collisions at $\sqrt{s} = 7$ TeV using the ATLAS detector at the LHC*, arXiv:1302.4393 [hep-ex].

[18] G. Corcella *et al.*, *HERWIG 6.5: an Event Generator for Hadron Emission Reactions With Interfering Gluons (including supersymmetric processes)*, *JHEP* **0101** (2001) 010, arXiv:hep-ph/0011363.

[19] J. M. Butterworth, J. R. Forshaw and M. H. Seymour, *Multiparton Interactions in Photoproduction at HERA*, *Z. Phys.* **C 72** (1996) 637, arXiv:hep-ph/9601371.

[20] ATLAS Collaboration, *New ATLAS event generator tunes to 2010 data*, ATL-PHYS-PUB-2011-008, `http://cdsweb.cern.ch/record/1345343`.

[21] T. Sjöstrand, S. Mrenna and P. Z. Skands, *PYTHIA 6.4 Physics and Manual*, *JHEP* **0605**, 026 (2006), arXiv:hep-ph/0603175.

[22] P. Skands, *Tuning Monte Carlo Generators: The Perugia Tunes*, *Phys. Rev.* **D 82** (2010) 074018, arXiv:1005.3457 [hep-ph].

[23] J. Pumplin *et al.*, *New Generation of Parton Distributions with Uncertainties from Global QCD Analysis*, *JHEP* **0207** (2002) 012, arXiv:hep-ph/0201195.

[24] S. Frixione and B. R. Webber, *Matching NLO QCD Computations and Parton Shower Simulations*, *JHEP* **0206** (2002) 029, arXiv:hep-ph/0204244.

[25] H.-L. Lai *et al.*, *New parton distributions for collider physics*, *Phys. Rev.* **D 82** (2010) 074024, arXiv:1007.2241 [hep-ph].

[26] P. Golonka and Z. Wąs, *Next-to-leading Logarithms and the PHOTOS Monte Carlo*, *Eur. Phys. J.* **C 50** (2007) 53, arXiv:hep-ph/0604232.

[27] D. R. Yennie, S. C. Frautschi and H. Suura, *The Infrared Divergence Phenomena and High-energy Processes*, *Ann. Phys.* **13** (1961) 379.

[28] C. Anastasiou, L. Dixon, K. Melnikov and F. Petriello, *High-precision QCD at hadron colliders: electroweak gauge boson rapidity distributions at NNLO*, *Phys. Rev.* **D 69** (2004) 094008, arXiv:hep-ph/0312266.

[29] A. D. Martin, W. J. Stirling, R. S. Thorne and G. Watt, *Parton distributions for the LHC*, *Eur. Phys. J.* **C 63** (2009) 189, arXiv:0901.0002 [hep-ph].

[30] ATLAS Collaboration, *Measurement of the inclusive $W^\pm$ and Z/γ^* cross sections in the electron and muon decay channels in pp collisions at $\sqrt{s} = 7$ TeV with the ATLAS detector*, *Phys. Rev.* **D 85** (2012) 072004, arXiv:1109.5141 [hep-ex].

[31] B. Kersevan and E. Richter-Wąs, *The Monte Carlo Event Generator AcerMC versions 2.0 to 3.8 with interfaces to PYTHIA 6.4, HERWIG 6.5 and ARIADNE 4.1*, Comput. Phys. Commun. **184** (2013) 919, arXiv:hep-ph/0405247.

[32] P. Nason, *A New Method for Combining NLO QCD with Shower Monte Carlo Algorithms*, *JHEP* **0411** (2004) 040, arXiv:hep-ph/0409146.

[33] S. Frixione, P. Nason and C. Oleari, *Matching NLO QCD computations with Parton Shower simulations: the POWHEG method*, *JHEP* **0711** (2007) 070, arXiv:0709.2092 [hep-ph].

[34] S. Agostinelli *et al.*, *GEANT4: A Simulation Toolkit*, *Nucl. Instrum. Meth.* **A 506** (2003) 250.

[35] ATLAS Collaboration, *The ATLAS Simulation Infrastructure*, *Eur. Phys. J.* **C 70** (2010) 823, arXiv:1005.4568 [physics.ins-det].

[36] ATLAS Collaboration, *Electron performance measurements with the ATLAS detector using the 2010 LHC proton–proton collision data*, Eur. Phys. J. **72** (2012) 1909, arXiv:1110.3174 [hep-ex].

[37] ATLAS Collaboration, *Measurement of the $W \to \ell\nu$ and $Z/\gamma^* \to \ell\ell$ production cross sections in proton–proton collisions at $\sqrt{s} = 7$ TeV with the ATLAS detector*, JHEP **1012** (2010) 060, arXiv:1010.2130 [hep-ex].

[38] M. Cacciari, G. P. Salam and G. Soyez, *The anti-k_t jet clustering algorithm*, JHEP **0804** (2008) 063, arXiv:0802.1189 [hep-ph].

[39] ATLAS Collaboration, *Jet energy measurement with the ATLAS detector in proton–proton collisions at $\sqrt{s} = 7$ TeV*, arXiv:1112.6426 [hep-ex].

[40] ATLAS Collaboration, *Jet energy scale and its systematic uncertainty in proton-proton collisions at $\sqrt{s} = 7$ TeV with the ATLAS 2011 data*, ATLAS-CONF-2013-004, http://cds.cern.ch/record/1509552.

[41] G. D'Agostini, *A Multidimensional Unfolding Method Based on Bayes' Theorem*, Nucl. Instrum. Meth. **A 362** (1995) 487.

[42] H1 Collaboration, F. D. Aaron *et al.*, *Measurement of the Inclusive ep Scattering Cross Section at low Q^2 and x at HERA*, Eur. Phys. J. **C 63** 625, arXiv:0904.0929 [hep-ex].

[43] I. W. Stewart and F. J. Tackmann, *Theory Uncertainties for Higgs Mass and other Searches using Jet Bins*, Phys. Rev. **D 85** (2012) 034011, arXiv:1107.2117 [hep-ph].

[44] A complete set of tables with the full results are available at the Durham HepData repository, http://hepdata.cedar.ac.uk.

[45] F. A. Berends *et al.*, *Multi-jet production in W, Z events at $p\bar{p}$ colliders*, Phys. Lett. **B 224** (1989) 237.

[46] A. Denner *et al.*, *Electroweak corrections to dilepton + jet production at hadron colliders*, JHEP **1106** (2011) 069, arXiv:1103.0914 [hep-ph].

[47] ATLAS Collaboration, *Study of jets produced in association with a W boson in pp collisions at $\sqrt{s} = 7$ TeV with the ATLAS detector*, Phys. Rev. **D 85** (2012) 092002, arXiv:1201.1276 [hep-ex].

[48] J. A. Maestre *et al.*, *The SM and NLO Multileg and SM MC Working Groups: Summary Report*, arXiv:1203.6803 [hep-ph].

The ATLAS Collaboration

G. Aad[48], T. Abajyan[21], B. Abbott[111], J. Abdallah[12], S. Abdel Khalek[115],
A.A. Abdelalim[49], O. Abdinov[11], R. Aben[105], B. Abi[112], M. Abolins[88], O.S. AbouZeid[158],
H. Abramowicz[153], H. Abreu[136], Y. Abulaiti[146a,146b], B.S. Acharya[164a,164b,a],
L. Adamczyk[38a], D.L. Adams[25], T.N. Addy[56], J. Adelman[176], S. Adomeit[98], T. Adye[129],
S. Aefsky[23], J.A. Aguilar-Saavedra[124b,b], M. Agustoni[17], S.P. Ahlen[22], F. Ahles[48],
A. Ahmad[148], M. Ahsan[41], G. Aielli[133a,133b], T.P.A. Åkesson[79], G. Akimoto[155],
A.V. Akimov[94], M.A. Alam[76], J. Albert[169], S. Albrand[55], M. Aleksa[30],
I.N. Aleksandrov[64], F. Alessandria[89a], C. Alexa[26a], G. Alexander[153], G. Alexandre[49],
T. Alexopoulos[10], M. Alhroob[164a,164c], M. Aliev[16], G. Alimonti[89a], J. Alison[31],
B.M.M. Allbrooke[18], L.J. Allison[71], P.P. Allport[73], S.E. Allwood-Spiers[53], J. Almond[82],
A. Aloisio[102a,102b], R. Alon[172], A. Alonso[36], F. Alonso[70], A. Altheimer[35],
B. Alvarez Gonzalez[88], M.G. Alviggi[102a,102b], K. Amako[65], C. Amelung[23],
V.V. Ammosov[128,*], S.P. Amor Dos Santos[124a], A. Amorim[124a,c], S. Amoroso[48],
N. Amram[153], C. Anastopoulos[30], L.S. Ancu[17], N. Andari[30], T. Andeen[35],
C.F. Anders[58b], G. Anders[58a], K.J. Anderson[31], A. Andreazza[89a,89b], V. Andrei[58a],
X.S. Anduaga[70], S. Angelidakis[9], P. Anger[44], A. Angerami[35], F. Anghinolfi[30],
A. Anisenkov[107], N. Anjos[124a], A. Annovi[47], A. Antonaki[9], M. Antonelli[47], A. Antonov[96],
J. Antos[144b], F. Anulli[132a], M. Aoki[101], L. Aperio Bella[18], R. Apolle[118,d], G. Arabidze[88],
I. Aracena[143], Y. Arai[65], A.T.H. Arce[45], S. Arfaoui[148], J-F. Arguin[93], S. Argyropoulos[42],
E. Arik[19a,*], M. Arik[19a], A.J. Armbruster[87], O. Arnaez[81], V. Arnal[80], A. Artamonov[95],
G. Artoni[132a,132b], D. Arutinov[21], S. Asai[155], N. Asbah[93], S. Ask[28], B. Åsman[146a,146b],
L. Asquith[6], K. Assamagan[25], R. Astalos[144a], A. Astbury[169], M. Atkinson[165],
B. Auerbach[6], E. Auge[115], K. Augsten[126], M. Aurousseau[145a], G. Avolio[30], D. Axen[168],
G. Azuelos[93,e], Y. Azuma[155], M.A. Baak[30], G. Baccaglioni[89a], C. Bacci[134a,134b],
A.M. Bach[15], H. Bachacou[136], K. Bachas[154], M. Backes[49], M. Backhaus[21],
J. Backus Mayes[143], E. Badescu[26a], P. Bagnaia[132a,132b], Y. Bai[33a], D.C. Bailey[158],
T. Bain[35], J.T. Baines[129], O.K. Baker[176], S. Baker[77], P. Balek[127], F. Balli[136], E. Banas[39],
P. Banerjee[93], Sw. Banerjee[173], D. Banfi[30], A. Bangert[150], V. Bansal[169], H.S. Bansil[18],
L. Barak[172], S.P. Baranov[94], T. Barber[48], E.L. Barberio[86], D. Barberis[50a,50b],
M. Barbero[83], D.Y. Bardin[64], T. Barillari[99], M. Barisonzi[175], T. Barklow[143], N. Barlow[28],
B.M. Barnett[129], R.M. Barnett[15], A. Baroncelli[134a], G. Barone[49], A.J. Barr[118],
F. Barreiro[80], J. Barreiro Guimarães da Costa[57], R. Bartoldus[143], A.E. Barton[71],
V. Bartsch[149], A. Basye[165], R.L. Bates[53], L. Batkova[144a], J.R. Batley[28], A. Battaglia[17],
M. Battistin[30], F. Bauer[136], H.S. Bawa[143,f], S. Beale[98], T. Beau[78], P.H. Beauchemin[161],
R. Beccherle[50a], P. Bechtle[21], H.P. Beck[17], K. Becker[175], S. Becker[98], M. Beckingham[138],
K.H. Becks[175], A.J. Beddall[19c], A. Beddall[19c], S. Bedikian[176], V.A. Bednyakov[64],
C.P. Bee[83], L.J. Beemster[105], T.A. Beermann[175], M. Begel[25], C. Belanger-Champagne[85],
P.J. Bell[49], W.H. Bell[49], G. Bella[153], L. Bellagamba[20a], A. Bellerive[29], M. Bellomo[30],
A. Belloni[57], O. Beloborodova[107,g], K. Belotskiy[96], O. Beltramello[30], O. Benary[153],
D. Benchekroun[135a], K. Bendtz[146a,146b], N. Benekos[165], Y. Benhammou[153],
E. Benhar Noccioli[49], J.A. Benitez Garcia[159b], D.P. Benjamin[45], J.R. Bensinger[23],

K. Benslama[130], S. Bentvelsen[105], D. Berge[30], E. Bergeaas Kuutmann[16], N. Berger[5],
F. Berghaus[169], E. Berglund[105], J. Beringer[15], P. Bernat[77], R. Bernhard[48], C. Bernius[25],
F.U. Bernlochner[169], T. Berry[76], C. Bertella[83], A. Bertin[20a,20b], F. Bertolucci[122a,122b],
M.I. Besana[89a,89b], G.J. Besjes[104], N. Besson[136], S. Bethke[99], W. Bhimji[46],
R.M. Bianchi[30], L. Bianchini[23], M. Bianco[72a,72b], O. Biebel[98], S.P. Bieniek[77],
K. Bierwagen[54], J. Biesiada[15], M. Biglietti[134a], H. Bilokon[47], M. Bindi[20a,20b], S. Binet[115],
A. Bingul[19c], C. Bini[132a,132b], C. Biscarat[178], B. Bittner[99], C.W. Black[150], J.E. Black[143],
K.M. Black[22], R.E. Blair[6], J.-B. Blanchard[136], T. Blazek[144a], I. Bloch[42], C. Blocker[23],
J. Blocki[39], W. Blum[81], U. Blumenschein[54], G.J. Bobbink[105], V.S. Bobrovnikov[107],
S.S. Bocchetta[79], A. Bocci[45], C.R. Boddy[118], M. Boehler[48], J. Boek[175], T.T. Boek[175],
N. Boelaert[36], J.A. Bogaerts[30], A. Bogdanchikov[107], A. Bogouch[90,*], C. Bohm[146a],
J. Bohm[125], V. Boisvert[76], T. Bold[38a], V. Boldea[26a], N.M. Bolnet[136], M. Bomben[78],
M. Bona[75], M. Boonekamp[136], S. Bordoni[78], C. Borer[17], A. Borisov[128], G. Borissov[71],
I. Borjanovic[13a], M. Borri[82], S. Borroni[42], J. Bortfeldt[98], V. Bortolotto[134a,134b], K. Bos[105],
D. Boscherini[20a], M. Bosman[12], H. Boterenbrood[105], J. Bouchami[93], J. Boudreau[123],
E.V. Bouhova-Thacker[71], D. Boumediene[34], C. Bourdarios[115], N. Bousson[83],
S. Boutouil[135d], A. Boveia[31], J. Boyd[30], I.R. Boyko[64], I. Bozovic-Jelisavcic[13b],
J. Bracinik[18], P. Branchini[134a], A. Brandt[8], G. Brandt[118], O. Brandt[54], U. Bratzler[156],
B. Brau[84], J.E. Brau[114], H.M. Braun[175,*], S.F. Brazzale[164a,164c], B. Brelier[158],
J. Bremer[30], K. Brendlinger[120], R. Brenner[166], S. Bressler[172], T.M. Bristow[145b],
D. Britton[53], F.M. Brochu[28], I. Brock[21], R. Brock[88], F. Broggi[89a], C. Bromberg[88],
J. Bronner[99], G. Brooijmans[35], T. Brooks[76], W.K. Brooks[32b], G. Brown[82],
P.A. Bruckman de Renstrom[39], D. Bruncko[144b], R. Bruneliere[48], S. Brunet[60], A. Bruni[20a],
G. Bruni[20a], M. Bruschi[20a], L. Bryngemark[79], T. Buanes[14], Q. Buat[55], F. Bucci[49],
J. Buchanan[118], P. Buchholz[141], R.M. Buckingham[118], A.G. Buckley[46], S.I. Buda[26a],
I.A. Budagov[64], B. Budick[108], L. Bugge[117], O. Bulekov[96], A.C. Bundock[73], M. Bunse[43],
T. Buran[117,*], H. Burckhart[30], S. Burdin[73], T. Burgess[14], S. Burke[129], E. Busato[34],
V. Büscher[81], P. Bussey[53], C.P. Buszello[166], B. Butler[57], J.M. Butler[22], C.M. Buttar[53],
J.M. Butterworth[77], W. Buttinger[28], M. Byszewski[30], S. Cabrera Urbán[167],
D. Caforio[20a,20b], O. Cakir[4a], P. Calafiura[15], G. Calderini[78], P. Calfayan[98], R. Calkins[106],
L.P. Caloba[24a], R. Caloi[132a,132b], D. Calvet[34], S. Calvet[34], R. Camacho Toro[49],
P. Camarri[133a,133b], D. Cameron[117], L.M. Caminada[15], R. Caminal Armadans[12],
S. Campana[30], M. Campanelli[77], V. Canale[102a,102b], F. Canelli[31], A. Canepa[159a],
J. Cantero[80], R. Cantrill[76], T. Cao[40], M.D.M. Capeans Garrido[30], I. Caprini[26a],
M. Caprini[26a], D. Capriotti[99], M. Capua[37a,37b], R. Caputo[81], R. Cardarelli[133a], T. Carli[30],
G. Carlino[102a], L. Carminati[89a,89b], S. Caron[104], E. Carquin[32b],
G.D. Carrillo-Montoya[145b], A.A. Carter[75], J.R. Carter[28], J. Carvalho[124a,h], D. Casadei[108],
M.P. Casado[12], M. Cascella[122a,122b], C. Caso[50a,50b,*], E. Castaneda-Miranda[173],
A. Castelli[105], V. Castillo Gimenez[167], N.F. Castro[124a], G. Cataldi[72a], P. Catastini[57],
A. Catinaccio[30], J.R. Catmore[30], A. Cattai[30], G. Cattani[133a,133b], S. Caughron[88],
V. Cavaliere[165], P. Cavalleri[78], D. Cavalli[89a], M. Cavalli-Sforza[12], V. Cavasinni[122a,122b],
F. Ceradini[134a,134b], B. Cerio[45], A.S. Cerqueira[24b], A. Cerri[15], L. Cerrito[75], F. Cerutti[15],
A. Cervelli[17], S.A. Cetin[19b], A. Chafaq[135a], D. Chakraborty[106], I. Chalupkova[127],

K. Chan[3], P. Chang[165], B. Chapleau[85], J.D. Chapman[28], J.W. Chapman[87],
D.G. Charlton[18], V. Chavda[82], C.A. Chavez Barajas[30], S. Cheatham[85], S. Chekanov[6],
S.V. Chekulaev[159a], G.A. Chelkov[64], M.A. Chelstowska[104], C. Chen[63], H. Chen[25],
S. Chen[33c], X. Chen[173], Y. Chen[35], Y. Cheng[31], A. Cheplakov[64],
R. Cherkaoui El Moursli[135e], V. Chernyatin[25], E. Cheu[7], S.L. Cheung[158], L. Chevalier[136],
V. Chiarella[47], G. Chiefari[102a,102b], J.T. Childers[30], A. Chilingarov[71], G. Chiodini[72a],
A.S. Chisholm[18], R.T. Chislett[77], A. Chitan[26a], M.V. Chizhov[64], G. Choudalakis[31],
S. Chouridou[9], B.K.B. Chow[98], I.A. Christidi[77], A. Christov[48], D. Chromek-Burckhart[30],
M.L. Chu[151], J. Chudoba[125], G. Ciapetti[132a,132b], A.K. Ciftci[4a], R. Ciftci[4a], D. Cinca[62],
V. Cindro[74], A. Ciocio[15], M. Cirilli[87], P. Cirkovic[13b], Z.H. Citron[172], M. Citterio[89a],
M. Ciubancan[26a], A. Clark[49], P.J. Clark[46], R.N. Clarke[15], J.C. Clemens[83], B. Clement[55],
C. Clement[146a,146b], Y. Coadou[83], M. Cobal[164a,164c], A. Coccaro[138], J. Cochran[63],
L. Coffey[23], J.G. Cogan[143], J. Coggeshall[165], J. Colas[5], S. Cole[106], A.P. Colijn[105],
N.J. Collins[18], C. Collins-Tooth[53], J. Collot[55], T. Colombo[119a,119b], G. Colon[84],
G. Compostella[99], P. Conde Muiño[124a], E. Coniavitis[166], M.C. Conidi[12],
S.M. Consonni[89a,89b], V. Consorti[48], S. Constantinescu[26a], C. Conta[119a,119b], G. Conti[57],
F. Conventi[102a,i], M. Cooke[15], B.D. Cooper[77], A.M. Cooper-Sarkar[118],
N.J. Cooper-Smith[76], K. Copic[15], T. Cornelissen[175], M. Corradi[20a], F. Corriveau[85,j],
A. Corso-Radu[163], A. Cortes-Gonzalez[165], G. Cortiana[99], G. Costa[89a], M.J. Costa[167],
D. Costanzo[139], D. Côté[30], G. Cottin[32a], L. Courneyea[169], G. Cowan[76], B.E. Cox[82],
K. Cranmer[108], S. Crépé-Renaudin[55], F. Crescioli[78], M. Cristinziani[21], G. Crosetti[37a,37b],
C.-M. Cuciuc[26a], C. Cuenca Almenar[176], T. Cuhadar Donszelmann[139], J. Cummings[176],
M. Curatolo[47], C.J. Curtis[18], C. Cuthbert[150], H. Czirr[141], P. Czodrowski[44],
Z. Czyczula[176], S. D'Auria[53], M. D'Onofrio[73], A. D'Orazio[132a,132b],
M.J. Da Cunha Sargedas De Sousa[124a], C. Da Via[82], W. Dabrowski[38a], A. Dafinca[118],
T. Dai[87], F. Dallaire[93], C. Dallapiccola[84], M. Dam[36], D.S. Damiani[137], A.C. Daniells[18],
H.O. Danielsson[30], V. Dao[104], G. Darbo[50a], G.L. Darlea[26b], S, Darmora[8],
J.A. Dassoulas[42], W. Davey[21], T. Davidek[127], N. Davidson[86], E. Davies[118,d], M. Davies[93],
O. Davignon[78], A.R. Davison[77], Y. Davygora[58a], E. Dawe[142], I. Dawson[139],
R.K. Daya-Ishmukhametova[23], K. De[8], R. de Asmundis[102a], S. De Castro[20a,20b],
S. De Cecco[78], J. de Graat[98], N. De Groot[104], P. de Jong[105], C. De La Taille[115],
H. De la Torre[80], F. De Lorenzi[63], L. De Nooij[105], D. De Pedis[132a], A. De Salvo[132a],
U. De Sanctis[164a,164c], A. De Santo[149], J.B. De Vivie De Regie[115], G. De Zorzi[132a,132b],
W.J. Dearnaley[71], R. Debbe[25], C. Debenedetti[46], B. Dechenaux[55], D.V. Dedovich[64],
J. Degenhardt[120], J. Del Peso[80], T. Del Prete[122a,122b], T. Delemontex[55],
M. Deliyergiyev[74], A. Dell'Acqua[30], L. Dell'Asta[22], M. Della Pietra[102a,i],
D. della Volpe[102a,102b], M. Delmastro[5], P.A. Delsart[55], C. Deluca[105], S. Demers[176],
M. Demichev[64], B. Demirkoz[12,k], S.P. Denisov[128], D. Derendarz[39], J.E. Derkaoui[135d],
F. Derue[78], P. Dervan[73], K. Desch[21], P.O. Deviveiros[105], A. Dewhurst[129], B. DeWilde[148],
S. Dhaliwal[105], R. Dhullipudi[25,l], A. Di Ciaccio[133a,133b], L. Di Ciaccio[5],
C. Di Donato[102a,102b], A. Di Girolamo[30], B. Di Girolamo[30], S. Di Luise[134a,134b],
A. Di Mattia[152], B. Di Micco[30], R. Di Nardo[47], A. Di Simone[133a,133b], R. Di Sipio[20a,20b],
M.A. Diaz[32a], E.B. Diehl[87], J. Dietrich[42], T.A. Dietzsch[58a], S. Diglio[86],

K. Dindar Yagci[40], J. Dingfelder[21], F. Dinut[26a], C. Dionisi[132a,132b], P. Dita[26a], S. Dita[26a],
F. Dittus[30], F. Djama[83], T. Djobava[51b], M.A.B. do Vale[24c], A. Do Valle Wemans[124a,m],
T.K.O. Doan[5], D. Dobos[30], E. Dobson[77], J. Dodd[35], C. Doglioni[49], T. Doherty[53],
T. Dohmae[155], Y. Doi[65,*], J. Dolejsi[127], Z. Dolezal[127], B.A. Dolgoshein[96,*],
M. Donadelli[24d], J. Donini[34], J. Dopke[30], A. Doria[102a], A. Dos Anjos[173], A. Dotti[122a,122b],
M.T. Dova[70], A.T. Doyle[53], M. Dris[10], J. Dubbert[87], S. Dube[15], E. Dubreuil[34],
E. Duchovni[172], G. Duckeck[98], D. Duda[175], A. Dudarev[30], F. Dudziak[63], L. Duflot[115],
M-A. Dufour[85], L. Duguid[76], M. Dührssen[30], M. Dunford[58a], H. Duran Yildiz[4a],
M. Düren[52], R. Duxfield[139], M. Dwuznik[38a], W.L. Ebenstein[45], J. Ebke[98], S. Eckweiler[81],
W. Edson[2], C.A. Edwards[76], N.C. Edwards[53], W. Ehrenfeld[21], T. Eifert[143], G. Eigen[14],
K. Einsweiler[15], E. Eisenhandler[75], T. Ekelof[166], M. El Kacimi[135c], M. Ellert[166], S. Elles[5],
F. Ellinghaus[81], K. Ellis[75], N. Ellis[30], J. Elmsheuser[98], M. Elsing[30], D. Emeliyanov[129],
Y. Enari[155], O.C. Endner[81], R. Engelmann[148], A. Engl[98], B. Epp[61], J. Erdmann[176],
A. Ereditato[17], D. Eriksson[146a], J. Ernst[2], M. Ernst[25], J. Ernwein[136], D. Errede[165],
S. Errede[165], E. Ertel[81], M. Escalier[115], H. Esch[43], C. Escobar[123], X. Espinal Curull[12],
B. Esposito[47], F. Etienne[83], A.I. Etienvre[136], E. Etzion[153], D. Evangelakou[54], H. Evans[60],
L. Fabbri[20a,20b], C. Fabre[30], G. Facini[30], R.M. Fakhrutdinov[128], S. Falciano[132a],
Y. Fang[33a], M. Fanti[89a,89b], A. Farbin[8], A. Farilla[134a], J. Farley[148], T. Farooque[158],
S. Farrell[163], S.M. Farrington[170], P. Farthouat[30], F. Fassi[167], P. Fassnacht[30],
D. Fassouliotis[9], B. Fatholahzadeh[158], A. Favareto[89a,89b], L. Fayard[115], P. Federic[144a],
O.L. Fedin[121], W. Fedorko[168], M. Fehling-Kaschek[48], L. Feligioni[83], C. Feng[33d],
E.J. Feng[6], H. Feng[87], A.B. Fenyuk[128], J. Ferencei[144b], W. Fernando[6], S. Ferrag[53],
J. Ferrando[53], V. Ferrara[42], A. Ferrari[166], P. Ferrari[105], R. Ferrari[119a],
D.E. Ferreira de Lima[53], A. Ferrer[167], D. Ferrere[49], C. Ferretti[87],
A. Ferretto Parodi[50a,50b], M. Fiascaris[31], F. Fiedler[81], A. Filipčič[74], F. Filthaut[104],
M. Fincke-Keeler[169], K.D. Finelli[45], M.C.N. Fiolhais[124a,h], L. Fiorini[167], A. Firan[40],
J. Fischer[175], M.J. Fisher[109], E.A. Fitzgerald[23], M. Flechl[48], I. Fleck[141],
P. Fleischmann[174], S. Fleischmann[175], G.T. Fletcher[139], G. Fletcher[75], T. Flick[175],
A. Floderus[79], L.R. Flores Castillo[173], A.C. Florez Bustos[159b], M.J. Flowerdew[99],
T. Fonseca Martin[17], A. Formica[136], A. Forti[82], D. Fortin[159a], D. Fournier[115],
A.J. Fowler[45], H. Fox[71], P. Francavilla[12], M. Franchini[20a,20b], S. Franchino[30], D. Francis[30],
M. Franklin[57], S. Franz[30], M. Fraternali[119a,119b], S. Fratina[120], S.T. French[28],
C. Friedrich[42], F. Friedrich[44], D. Froidevaux[30], J.A. Frost[28], C. Fukunaga[156],
E. Fullana Torregrosa[127], B.G. Fulsom[143], J. Fuster[167], C. Gabaldon[30], O. Gabizon[172],
A. Gabrielli[132a,132b], S. Gadatsch[105], T. Gadfort[25], S. Gadomski[49], G. Gagliardi[50a,50b],
P. Gagnon[60], C. Galea[98], B. Galhardo[124a], E.J. Gallas[118], V. Gallo[17], B.J. Gallop[129],
P. Gallus[126], K.K. Gan[109], R.P. Gandrajula[62], Y.S. Gao[143,f], A. Gaponenko[15],
F.M. Garay Walls[46], F. Garberson[176], C. García[167], J.E. García Navarro[167],
M. Garcia-Sciveres[15], R.W. Gardner[31], N. Garelli[143], V. Garonne[30], C. Gatti[47],
G. Gaudio[119a], B. Gaur[141], L. Gauthier[93], P. Gauzzi[132a,132b], I.L. Gavrilenko[94], C. Gay[168],
G. Gaycken[21], E.N. Gazis[10], P. Ge[33d,n], Z. Gecse[168], C.N.P. Gee[129], D.A.A. Geerts[105],
Ch. Geich-Gimbel[21], K. Gellerstedt[146a,146b], C. Gemme[50a], A. Gemmell[53], M.H. Genest[55],
S. Gentile[132a,132b], M. George[54], S. George[76], D. Gerbaudo[163], P. Gerlach[175],

A. Gershon[153], C. Geweniger[58a], H. Ghazlane[135b], N. Ghodbane[34], B. Giacobbe[20a],
S. Giagu[132a,132b], V. Giangiobbe[12], F. Gianotti[30], B. Gibbard[25], A. Gibson[158],
S.M. Gibson[30], M. Gilchriese[15], T.P.S. Gillam[28], D. Gillberg[30], A.R. Gillman[129],
D.M. Gingrich[3,e], N. Giokaris[9], M.P. Giordani[164c], R. Giordano[102a,102b], F.M. Giorgi[16],
P. Giovannini[99], P.F. Giraud[136], D. Giugni[89a], C. Giuliani[48], M. Giunta[93],
B.K. Gjelsten[117], L.K. Gladilin[97], C. Glasman[80], J. Glatzer[21], A. Glazov[42], G.L. Glonti[64],
J.R. Goddard[75], J. Godfrey[142], J. Godlewski[30], M. Goebel[42], C. Goeringer[81],
S. Goldfarb[87], T. Golling[176], D. Golubkov[128], A. Gomes[124a,c], L.S. Gomez Fajardo[42],
R. Gonçalo[76], J. Goncalves Pinto Firmino Da Costa[42], L. Gonella[21], S. González de la
Hoz[167], G. Gonzalez Parra[12], M.L. Gonzalez Silva[27], S. Gonzalez-Sevilla[49],
J.J. Goodson[148], L. Goossens[30], T. Göpfert[44], P.A. Gorbounov[95], H.A. Gordon[25],
I. Gorelov[103], G. Gorfine[175], B. Gorini[30], E. Gorini[72a,72b], A. Gorišek[74], E. Gornicki[39],
A.T. Goshaw[6], C. Gössling[43], M.I. Gostkin[64], I. Gough Eschrich[163], M. Gouighri[135a],
D. Goujdami[135c], M.P. Goulette[49], A.G. Goussiou[138], C. Goy[5], S. Gozpinar[23],
L. Graber[54], I. Grabowska-Bold[38a], P. Grafström[20a,20b], K-J. Grahn[42], E. Gramstad[117],
F. Grancagnolo[72a], S. Grancagnolo[16], V. Grassi[148], V. Gratchev[121], H.M. Gray[30],
J.A. Gray[148], E. Graziani[134a], O.G. Grebenyuk[121], T. Greenshaw[73], Z.D. Greenwood[25,l],
K. Gregersen[36], I.M. Gregor[42], P. Grenier[143], J. Griffiths[8], N. Grigalashvili[64],
A.A. Grillo[137], K. Grimm[71], S. Grinstein[12], Ph. Gris[34], Y.V. Grishkevich[97],
J.-F. Grivaz[115], J.P. Grohs[44], A. Grohsjean[42], E. Gross[172], J. Grosse-Knetter[54],
J. Groth-Jensen[172], K. Grybel[141], D. Guest[176], O. Gueta[153], C. Guicheney[34],
E. Guido[50a,50b], T. Guillemin[115], S. Guindon[2], U. Gul[53], J. Gunther[126], B. Guo[158],
J. Guo[35], P. Gutierrez[111], N. Guttman[153], O. Gutzwiller[173], C. Guyot[136], C. Gwenlan[118],
C.B. Gwilliam[73], A. Haas[108], S. Haas[30], C. Haber[15], H.K. Hadavand[8], P. Haefner[21],
Z. Hajduk[39], H. Hakobyan[177], D. Hall[118], G. Halladjian[62], K. Hamacher[175], P. Hamal[113],
K. Hamano[86], M. Hamer[54], A. Hamilton[145b,o], S. Hamilton[161], L. Han[33b], K. Hanagaki[116],
K. Hanawa[160], M. Hance[15], C. Handel[81], P. Hanke[58a], J.R. Hansen[36], J.B. Hansen[36],
J.D. Hansen[36], P.H. Hansen[36], P. Hansson[143], K. Hara[160], A.S. Hard[173], T. Harenberg[175],
S. Harkusha[90], D. Harper[87], R.D. Harrington[46], O.M. Harris[138], J. Hartert[48],
F. Hartjes[105], T. Haruyama[65], A. Harvey[56], S. Hasegawa[101], Y. Hasegawa[140],
S. Hassani[136], S. Haug[17], M. Hauschild[30], R. Hauser[88], M. Havranek[21], C.M. Hawkes[18],
R.J. Hawkings[30], A.D. Hawkins[79], T. Hayakawa[66], T. Hayashi[160], D. Hayden[76],
C.P. Hays[118], H.S. Hayward[73], S.J. Haywood[129], S.J. Head[18], T. Heck[81], V. Hedberg[79],
L. Heelan[8], S. Heim[120], B. Heinemann[15], S. Heisterkamp[36], L. Helary[22], C. Heller[98],
M. Heller[30], S. Hellman[146a,146b], D. Hellmich[21], C. Helsens[12], J. Henderson[118],
R.C.W. Henderson[71], M. Henke[58a], A. Henrichs[176], A.M. Henriques Correia[30],
S. Henrot-Versille[115], C. Hensel[54], G.H. Herbert[16], C.M. Hernandez[8], Y. Hernández
Jiménez[167], R. Herrberg[16], G. Herten[48], R. Hertenberger[98], L. Hervas[30], G.G. Hesketh[77],
N.P. Hessey[105], R. Hickling[75], E. Higón-Rodriguez[167], J.C. Hill[28], K.H. Hiller[42],
S. Hillert[21], S.J. Hillier[18], I. Hinchliffe[15], E. Hines[120], M. Hirose[116], D. Hirschbuehl[175],
J. Hobbs[148], N. Hod[105], M.C. Hodgkinson[139], P. Hodgson[139], A. Hoecker[30],
M.R. Hoeferkamp[103], J. Hoffman[40], D. Hoffmann[83], J.I. Hofmann[58a], M. Hohlfeld[81],
S.O. Holmgren[146a], J.L. Holzbauer[88], T.M. Hong[120], L. Hooft van Huysduynen[108],

J-Y. Hostachy[55], S. Hou[151], A. Hoummada[135a], J. Howard[118], J. Howarth[82],
M. Hrabovsky[113], I. Hristova[16], J. Hrivnac[115], T. Hryn'ova[5], P.J. Hsu[81], S.-C. Hsu[138],
D. Hu[35], Z. Hubacek[30], F. Hubaut[83], F. Huegging[21], A. Huettmann[42], T.B. Huffman[118],
E.W. Hughes[35], G. Hughes[71], M. Huhtinen[30], T.A. Hülsing[81], M. Hurwitz[15],
N. Huseynov[64,p], J. Huston[88], J. Huth[57], G. Iacobucci[49], G. Iakovidis[10], I. Ibragimov[141],
L. Iconomidou-Fayard[115], J. Idarraga[115], P. Iengo[102a], O. Igonkina[105], Y. Ikegami[65],
K. Ikematsu[141], M. Ikeno[65], D. Iliadis[154], N. Ilic[158], T. Ince[99], P. Ioannou[9], M. Iodice[134a],
K. Iordanidou[9], V. Ippolito[132a,132b], A. Irles Quiles[167], C. Isaksson[166], M. Ishino[67],
M. Ishitsuka[157], R. Ishmukhametov[109], C. Issever[118], S. Istin[19a], A.V. Ivashin[128],
W. Iwanski[39], H. Iwasaki[65], J.M. Izen[41], V. Izzo[102a], B. Jackson[120], J.N. Jackson[73],
P. Jackson[1], M.R. Jaekel[30], V. Jain[2], K. Jakobs[48], S. Jakobsen[36], T. Jakoubek[125],
J. Jakubek[126], D.O. Jamin[151], D.K. Jana[111], E. Jansen[77], H. Jansen[30], J. Janssen[21],
A. Jantsch[99], M. Janus[48], R.C. Jared[173], G. Jarlskog[79], L. Jeanty[57], G.-Y. Jeng[150],
I. Jen-La Plante[31], D. Jennens[86], P. Jenni[30], C. Jeske[170], P. Jež[36], S. Jézéquel[5],
M.K. Jha[20a], H. Ji[173], W. Ji[81], J. Jia[148], Y. Jiang[33b], M. Jimenez Belenguer[42], S. Jin[33a],
O. Jinnouchi[157], M.D. Joergensen[36], D. Joffe[40], M. Johansen[146a,146b], K.E. Johansson[146a],
P. Johansson[139], S. Johnert[42], K.A. Johns[7], K. Jon-And[146a,146b], G. Jones[170],
R.W.L. Jones[71], T.J. Jones[73], C. Joram[30], P.M. Jorge[124a], K.D. Joshi[82], J. Jovicevic[147],
T. Jovin[13b], X. Ju[173], C.A. Jung[43], R.M. Jungst[30], P. Jussel[61], A. Juste Rozas[12],
S. Kabana[17], M. Kaci[167], A. Kaczmarska[39], P. Kadlecik[36], M. Kado[115], H. Kagan[109],
M. Kagan[57], E. Kajomovitz[152], S. Kalinin[175], S. Kama[40], N. Kanaya[155], M. Kaneda[30],
S. Kaneti[28], T. Kanno[157], V.A. Kantserov[96], J. Kanzaki[65], B. Kaplan[108], A. Kapliy[31],
D. Kar[53], M. Karagounis[21], K. Karakostas[10], M. Karnevskiy[81], V. Kartvelishvili[71],
A.N. Karyukhin[128], L. Kashif[173], G. Kasieczka[58b], R.D. Kass[109], A. Kastanas[14],
Y. Kataoka[155], J. Katzy[42], V. Kaushik[7], K. Kawagoe[69], T. Kawamoto[155],
G. Kawamura[54], S. Kazama[155], V.F. Kazanin[107], M.Y. Kazarinov[64], R. Keeler[169],
P.T. Keener[120], R. Kehoe[40], M. Keil[54], J.S. Keller[138], H. Keoshkerian[5], O. Kepka[125],
B.P. Kerševan[74], S. Kersten[175], K. Kessoku[155], J. Keung[158], F. Khalil-zada[11],
H. Khandanyan[146a,146b], A. Khanov[112], D. Kharchenko[64], A. Khodinov[96], A. Khomich[58a],
T.J. Khoo[28], G. Khoriauli[21], A. Khoroshilov[175], V. Khovanskiy[95], E. Khramov[64],
J. Khubua[51b], H. Kim[146a,146b], S.H. Kim[160], N. Kimura[171], O. Kind[16], B.T. King[73],
M. King[66], R.S.B. King[118], S.B. King[168], J. Kirk[129], A.E. Kiryunin[99], T. Kishimoto[66],
D. Kisielewska[38a], T. Kitamura[66], T. Kittelmann[123], K. Kiuchi[160], E. Kladiva[144b],
M. Klein[73], U. Klein[73], K. Kleinknecht[81], M. Klemetti[85], A. Klier[172], P. Klimek[146a,146b],
A. Klimentov[25], R. Klingenberg[43], J.A. Klinger[82], E.B. Klinkby[36], T. Klioutchnikova[30],
P.F. Klok[104], S. Klous[105], E.-E. Kluge[58a], P. Kluit[105], S. Kluth[99], E. Kneringer[61],
E.B.F.G. Knoops[83], A. Knue[54], B.R. Ko[45], T. Kobayashi[155], M. Kobel[44], M. Kocian[143],
P. Kodys[127], S. Koenig[81], F. Koetsveld[104], P. Koevesarki[21], T. Koffas[29], E. Koffeman[105],
L.A. Kogan[118], S. Kohlmann[175], F. Kohn[54], Z. Kohout[126], T. Kohriki[65], T. Koi[143],
H. Kolanoski[16], I. Koletsou[89a], J. Koll[88], A.A. Komar[94], Y. Komori[155], T. Kondo[65],
K. Köneke[30], A.C. König[104], T. Kono[42,q], A.I. Kononov[48], R. Konoplich[108,r],
N. Konstantinidis[77], R. Kopeliansky[152], S. Koperny[38a], L. Köpke[81], A.K. Kopp[48],
K. Korcyl[39], K. Kordas[154], A. Korn[46], A. Korol[107], I. Korolkov[12], E.V. Korolkova[139],

V.A. Korotkov[128], O. Kortner[99], S. Kortner[99], V.V. Kostyukhin[21], S. Kotov[99],
V.M. Kotov[64], A. Kotwal[45], C. Kourkoumelis[9], V. Kouskoura[154], A. Koutsman[159a],
R. Kowalewski[169], T.Z. Kowalski[38a], W. Kozanecki[136], A.S. Kozhin[128], V. Kral[126],
V.A. Kramarenko[97], G. Kramberger[74], M.W. Krasny[78], A. Krasznahorkay[108],
J.K. Kraus[21], A. Kravchenko[25], S. Kreiss[108], J. Kretzschmar[73], K. Kreutzfeldt[52],
N. Krieger[54], P. Krieger[158], K. Kroeninger[54], H. Kroha[99], J. Kroll[120], J. Kroseberg[21],
J. Krstic[13a], U. Kruchonak[64], H. Krüger[21], T. Kruker[17], N. Krumnack[63],
Z.V. Krumshteyn[64], M.K. Kruse[45], T. Kubota[86], S. Kuday[4a], S. Kuehn[48], A. Kugel[58c],
T. Kuhl[42], V. Kukhtin[64], Y. Kulchitsky[90], S. Kuleshov[32b], M. Kuna[78], J. Kunkle[120],
A. Kupco[125], H. Kurashige[66], M. Kurata[160], Y.A. Kurochkin[90], V. Kus[125],
E.S. Kuwertz[147], M. Kuze[157], J. Kvita[142], R. Kwee[16], A. La Rosa[49], L. La Rotonda[37a,37b],
L. Labarga[80], S. Lablak[135a], C. Lacasta[167], F. Lacava[132a,132b], J. Lacey[29], H. Lacker[16],
D. Lacour[78], V.R. Lacuesta[167], E. Ladygin[64], R. Lafaye[5], B. Laforge[78], T. Lagouri[176],
S. Lai[48], H. Laier[58a], E. Laisne[55], L. Lambourne[77], C.L. Lampen[7], W. Lampl[7],
E. Lançon[136], U. Landgraf[48], M.P.J. Landon[75], V.S. Lang[58a], C. Lange[42],
A.J. Lankford[163], F. Lanni[25], K. Lantzsch[30], A. Lanza[119a], S. Laplace[78], C. Lapoire[21],
J.F. Laporte[136], T. Lari[89a], A. Larner[118], M. Lassnig[30], P. Laurelli[47], V. Lavorini[37a,37b],
W. Lavrijsen[15], P. Laycock[73], O. Le Dortz[78], E. Le Guirriec[83], E. Le Menedeu[12],
T. LeCompte[6], F. Ledroit-Guillon[55], H. Lee[105], J.S.H. Lee[116], S.C. Lee[151], L. Lee[176],
M. Lefebvre[169], M. Legendre[136], F. Legger[98], C. Leggett[15], M. Lehmacher[21],
G. Lehmann Miotto[30], A.G. Leister[176], M.A.L. Leite[24d], R. Leitner[127], D. Lellouch[172],
B. Lemmer[54], V. Lendermann[58a], K.J.C. Leney[145b], T. Lenz[105], G. Lenzen[175], B. Lenzi[30],
K. Leonhardt[44], S. Leontsinis[10], F. Lepold[58a], C. Leroy[93], J-R. Lessard[169], C.G. Lester[28],
C.M. Lester[120], J. Levêque[5], D. Levin[87], L.J. Levinson[172], A. Lewis[118], G.H. Lewis[108],
A.M. Leyko[21], M. Leyton[16], B. Li[33b], B. Li[83], H. Li[148], H.L. Li[31], S. Li[33b,s], X. Li[87],
Z. Liang[118,t], H. Liao[34], B. Liberti[133a], P. Lichard[30], K. Lie[165], J. Liebal[21], W. Liebig[14],
C. Limbach[21], A. Limosani[86], M. Limper[62], S.C. Lin[151,u], F. Linde[105], B.E. Lindquist[148],
J.T. Linnemann[88], E. Lipeles[120], A. Lipniacka[14], M. Lisovyi[42], T.M. Liss[165], D. Lissauer[25],
A. Lister[168], A.M. Litke[137], D. Liu[151], J.B. Liu[33b], K. Liu[33b,v], L. Liu[87], M. Liu[33b],
Y. Liu[33b], M. Livan[119a,119b], S.S.A. Livermore[118], A. Lleres[55], J. Llorente Merino[80],
S.L. Lloyd[75], F. Lo Sterzo[132a,132b], E. Lobodzinska[42], P. Loch[7], W.S. Lockman[137],
T. Loddenkoetter[21], F.K. Loebinger[82], A.E. Loevschall-Jensen[36], A. Loginov[176],
C.W. Loh[168], T. Lohse[16], K. Lohwasser[48], M. Lokajicek[125], V.P. Lombardo[5], R.E. Long[71],
L. Lopes[124a], D. Lopez Mateos[57], J. Lorenz[98], N. Lorenzo Martinez[115], M. Losada[162],
P. Loscutoff[15], M.J. Losty[159a,*], X. Lou[41], A. Lounis[115], K.F. Loureiro[162], J. Love[6],
P.A. Love[71], A.J. Lowe[143,f], F. Lu[33a], H.J. Lubatti[138], C. Luci[132a,132b], A. Lucotte[55],
D. Ludwig[42], I. Ludwig[48], J. Ludwig[48], F. Luehring[60], W. Lukas[61], L. Luminari[132a],
E. Lund[117], B. Lundberg[79], J. Lundberg[146a,146b], O. Lundberg[146a,146b],
B. Lund-Jensen[147], J. Lundquist[36], M. Lungwitz[81], D. Lynn[25], R. Lysak[125], E. Lytken[79],
H. Ma[25], L.L. Ma[173], G. Maccarrone[47], A. Macchiolo[99], B. Maček[74],
J. Machado Miguens[124a], D. Macina[30], R. Mackeprang[36], R. Madar[48], R.J. Madaras[15],
H.J. Maddocks[71], W.F. Mader[44], A. Madsen[166], M. Maeno[5], T. Maeno[25], L. Magnoni[163],
E. Magradze[54], K. Mahboubi[48], J. Mahlstedt[105], S. Mahmoud[73], G. Mahout[18],

C. Maiani[136], C. Maidantchik[24a], A. Maio[124a,c], S. Majewski[25], Y. Makida[65],
N. Makovec[115], P. Mal[136,w], B. Malaescu[78], Pa. Malecki[39], P. Malecki[39], V.P. Maleev[121],
F. Malek[55], U. Mallik[62], D. Malon[6], C. Malone[143], S. Maltezos[10], V. Malyshev[107],
S. Malyukov[30], J. Mamuzic[13b], L. Mandelli[89a], I. Mandić[74], R. Mandrysch[62],
J. Maneira[124a], A. Manfredini[99], L. Manhaes de Andrade Filho[24b],
J.A. Manjarres Ramos[136], A. Mann[98], P.M. Manning[137], A. Manousakis-Katsikakis[9],
B. Mansoulie[136], R. Mantifel[85], L. Mapelli[30], L. March[167], J.F. Marchand[29],
F. Marchese[133a,133b], G. Marchiori[78], M. Marcisovsky[125], C.P. Marino[169],
F. Marroquim[24a], Z. Marshall[30], L.F. Marti[17], S. Marti-Garcia[167], B. Martin[30],
B. Martin[88], J.P. Martin[93], T.A. Martin[170], V.J. Martin[46], B. Martin dit Latour[49],
H. Martinez[136], M. Martinez[12], S. Martin-Haugh[149], A.C. Martyniuk[169], M. Marx[82],
F. Marzano[132a], A. Marzin[111], L. Masetti[81], T. Mashimo[155], R. Mashinistov[94], J. Masik[82],
A.L. Maslennikov[107], I. Massa[20a,20b], N. Massol[5], P. Mastrandrea[148],
A. Mastroberardino[37a,37b], T. Masubuchi[155], H. Matsunaga[155], T. Matsushita[66],
P. Mättig[175], S. Mättig[42], C. Mattravers[118,d], J. Maurer[83], S.J. Maxfield[73],
D.A. Maximov[107,g], R. Mazini[151], M. Mazur[21], L. Mazzaferro[133a,133b], M. Mazzanti[89a],
S.P. Mc Kee[87], A. McCarn[165], R.L. McCarthy[148], T.G. McCarthy[29], N.A. McCubbin[129],
K.W. McFarlane[56,*], J.A. Mcfayden[139], G. Mchedlidze[51b], T. Mclaughlan[18],
S.J. McMahon[129], R.A. McPherson[169,j], A. Meade[84], J. Mechnich[105], M. Mechtel[175],
M. Medinnis[42], S. Meehan[31], R. Meera-Lebbai[111], T. Meguro[116], S. Mehlhase[36],
A. Mehta[73], K. Meier[58a], C. Meineck[98], B. Meirose[79], C. Melachrinos[31],
B.R. Mellado Garcia[173], F. Meloni[89a,89b], L. Mendoza Navas[162], A. Mengarelli[20a,20b],
S. Menke[99], E. Meoni[161], K.M. Mercurio[57], N. Meric[136], P. Mermod[49], L. Merola[102a,102b],
C. Meroni[89a], F.S. Merritt[31], H. Merritt[109], A. Messina[30,x], J. Metcalfe[25], A.S. Mete[163],
C. Meyer[81], C. Meyer[31], J-P. Meyer[136], J. Meyer[30], J. Meyer[54], S. Michal[30],
R.P. Middleton[129], S. Migas[73], L. Mijović[136], G. Mikenberg[172], M. Mikestikova[125],
M. Mikuž[74], D.W. Miller[31], W.J. Mills[168], C. Mills[57], A. Milov[172], D.A. Milstead[146a,146b],
D. Milstein[172], A.A. Minaenko[128], M. Miñano Moya[167], I.A. Minashvili[64], A.I. Mincer[108],
B. Mindur[38a], M. Mineev[64], Y. Ming[173], L.M. Mir[12], G. Mirabelli[132a], J. Mitrevski[137],
V.A. Mitsou[167], S. Mitsui[65], P.S. Miyagawa[139], J.U. Mjörnmark[79], T. Moa[146a,146b],
V. Moeller[28], S. Mohapatra[148], W. Mohr[48], R. Moles-Valls[167], A. Molfetas[30], K. Mönig[42],
C. Monini[55], J. Monk[36], E. Monnier[83], J. Montejo Berlingen[12], F. Monticelli[70],
S. Monzani[20a,20b], R.W. Moore[3], C. Mora Herrera[49], A. Moraes[53], N. Morange[62],
J. Morel[54], D. Moreno[81], M. Moreno Llácer[167], P. Morettini[50a], M. Morgenstern[44],
M. Morii[57], A.K. Morley[30], G. Mornacchi[30], J.D. Morris[75], L. Morvaj[101], N. Möser[21],
H.G. Moser[99], M. Mosidze[51b], J. Moss[109], R. Mount[143], E. Mountricha[10,y],
S.V. Mouraviev[94,*], E.J.W. Moyse[84], R.D. Mudd[18], F. Mueller[58a], J. Mueller[123],
K. Mueller[21], T. Mueller[28], T. Mueller[81], D. Muenstermann[30], T.A. Müller[98],
Y. Munwes[153], J.A. Murillo Quijada[18], W.J. Murray[129], I. Mussche[105], E. Musto[152],
A.G. Myagkov[128], M. Myska[125], O. Nackenhorst[54], J. Nadal[12], K. Nagai[160], R. Nagai[157],
Y. Nagai[83], K. Nagano[65], A. Nagarkar[109], Y. Nagasaka[59], M. Nagel[99], A.M. Nairz[30],
Y. Nakahama[30], K. Nakamura[65], T. Nakamura[155], I. Nakano[110], H. Namasivayam[41],
G. Nanava[21], A. Napier[161], R. Narayan[58b], M. Nash[77,d], T. Nattermann[21], T. Naumann[42],

G. Navarro[162], H.A. Neal[87], P.Yu. Nechaeva[94], T.J. Neep[82], A. Negri[119a,119b], G. Negri[30],
M. Negrini[20a], S. Nektarijevic[49], A. Nelson[163], T.K. Nelson[143], S. Nemecek[125],
P. Nemethy[108], A.A. Nepomuceno[24a], M. Nessi[30,z], M.S. Neubauer[165], M. Neumann[175],
A. Neusiedl[81], R.M. Neves[108], P. Nevski[25], F.M. Newcomer[120], P.R. Newman[18],
D.H. Nguyen[6], V. Nguyen Thi Hong[136], R.B. Nickerson[118], R. Nicolaidou[136],
B. Nicquevert[30], F. Niedercorn[115], J. Nielsen[137], N. Nikiforou[35], A. Nikiforov[16],
V. Nikolaenko[128], I. Nikolic-Audit[78], K. Nikolics[49], K. Nikolopoulos[18], P. Nilsson[8],
Y. Ninomiya[155], A. Nisati[132a], R. Nisius[99], T. Nobe[157], L. Nodulman[6], M. Nomachi[116],
I. Nomidis[154], S. Norberg[111], M. Nordberg[30], J. Novakova[127], M. Nozaki[65], L. Nozka[113],
A.-E. Nuncio-Quiroz[21], G. Nunes Hanninger[86], T. Nunnemann[98], E. Nurse[77],
B.J. O'Brien[46], D.C. O'Neil[142], V. O'Shea[53], L.B. Oakes[98], F.G. Oakham[29,e],
H. Oberlack[99], J. Ocariz[78], A. Ochi[66], M.I. Ochoa[77], S. Oda[69], S. Odaka[65], J. Odier[83],
H. Ogren[60], A. Oh[82], S.H. Oh[45], C.C. Ohm[30], T. Ohshima[101], W. Okamura[116],
H. Okawa[25], Y. Okumura[31], T. Okuyama[155], A. Olariu[26a], A.G. Olchevski[64],
S.A. Olivares Pino[46], M. Oliveira[124a,h], D. Oliveira Damazio[25], E. Oliver Garcia[167],
D. Olivito[120], A. Olszewski[39], J. Olszowska[39], A. Onofre[124a,aa], P.U.E. Onyisi[31,ab],
C.J. Oram[159a], M.J. Oreglia[31], Y. Oren[153], D. Orestano[134a,134b], N. Orlando[72a,72b],
C. Oropeza Barrera[53], R.S. Orr[158], B. Osculati[50a,50b], R. Ospanov[120], C. Osuna[12],
G. Otero y Garzon[27], J.P. Ottersbach[105], M. Ouchrif[135d], E.A. Ouellette[169],
F. Ould-Saada[117], A. Ouraou[136], Q. Ouyang[33a], A. Ovcharova[15], M. Owen[82], S. Owen[139],
V.E. Ozcan[19a], N. Ozturk[8], A. Pacheco Pages[12], C. Padilla Aranda[12], S. Pagan Griso[15],
E. Paganis[139], C. Pahl[99], F. Paige[25], P. Pais[84], K. Pajchel[117], G. Palacino[159b],
C.P. Paleari[7], S. Palestini[30], D. Pallin[34], A. Palma[124a], J.D. Palmer[18], Y.B. Pan[173],
E. Panagiotopoulou[10], J.G. Panduro Vazquez[76], P. Pani[105], N. Panikashvili[87],
S. Panitkin[25], D. Pantea[26a], A. Papadelis[146a], Th.D. Papadopoulou[10], A. Paramonov[6],
D. Paredes Hernandez[34], W. Park[25,ac], M.A. Parker[28], F. Parodi[50a,50b], J.A. Parsons[35],
U. Parzefall[48], S. Pashapour[54], E. Pasqualucci[132a], S. Passaggio[50a], A. Passeri[134a],
F. Pastore[134a,134b,*], Fr. Pastore[76], G. Pásztor[49,ad], S. Pataraia[175], N.D. Patel[150],
J.R. Pater[82], S. Patricelli[102a,102b], T. Pauly[30], J. Pearce[169], M. Pedersen[117],
S. Pedraza Lopez[167], M.I. Pedraza Morales[173], S.V. Peleganchuk[107], D. Pelikan[166],
H. Peng[33b], B. Penning[31], A. Penson[35], J. Penwell[60], T. Perez Cavalcanti[42],
E. Perez Codina[159a], M.T. Pérez García-Estañ[167], V. Perez Reale[35], L. Perini[89a,89b],
H. Pernegger[30], R. Perrino[72a], P. Perrodo[5], V.D. Peshekhonov[64], K. Peters[30],
R.F.Y. Peters[54,ae], B.A. Petersen[30], J. Petersen[30], T.C. Petersen[36], E. Petit[5],
A. Petridis[146a,146b], C. Petridou[154], E. Petrolo[132a], F. Petrucci[134a,134b], D. Petschull[42],
M. Petteni[142], R. Pezoa[32b], A. Phan[86], P.W. Phillips[129], G. Piacquadio[143], E. Pianori[170],
A. Picazio[49], E. Piccaro[75], M. Piccinini[20a,20b], S.M. Piec[42], R. Piegaia[27], D.T. Pignotti[109],
J.E. Pilcher[31], A.D. Pilkington[82], J. Pina[124a,c], M. Pinamonti[164a,164c,af], A. Pinder[118],
J.L. Pinfold[3], A. Pingel[36], B. Pinto[124a], C. Pizio[89a,89b], M.-A. Pleier[25], V. Pleskot[127],
E. Plotnikova[64], P. Plucinski[146a,146b], A. Poblaguev[25], S. Poddar[58a], F. Podlyski[34],
R. Poettgen[81], L. Poggioli[115], D. Pohl[21], M. Pohl[49], G. Polesello[119a], A. Policicchio[37a,37b],
R. Polifka[158], A. Polini[20a], V. Polychronakos[25], D. Pomeroy[23], K. Pommès[30],
L. Pontecorvo[132a], B.G. Pope[88], G.A. Popeneciu[26a], D.S. Popovic[13a], A. Poppleton[30],

X. Portell Bueso[30], G.E. Pospelov[99], S. Pospisil[126], I.N. Potrap[64], C.J. Potter[149],
C.T. Potter[114], G. Poulard[30], J. Poveda[60], V. Pozdnyakov[64], R. Prabhu[77], P. Pralavorio[83],
A. Pranko[15], S. Prasad[30], R. Pravahan[25], S. Prell[63], K. Pretzl[17], D. Price[60], J. Price[73],
L.E. Price[6], D. Prieur[123], M. Primavera[72a], M. Proissl[46], K. Prokofiev[108], F. Prokoshin[32b],
E. Protopapadaki[136], S. Protopopescu[25], J. Proudfoot[6], X. Prudent[44], M. Przybycien[38a],
H. Przysiezniak[5], S. Psoroulas[21], E. Ptacek[114], E. Pueschel[84], D. Puldon[148],
M. Purohit[25,ac], P. Puzo[115], Y. Pylypchenko[62], J. Qian[87], A. Quadt[54], D.R. Quarrie[15],
W.B. Quayle[173], D. Quilty[53], M. Raas[104], V. Radeka[25], V. Radescu[42], P. Radloff[114],
F. Ragusa[89a,89b], G. Rahal[178], S. Rajagopalan[25], M. Rammensee[48], M. Rammes[141],
A.S. Randle-Conde[40], K. Randrianarivony[29], C. Rangel-Smith[78], K. Rao[163],
F. Rauscher[98], T.C. Rave[48], T. Ravenscroft[53], M. Raymond[30], A.L. Read[117],
D.M. Rebuzzi[119a,119b], A. Redelbach[174], G. Redlinger[25], R. Reece[120], K. Reeves[41],
A. Reinsch[114], I. Reisinger[43], M. Relich[163], C. Rembser[30], Z.L. Ren[151], A. Renaud[115],
M. Rescigno[132a], S. Resconi[89a], B. Resende[136], P. Reznicek[98], R. Rezvani[158], R. Richter[99],
E. Richter-Was[38b], M. Ridel[78], P. Rieck[16], M. Rijssenbeek[148], A. Rimoldi[119a,119b],
L. Rinaldi[20a], R.R. Rios[40], E. Ritsch[61], I. Riu[12], G. Rivoltella[89a,89b], F. Rizatdinova[112],
E. Rizvi[75], S.H. Robertson[85,j], A. Robichaud-Veronneau[118], D. Robinson[28],
J.E.M. Robinson[82], A. Robson[53], J.G. Rocha de Lima[106], C. Roda[122a,122b],
D. Roda Dos Santos[30], A. Roe[54], S. Roe[30], O. Røhne[117], S. Rolli[161], A. Romaniouk[96],
M. Romano[20a,20b], G. Romeo[27], E. Romero Adam[167], N. Rompotis[138], L. Roos[78],
E. Ros[167], S. Rosati[132a], K. Rosbach[49], A. Rose[149], M. Rose[76], G.A. Rosenbaum[158],
P.L. Rosendahl[14], O. Rosenthal[141], L. Rosselet[49], V. Rossetti[12], E. Rossi[132a,132b],
L.P. Rossi[50a], M. Rotaru[26a], I. Roth[172], J. Rothberg[138], D. Rousseau[115], C.R. Royon[136],
A. Rozanov[83], Y. Rozen[152], X. Ruan[33a,ag], F. Rubbo[12], I. Rubinskiy[42], N. Ruckstuhl[105],
V.I. Rud[97], C. Rudolph[44], M.S. Rudolph[158], F. Rühr[7], A. Ruiz-Martinez[63],
L. Rumyantsev[64], Z. Rurikova[48], N.A. Rusakovich[64], A. Ruschke[98], J.P. Rutherfoord[7],
N. Ruthmann[48], P. Ruzicka[125], Y.F. Ryabov[121], M. Rybar[127], G. Rybkin[115],
N.C. Ryder[118], A.F. Saavedra[150], A. Saddique[3], I. Sadeh[153], H.F-W. Sadrozinski[137],
R. Sadykov[64], F. Safai Tehrani[132a], H. Sakamoto[155], G. Salamanna[75], A. Salamon[133a],
M. Saleem[111], D. Salek[30], D. Salihagic[99], A. Salnikov[143], J. Salt[167],
B.M. Salvachua Ferrando[6], D. Salvatore[37a,37b], F. Salvatore[149], A. Salvucci[104],
A. Salzburger[30], D. Sampsonidis[154], A. Sanchez[102a,102b], J. Sánchez[167],
V. Sanchez Martinez[167], H. Sandaker[14], H.G. Sander[81], M.P. Sanders[98], M. Sandhoff[175],
T. Sandoval[28], C. Sandoval[162], R. Sandstroem[99], D.P.C. Sankey[129], A. Sansoni[47],
C. Santoni[34], R. Santonico[133a,133b], H. Santos[124a], I. Santoyo Castillo[149], K. Sapp[123],
J.G. Saraiva[124a], T. Sarangi[173], E. Sarkisyan-Grinbaum[8], B. Sarrazin[21], F. Sarri[122a,122b],
G. Sartisohn[175], O. Sasaki[65], Y. Sasaki[155], N. Sasao[67], I. Satsounkevitch[90], G. Sauvage[5,*],
E. Sauvan[5], J.B. Sauvan[115], P. Savard[158,e], V. Savinov[123], D.O. Savu[30], C. Sawyer[118],
L. Sawyer[25,l], D.H. Saxon[53], J. Saxon[120], C. Sbarra[20a], A. Sbrizzi[3], D.A. Scannicchio[163],
M. Scarcella[150], J. Schaarschmidt[115], P. Schacht[99], D. Schaefer[120], A. Schaelicke[46],
S. Schaepe[21], S. Schaetzel[58b], U. Schäfer[81], A.C. Schaffer[115], D. Schaile[98],
R.D. Schamberger[148], V. Scharf[58a], V.A. Schegelsky[121], D. Scheirich[87], M. Schernau[163],
M.I. Scherzer[35], C. Schiavi[50a,50b], J. Schieck[98], C. Schillo[48], M. Schioppa[37a,37b],

S. Schlenker[30], E. Schmidt[48], K. Schmieden[21], C. Schmitt[81], C. Schmitt[98], S. Schmitt[58b],
B. Schneider[17], Y.J. Schnellbach[73], U. Schnoor[44], L. Schoeffel[136], A. Schoening[58b],
A.L.S. Schorlemmer[54], M. Schott[81], D. Schouten[159a], J. Schovancova[125], M. Schram[85],
C. Schroeder[81], N. Schroer[58c], M.J. Schultens[21], J. Schultes[175], H.-C. Schultz-Coulon[58a],
H. Schulz[16], M. Schumacher[48], B.A. Schumm[137], Ph. Schune[136], A. Schwartzman[143],
Ph. Schwegler[99], Ph. Schwemling[136], R. Schwienhorst[88], J. Schwindling[136], T. Schwindt[21],
M. Schwoerer[5], F.G. Sciacca[17], E. Scifo[115], G. Sciolla[23], W.G. Scott[129], F. Scutti[21],
J. Searcy[87], G. Sedov[42], E. Sedykh[121], S.C. Seidel[103], A. Seiden[137], F. Seifert[44],
J.M. Seixas[24a], G. Sekhniaidze[102a], S.J. Sekula[40], K.E. Selbach[46], D.M. Seliverstov[121],
G. Sellers[73], M. Seman[144b], N. Semprini-Cesari[20a,20b], C. Serfon[30], L. Serin[115],
L. Serkin[54], T. Serre[83], R. Seuster[159a], H. Severini[111], A. Sfyrla[30], E. Shabalina[54],
M. Shamim[114], L.Y. Shan[33a], J.T. Shank[22], Q.T. Shao[86], M. Shapiro[15], P.B. Shatalov[95],
K. Shaw[164a,164c], P. Sherwood[77], S. Shimizu[101], M. Shimojima[100], T. Shin[56],
M. Shiyakova[64], A. Shmeleva[94], M.J. Shochet[31], D. Short[118], S. Shrestha[63], E. Shulga[96],
M.A. Shupe[7], P. Sicho[125], A. Sidoti[132a], F. Siegert[48], Dj. Sijacki[13a], O. Silbert[172],
J. Silva[124a], Y. Silver[153], D. Silverstein[143], S.B. Silverstein[146a], V. Simak[126], O. Simard[5],
Lj. Simic[13a], S. Simion[115], E. Simioni[81], B. Simmons[77], R. Simoniello[89a,89b],
M. Simonyan[36], P. Sinervo[158], N.B. Sinev[114], V. Sipica[141], G. Siragusa[174], A. Sircar[25],
A.N. Sisakyan[64,*], S.Yu. Sivoklokov[97], J. Sjölin[146a,146b], T.B. Sjursen[14], L.A. Skinnari[15],
H.P. Skottowe[57], K. Skovpen[107], P. Skubic[111], M. Slater[18], T. Slavicek[126], K. Sliwa[161],
V. Smakhtin[172], B.H. Smart[46], L. Smestad[117], S.Yu. Smirnov[96], Y. Smirnov[96],
L.N. Smirnova[97,ah], O. Smirnova[79], K.M. Smith[53], M. Smizanska[71], K. Smolek[126],
A.A. Snesarev[94], G. Snidero[75], J. Snow[111], S. Snyder[25], R. Sobie[169,j], J. Sodomka[126],
A. Soffer[153], D.A. Soh[151,t], C.A. Solans[30], M. Solar[126], J. Solc[126], E.Yu. Soldatov[96],
U. Soldevila[167], E. Solfaroli Camillocci[132a,132b], A.A. Solodkov[128], O.V. Solovyanov[128],
V. Solovyev[121], N. Soni[1], A. Sood[15], V. Sopko[126], B. Sopko[126], M. Sosebee[8],
R. Soualah[164a,164c], P. Soueid[93], A. Soukharev[107], D. South[42], S. Spagnolo[72a,72b],
F. Spanò[76], R. Spighi[20a], G. Spigo[30], R. Spiwoks[30], M. Spousta[127,ai], T. Spreitzer[158],
B. Spurlock[8], R.D. St. Denis[53], J. Stahlman[120], R. Stamen[58a], E. Stanecka[39],
R.W. Stanek[6], C. Stanescu[134a], M. Stanescu-Bellu[42], M.M. Stanitzki[42], S. Stapnes[117],
E.A. Starchenko[128], J. Stark[55], P. Staroba[125], P. Starovoitov[42], R. Staszewski[39],
A. Staude[98], P. Stavina[144a,*], G. Steele[53], P. Steinbach[44], P. Steinberg[25], I. Stekl[126],
B. Stelzer[142], H.J. Stelzer[88], O. Stelzer-Chilton[159a], H. Stenzel[52], S. Stern[99],
G.A. Stewart[30], J.A. Stillings[21], M.C. Stockton[85], M. Stoebe[85], K. Stoerig[48],
G. Stoicea[26a], S. Stonjek[99], A.R. Stradling[8], A. Straessner[44], J. Strandberg[147],
S. Strandberg[146a,146b], A. Strandlie[117], M. Strang[109], E. Strauss[143], M. Strauss[111],
P. Strizenec[144b], R. Ströhmer[174], D.M. Strom[114], J.A. Strong[76,*], R. Stroynowski[40],
B. Stugu[14], I. Stumer[25,*], J. Stupak[148], P. Sturm[175], N.A. Styles[42], D. Su[143],
HS. Subramania[3], R. Subramaniam[25], A. Succurro[12], Y. Sugaya[116], C. Suhr[106],
M. Suk[126], V.V. Sulin[94], S. Sultansoy[4c], T. Sumida[67], X. Sun[55], J.E. Sundermann[48],
K. Suruliz[139], G. Susinno[37a,37b], M.R. Sutton[149], Y. Suzuki[65], Y. Suzuki[66], M. Svatos[125],
S. Swedish[168], M. Swiatlowski[143], I. Sykora[144a], T. Sykora[127], D. Ta[105], K. Tackmann[42],
A. Taffard[163], R. Tafirout[159a], N. Taiblum[153], Y. Takahashi[101], H. Takai[25],

R. Takashima[68], H. Takeda[66], T. Takeshita[140], Y. Takubo[65], M. Talby[83], A. Talyshev[107,g],
J.Y.C. Tam[174], M.C. Tamsett[25], K.G. Tan[86], J. Tanaka[155], R. Tanaka[115], S. Tanaka[131],
S. Tanaka[65], A.J. Tanasijczuk[142], K. Tani[66], N. Tannoury[83], S. Tapprogge[81], D. Tardif[158],
S. Tarem[152], F. Tarrade[29], G.F. Tartarelli[89a], P. Tas[127], M. Tasevsky[125], E. Tassi[37a,37b],
Y. Tayalati[135d], C. Taylor[77], F.E. Taylor[92], G.N. Taylor[86], W. Taylor[159b],
M. Teinturier[115], F.A. Teischinger[30], M. Teixeira Dias Castanheira[75], P. Teixeira-Dias[76],
K.K. Temming[48], H. Ten Kate[30], P.K. Teng[151], S. Terada[65], K. Terashi[155], J. Terron[80],
M. Testa[47], R.J. Teuscher[158,j], J. Therhaag[21], T. Theveneaux-Pelzer[34], S. Thoma[48],
J.P. Thomas[18], E.N. Thompson[35], P.D. Thompson[18], P.D. Thompson[158],
A.S. Thompson[53], L.A. Thomsen[36], E. Thomson[120], M. Thomson[28], W.M. Thong[86],
R.P. Thun[87,*], F. Tian[35], M.J. Tibbetts[15], T. Tic[125], V.O. Tikhomirov[94],
Y.A. Tikhonov[107,g], S. Timoshenko[96], E. Tiouchichine[83], P. Tipton[176], S. Tisserant[83],
T. Todorov[5], S. Todorova-Nova[161], B. Toggerson[163], J. Tojo[69], S. Tokár[144a],
K. Tokushuku[65], K. Tollefson[88], L. Tomlinson[82], M. Tomoto[101], L. Tompkins[31],
K. Toms[103], A. Tonoyan[14], C. Topfel[17], N.D. Topilin[64], E. Torrence[114], H. Torres[78],
E. Torró Pastor[167], J. Toth[83,ad], F. Touchard[83], D.R. Tovey[139], H.L. Tran[115],
T. Trefzger[174], L. Tremblet[30], A. Tricoli[30], I.M. Trigger[159a], S. Trincaz-Duvoid[78],
M.F. Tripiana[70], N. Triplett[25], W. Trischuk[158], B. Trocmé[55], C. Troncon[89a],
M. Trottier-McDonald[142], M. Trovatelli[134a,134b], P. True[88], M. Trzebinski[39], A. Trzupek[39],
C. Tsarouchas[30], J.C-L. Tseng[118], M. Tsiakiris[105], P.V. Tsiareshka[90], D. Tsionou[136],
G. Tsipolitis[10], S. Tsiskaridze[12], V. Tsiskaridze[48], E.G. Tskhadadze[51a], I.I. Tsukerman[95],
V. Tsulaia[15], J.-W. Tsung[21], S. Tsuno[65], D. Tsybychev[148], A. Tua[139], A. Tudorache[26a],
V. Tudorache[26a], J.M. Tuggle[31], A.N. Tuna[120], M. Turala[39], D. Turecek[126],
I. Turk Cakir[4d], R. Turra[89a,89b], P.M. Tuts[35], A. Tykhonov[74], M. Tylmad[146a,146b],
M. Tyndel[129], G. Tzanakos[9], K. Uchida[21], I. Ueda[155], R. Ueno[29], M. Ughetto[83],
M. Ugland[14], M. Uhlenbrock[21], F. Ukegawa[160], G. Unal[30], A. Undrus[25], G. Unel[163],
F.C. Ungaro[48], Y. Unno[65], D. Urbaniec[35], P. Urquijo[21], G. Usai[8], L. Vacavant[83],
V. Vacek[126], B. Vachon[85], S. Vahsen[15], N. Valencic[105], S. Valentinetti[20a,20b], A. Valero[167],
L. Valery[34], S. Valkar[127], E. Valladolid Gallego[167], S. Vallecorsa[152], J.A. Valls Ferrer[167],
R. Van Berg[120], P.C. Van Der Deijl[105], R. van der Geer[105], H. van der Graaf[105],
R. Van Der Leeuw[105], E. van der Poel[105], D. van der Ster[30], N. van Eldik[30],
P. van Gemmeren[6], J. Van Nieuwkoop[142], I. van Vulpen[105], M. Vanadia[99], W. Vandelli[30],
A. Vaniachine[6], P. Vankov[42], F. Vannucci[78], R. Vari[132a], E.W. Varnes[7], T. Varol[84],
D. Varouchas[15], A. Vartapetian[8], K.E. Varvell[150], V.I. Vassilakopoulos[56], F. Vazeille[34],
T. Vazquez Schroeder[54], F. Veloso[124a], S. Veneziano[132a], A. Ventura[72a,72b], D. Ventura[84],
M. Venturi[48], N. Venturi[158], V. Vercesi[119a], M. Verducci[138], W. Verkerke[105],
J.C. Vermeulen[105], A. Vest[44], M.C. Vetterli[142,e], I. Vichou[165], T. Vickey[145b,aj],
O.E. Vickey Boeriu[145b], G.H.A. Viehhauser[118], S. Viel[168], M. Villa[20a,20b],
M. Villaplana Perez[167], E. Vilucchi[47], M.G. Vincter[29], V.B. Vinogradov[64], J. Virzi[15],
O. Vitells[172], M. Viti[42], I. Vivarelli[48], F. Vives Vaque[3], S. Vlachos[10], D. Vladoiu[98],
M. Vlasak[126], A. Vogel[21], P. Vokac[126], G. Volpi[47], M. Volpi[86], G. Volpini[89a],
H. von der Schmitt[99], H. von Radziewski[48], E. von Toerne[21], V. Vorobel[127], M. Vos[167],
R. Voss[30], J.H. Vossebeld[73], N. Vranjes[136], M. Vranjes Milosavljevic[105], V. Vrba[125],

M. Vreeswijk[105], T. Vu Anh[48], R. Vuillermet[30], I. Vukotic[31], Z. Vykydal[126],
W. Wagner[175], P. Wagner[21], H. Wahlen[175], S. Wahrmund[44], J. Wakabayashi[101],
S. Walch[87], J. Walder[71], R. Walker[98], W. Walkowiak[141], R. Wall[176], P. Waller[73],
B. Walsh[176], C. Wang[45], H. Wang[173], H. Wang[40], J. Wang[151], J. Wang[33a], K. Wang[85],
R. Wang[103], S.M. Wang[151], T. Wang[21], X. Wang[176], A. Warburton[85], C.P. Ward[28],
D.R. Wardrope[77], M. Warsinsky[48], A. Washbrook[46], C. Wasicki[42], I. Watanabe[66],
P.M. Watkins[18], A.T. Watson[18], I.J. Watson[150], M.F. Watson[18], G. Watts[138], S. Watts[82],
A.T. Waugh[150], B.M. Waugh[77], M.S. Weber[17], J.S. Webster[31], A.R. Weidberg[118],
P. Weigell[99], J. Weingarten[54], C. Weiser[48], P.S. Wells[30], T. Wenaus[25], D. Wendland[16],
Z. Weng[151,t], T. Wengler[30], S. Wenig[30], N. Wermes[21], M. Werner[48], P. Werner[30],
M. Werth[163], M. Wessels[58a], J. Wetter[161], K. Whalen[29], A. White[8], M.J. White[86],
S. White[122a,122b], S.R. Whitehead[118], D. Whiteson[163], D. Whittington[60], D. Wicke[175],
F.J. Wickens[129], W. Wiedenmann[173], M. Wielers[79], P. Wienemann[21], C. Wiglesworth[36],
L.A.M. Wiik-Fuchs[21], P.A. Wijeratne[77], A. Wildauer[99], M.A. Wildt[42,q], I. Wilhelm[127],
H.G. Wilkens[30], J.Z. Will[98], E. Williams[35], H.H. Williams[120], S. Williams[28], W. Willis[35,*],
S. Willocq[84], J.A. Wilson[18], A. Wilson[87], I. Wingerter-Seez[5], S. Winkelmann[48],
F. Winklmeier[30], M. Wittgen[143], T. Wittig[43], J. Wittkowski[98], S.J. Wollstadt[81],
M.W. Wolter[39], H. Wolters[124a,h], W.C. Wong[41], G. Wooden[87], B.K. Wosiek[39],
J. Wotschack[30], M.J. Woudstra[82], K.W. Wozniak[39], K. Wraight[53], M. Wright[53],
B. Wrona[73], S.L. Wu[173], X. Wu[49], Y. Wu[87], E. Wulf[35], B.M. Wynne[46], S. Xella[36],
M. Xiao[136], S. Xie[48], C. Xu[33b,y], D. Xu[33a], L. Xu[33b], B. Yabsley[150], S. Yacoob[145a,ak],
M. Yamada[65], H. Yamaguchi[155], Y. Yamaguchi[155], A. Yamamoto[65], K. Yamamoto[63],
S. Yamamoto[155], T. Yamamura[155], T. Yamanaka[155], K. Yamauchi[101], T. Yamazaki[155],
Y. Yamazaki[66], Z. Yan[22], H. Yang[33e], H. Yang[173], U.K. Yang[82], Y. Yang[109],
Z. Yang[146a,146b], S. Yanush[91], L. Yao[33a], Y. Yasu[65], E. Yatsenko[42], K.H. Yau Wong[21],
J. Ye[40], S. Ye[25], A.L. Yen[57], E. Yildirim[42], M. Yilmaz[4b], R. Yoosoofmiya[123], K. Yorita[171],
R. Yoshida[6], K. Yoshihara[155], C. Young[143], C.J.S. Young[118], S. Youssef[22], D. Yu[25],
D.R. Yu[15], J. Yu[8], J. Yu[112], L. Yuan[66], A. Yurkewicz[106], B. Zabinski[39], R. Zaidan[62],
A.M. Zaitsev[128], S. Zambito[23], L. Zanello[132a,132b], D. Zanzi[99], A. Zaytsev[25], C. Zeitnitz[175],
M. Zeman[126], A. Zemla[39], O. Zenin[128], T. Ženiš[144a], D. Zerwas[115], G. Zevi della Porta[57],
D. Zhang[87], H. Zhang[88], J. Zhang[6], L. Zhang[151], X. Zhang[33d], Z. Zhang[115], Z. Zhao[33b],
A. Zhemchugov[64], J. Zhong[118], B. Zhou[87], N. Zhou[163], Y. Zhou[151], C.G. Zhu[33d],
H. Zhu[42], J. Zhu[87], Y. Zhu[33b], X. Zhuang[33a], V. Zhuravlov[99], A. Zibell[98], D. Zieminska[60],
N.I. Zimin[64], R. Zimmermann[21], S. Zimmermann[21], S. Zimmermann[48],
Z. Zinonos[122a,122b], M. Ziolkowski[141], R. Zitoun[5], L. Živković[35], V.V. Zmouchko[128,*],
G. Zobernig[173], A. Zoccoli[20a,20b], M. zur Nedden[16], V. Zutshi[106], L. Zwalinski[30].

[1] School of Chemistry and Physics, University of Adelaide, Adelaide, Australia
[2] Physics Department, SUNY Albany, Albany NY, United States of America
[3] Department of Physics, University of Alberta, Edmonton AB, Canada
[4] (a)Department of Physics, Ankara University, Ankara; (b)Department of Physics, Gazi University, Ankara; (c)Division of Physics, TOBB University of Economics and Technology, Ankara; (d)Turkish Atomic Energy Authority, Ankara, Turkey

[5] LAPP, CNRS/IN2P3 and Université de Savoie, Annecy-le-Vieux, France

[6] High Energy Physics Division, Argonne National Laboratory, Argonne IL, United States of America

[7] Department of Physics, University of Arizona, Tucson AZ, United States of America

[8] Department of Physics, The University of Texas at Arlington, Arlington TX, United States of America

[9] Physics Department, University of Athens, Athens, Greece

[10] Physics Department, National Technical University of Athens, Zografou, Greece

[11] Institute of Physics, Azerbaijan Academy of Sciences, Baku, Azerbaijan

[12] Institut de Física d'Altes Energies and Departament de Física de la Universitat Autònoma de Barcelona and ICREA, Barcelona, Spain

[13] [a]Institute of Physics, University of Belgrade, Belgrade; [b]Vinca Institute of Nuclear Sciences, University of Belgrade, Belgrade, Serbia

[14] Department for Physics and Technology, University of Bergen, Bergen, Norway

[15] Physics Division, Lawrence Berkeley National Laboratory and University of California, Berkeley CA, United States of America

[16] Department of Physics, Humboldt University, Berlin, Germany

[17] Albert Einstein Center for Fundamental Physics and Laboratory for High Energy Physics, University of Bern, Bern, Switzerland

[18] School of Physics and Astronomy, University of Birmingham, Birmingham, United Kingdom

[19] [a]Department of Physics, Bogazici University, Istanbul; [b]Division of Physics, Dogus University, Istanbul; [c]Department of Physics Engineering, Gaziantep University, Gaziantep, Turkey

[20] [a]INFN Sezione di Bologna; [b]Dipartimento di Fisica, Università di Bologna, Bologna, Italy

[21] Physikalisches Institut, University of Bonn, Bonn, Germany

[22] Department of Physics, Boston University, Boston MA, United States of America

[23] Department of Physics, Brandeis University, Waltham MA, United States of America

[24] [a]Universidade Federal do Rio De Janeiro COPPE/EE/IF, Rio de Janeiro; [b]Federal University of Juiz de Fora (UFJF), Juiz de Fora; [c]Federal University of Sao Joao del Rei (UFSJ), Sao Joao del Rei; [d]Instituto de Fisica, Universidade de Sao Paulo, Sao Paulo, Brazil

[25] Physics Department, Brookhaven National Laboratory, Upton NY, United States of America

[26] [a]National Institute of Physics and Nuclear Engineering, Bucharest; [b]University Politehnica Bucharest, Bucharest; [c]West University in Timisoara, Timisoara, Romania

[27] Departamento de Física, Universidad de Buenos Aires, Buenos Aires, Argentina

[28] Cavendish Laboratory, University of Cambridge, Cambridge, United Kingdom

[29] Department of Physics, Carleton University, Ottawa ON, Canada

[30] CERN, Geneva, Switzerland

[31] Enrico Fermi Institute, University of Chicago, Chicago IL, United States of America

[32] [a]Departamento de Física, Pontificia Universidad Católica de Chile, Santiago;

$^{(b)}$Departamento de Física, Universidad Técnica Federico Santa María, Valparaíso, Chile
33 $^{(a)}$Institute of High Energy Physics, Chinese Academy of Sciences, Beijing;
$^{(b)}$Department of Modern Physics, University of Science and Technology of China, Anhui;
$^{(c)}$Department of Physics, Nanjing University, Jiangsu; $^{(d)}$School of Physics, Shandong
University, Shandong; $^{(e)}$Physics Department, Shanghai Jiao Tong University, Shanghai,
China
34 Laboratoire de Physique Corpusculaire, Clermont Université and Université Blaise
Pascal and CNRS/IN2P3, Clermont-Ferrand, France
35 Nevis Laboratory, Columbia University, Irvington NY, United States of America
36 Niels Bohr Institute, University of Copenhagen, Kobenhavn, Denmark
37 $^{(a)}$INFN Gruppo Collegato di Cosenza; $^{(b)}$Dipartimento di Fisica, Università della
Calabria, Rende, Italy
38 $^{(a)}$AGH University of Science and Technology, Faculty of Physics and Applied
Computer Science, Krakow; $^{(b)}$Marian Smoluchowski Institute of Physics, Jagiellonian
University, Krakow, Poland
39 The Henryk Niewodniczanski Institute of Nuclear Physics, Polish Academy of Sciences,
Krakow, Poland
40 Physics Department, Southern Methodist University, Dallas TX, United States of
America
41 Physics Department, University of Texas at Dallas, Richardson TX, United States of
America
42 DESY, Hamburg and Zeuthen, Germany
43 Institut für Experimentelle Physik IV, Technische Universität Dortmund, Dortmund,
Germany
44 Institut für Kern-Âăund Teilchenphysik, Technical University Dresden, Dresden,
Germany
45 Department of Physics, Duke University, Durham NC, United States of America
46 SUPA - School of Physics and Astronomy, University of Edinburgh, Edinburgh, United
Kingdom
47 INFN Laboratori Nazionali di Frascati, Frascati, Italy
48 Fakultät für Mathematik und Physik, Albert-Ludwigs-Universität, Freiburg, Germany
49 Section de Physique, Université de Genève, Geneva, Switzerland
50 $^{(a)}$INFN Sezione di Genova; $^{(b)}$Dipartimento di Fisica, Università di Genova, Genova,
Italy
51 $^{(a)}$E. Andronikashvili Institute of Physics, Iv. Javakhishvili Tbilisi State University,
Tbilisi; $^{(b)}$High Energy Physics Institute, Tbilisi State University, Tbilisi, Georgia
52 II Physikalisches Institut, Justus-Liebig-Universität Giessen, Giessen, Germany
53 SUPA - School of Physics and Astronomy, University of Glasgow, Glasgow, United
Kingdom
54 II Physikalisches Institut, Georg-August-Universität, Göttingen, Germany
55 Laboratoire de Physique Subatomique et de Cosmologie, Université Joseph Fourier and
CNRS/IN2P3 and Institut National Polytechnique de Grenoble, Grenoble, France
56 Department of Physics, Hampton University, Hampton VA, United States of America

[57] Laboratory for Particle Physics and Cosmology, Harvard University, Cambridge MA, United States of America

[58] [a]Kirchhoff-Institut für Physik, Ruprecht-Karls-Universität Heidelberg, Heidelberg; [b]Physikalisches Institut, Ruprecht-Karls-Universität Heidelberg, Heidelberg; [c]ZITI Institut für technische Informatik, Ruprecht-Karls-Universität Heidelberg, Mannheim, Germany

[59] Faculty of Applied Information Science, Hiroshima Institute of Technology, Hiroshima, Japan

[60] Department of Physics, Indiana University, Bloomington IN, United States of America

[61] Institut für Astro-Âǎund Teilchenphysik, Leopold-Franzens-Universität, Innsbruck, Austria

[62] University of Iowa, Iowa City IA, United States of America

[63] Department of Physics and Astronomy, Iowa State University, Ames IA, United States of America

[64] Joint Institute for Nuclear Research, JINR Dubna, Dubna, Russia

[65] KEK, High Energy Accelerator Research Organization, Tsukuba, Japan

[66] Graduate School of Science, Kobe University, Kobe, Japan

[67] Faculty of Science, Kyoto University, Kyoto, Japan

[68] Kyoto University of Education, Kyoto, Japan

[69] Department of Physics, Kyushu University, Fukuoka, Japan

[70] Instituto de Física La Plata, Universidad Nacional de La Plata and CONICET, La Plata, Argentina

[71] Physics Department, Lancaster University, Lancaster, United Kingdom

[72] [a]INFN Sezione di Lecce; [b]Dipartimento di Matematica e Fisica, Università del Salento, Lecce, Italy

[73] Oliver Lodge Laboratory, University of Liverpool, Liverpool, United Kingdom

[74] Department of Physics, Jožef Stefan Institute and University of Ljubljana, Ljubljana, Slovenia

[75] School of Physics and Astronomy, Queen Mary University of London, London, United Kingdom

[76] Department of Physics, Royal Holloway University of London, Surrey, United Kingdom

[77] Department of Physics and Astronomy, University College London, London, United Kingdom

[78] Laboratoire de Physique Nucléaire et de Hautes Energies, UPMC and Université Paris-Diderot and CNRS/IN2P3, Paris, France

[79] Fysiska institutionen, Lunds universitet, Lund, Sweden

[80] Departamento de Fisica Teorica C-15, Universidad Autonoma de Madrid, Madrid, Spain

[81] Institut für Physik, Universität Mainz, Mainz, Germany

[82] School of Physics and Astronomy, University of Manchester, Manchester, United Kingdom

[83] CPPM, Aix-Marseille Université and CNRS/IN2P3, Marseille, France

[84] Department of Physics, University of Massachusetts, Amherst MA, United States of

America

[85] Department of Physics, McGill University, Montreal QC, Canada

[86] School of Physics, University of Melbourne, Victoria, Australia

[87] Department of Physics, The University of Michigan, Ann Arbor MI, United States of America

[88] Department of Physics and Astronomy, Michigan State University, East Lansing MI, United States of America

[89] [a]INFN Sezione di Milano; [b]Dipartimento di Fisica, Università di Milano, Milano, Italy

[90] B.I. Stepanov Institute of Physics, National Academy of Sciences of Belarus, Minsk, Republic of Belarus

[91] National Scientific and Educational Centre for Particle and High Energy Physics, Minsk, Republic of Belarus

[92] Department of Physics, Massachusetts Institute of Technology, Cambridge MA, United States of America

[93] Group of Particle Physics, University of Montreal, Montreal QC, Canada

[94] P.N. Lebedev Institute of Physics, Academy of Sciences, Moscow, Russia

[95] Institute for Theoretical and Experimental Physics (ITEP), Moscow, Russia

[96] Moscow Engineering and Physics Institute (MEPhI), Moscow, Russia

[97] D.V.Skobeltsyn Institute of Nuclear Physics, M.V.Lomonosov Moscow State University, Moscow, Russia

[98] Fakultät für Physik, Ludwig-Maximilians-Universität München, München, Germany

[99] Max-Planck-Institut für Physik (Werner-Heisenberg-Institut), München, Germany

[100] Nagasaki Institute of Applied Science, Nagasaki, Japan

[101] Graduate School of Science and Kobayashi-Maskawa Institute, Nagoya University, Nagoya, Japan

[102] [a]INFN Sezione di Napoli; [b]Dipartimento di Scienze Fisiche, Università di Napoli, Napoli, Italy

[103] Department of Physics and Astronomy, University of New Mexico, Albuquerque NM, United States of America

[104] Institute for Mathematics, Astrophysics and Particle Physics, Radboud University Nijmegen/Nikhef, Nijmegen, Netherlands

[105] Nikhef National Institute for Subatomic Physics and University of Amsterdam, Amsterdam, Netherlands

[106] Department of Physics, Northern Illinois University, DeKalb IL, United States of America

[107] Budker Institute of Nuclear Physics, SB RAS, Novosibirsk, Russia

[108] Department of Physics, New York University, New York NY, United States of America

[109] Ohio State University, Columbus OH, United States of America

[110] Faculty of Science, Okayama University, Okayama, Japan

[111] Homer L. Dodge Department of Physics and Astronomy, University of Oklahoma, Norman OK, United States of America

[112] Department of Physics, Oklahoma State University, Stillwater OK, United States of

America

[113] Palacký University, RCPTM, Olomouc, Czech Republic

[114] Center for High Energy Physics, University of Oregon, Eugene OR, United States of America

[115] LAL, Université Paris-Sud and CNRS/IN2P3, Orsay, France

[116] Graduate School of Science, Osaka University, Osaka, Japan

[117] Department of Physics, University of Oslo, Oslo, Norway

[118] Department of Physics, Oxford University, Oxford, United Kingdom

[119] [a]INFN Sezione di Pavia; [b]Dipartimento di Fisica, Università di Pavia, Pavia, Italy

[120] Department of Physics, University of Pennsylvania, Philadelphia PA, United States of America

[121] Petersburg Nuclear Physics Institute, Gatchina, Russia

[122] [a]INFN Sezione di Pisa; [b]Dipartimento di Fisica E. Fermi, Università di Pisa, Pisa, Italy

[123] Department of Physics and Astronomy, University of Pittsburgh, Pittsburgh PA, United States of America

[124] [a]Laboratorio de Instrumentacao e Fisica Experimental de Particulas - LIP, Lisboa, Portugal; [b]Departamento de Fisica Teorica y del Cosmos and CAFPE, Universidad de Granada, Granada, Spain

[125] Institute of Physics, Academy of Sciences of the Czech Republic, Praha, Czech Republic

[126] Czech Technical University in Prague, Praha, Czech Republic

[127] Faculty of Mathematics and Physics, Charles University in Prague, Praha, Czech Republic

[128] State Research Center Institute for High Energy Physics, Protvino, Russia

[129] Particle Physics Department, Rutherford Appleton Laboratory, Didcot, United Kingdom

[130] Physics Department, University of Regina, Regina SK, Canada

[131] Ritsumeikan University, Kusatsu, Shiga, Japan

[132] [a]INFN Sezione di Roma I; [b]Dipartimento di Fisica, Università La Sapienza, Roma, Italy

[133] [a]INFN Sezione di Roma Tor Vergata; [b]Dipartimento di Fisica, Università di Roma Tor Vergata, Roma, Italy

[134] [a]INFN Sezione di Roma Tre; [b]Dipartimento di Matematica e Fisica, Università Roma Tre, Roma, Italy

[135] [a]Faculté des Sciences Ain Chock, Réseau Universitaire de Physique des Hautes Energies - Université Hassan II, Casablanca; [b]Centre National de l'Energie des Sciences Techniques Nucleaires, Rabat; [c]Faculté des Sciences Semlalia, Université Cadi Ayyad, LPHEA-Marrakech; [d]Faculté des Sciences, Université Mohamed Premier and LPTPM, Oujda; [e]Faculté des sciences, Université Mohammed V-Agdal, Rabat, Morocco

[136] DSM/IRFU (Institut de Recherches sur les Lois Fondamentales de l'Univers), CEA Saclay (Commissariat à l'Energie Atomique et aux Energies Alternatives), Gif-sur-Yvette, France

[137] Santa Cruz Institute for Particle Physics, University of California Santa Cruz, Santa Cruz CA, United States of America

[138] Department of Physics, University of Washington, Seattle WA, United States of America

[139] Department of Physics and Astronomy, University of Sheffield, Sheffield, United Kingdom

[140] Department of Physics, Shinshu University, Nagano, Japan

[141] Fachbereich Physik, Universität Siegen, Siegen, Germany

[142] Department of Physics, Simon Fraser University, Burnaby BC, Canada

[143] SLAC National Accelerator Laboratory, Stanford CA, United States of America

[144] [a]Faculty of Mathematics, Physics & Informatics, Comenius University, Bratislava; [b]Department of Subnuclear Physics, Institute of Experimental Physics of the Slovak Academy of Sciences, Kosice, Slovak Republic

[145] [a]Department of Physics, University of Johannesburg, Johannesburg; [b]School of Physics, University of the Witwatersrand, Johannesburg, South Africa

[146] [a]Department of Physics, Stockholm University; [b]The Oskar Klein Centre, Stockholm, Sweden

[147] Physics Department, Royal Institute of Technology, Stockholm, Sweden

[148] Departments of Physics & Astronomy and Chemistry, Stony Brook University, Stony Brook NY, United States of America

[149] Department of Physics and Astronomy, University of Sussex, Brighton, United Kingdom

[150] School of Physics, University of Sydney, Sydney, Australia

[151] Institute of Physics, Academia Sinica, Taipei, Taiwan

[152] Department of Physics, Technion: Israel Institute of Technology, Haifa, Israel

[153] Raymond and Beverly Sackler School of Physics and Astronomy, Tel Aviv University, Tel Aviv, Israel

[154] Department of Physics, Aristotle University of Thessaloniki, Thessaloniki, Greece

[155] International Center for Elementary Particle Physics and Department of Physics, The University of Tokyo, Tokyo, Japan

[156] Graduate School of Science and Technology, Tokyo Metropolitan University, Tokyo, Japan

[157] Department of Physics, Tokyo Institute of Technology, Tokyo, Japan

[158] Department of Physics, University of Toronto, Toronto ON, Canada

[159] [a]TRIUMF, Vancouver BC; [b]Department of Physics and Astronomy, York University, Toronto ON, Canada

[160] Faculty of Pure and Applied Sciences, University of Tsukuba, Tsukuba, Japan

[161] Department of Physics and Astronomy, Tufts University, Medford MA, United States of America

[162] Centro de Investigaciones, Universidad Antonio Narino, Bogota, Colombia

[163] Department of Physics and Astronomy, University of California Irvine, Irvine CA, United States of America

[164] [a]INFN Gruppo Collegato di Udine; [b]ICTP, Trieste; [c]Dipartimento di Chimica,

Fisica e Ambiente, Università di Udine, Udine, Italy

[165] Department of Physics, University of Illinois, Urbana IL, United States of America

[166] Department of Physics and Astronomy, University of Uppsala, Uppsala, Sweden

[167] Instituto de Física Corpuscular (IFIC) and Departamento de Física Atómica, Molecular y Nuclear and Departamento de Ingeniería Electrónica and Instituto de Microelectrónica de Barcelona (IMB-CNM), University of Valencia and CSIC, Valencia, Spain

[168] Department of Physics, University of British Columbia, Vancouver BC, Canada

[169] Department of Physics and Astronomy, University of Victoria, Victoria BC, Canada

[170] Department of Physics, University of Warwick, Coventry, United Kingdom

[171] Waseda University, Tokyo, Japan

[172] Department of Particle Physics, The Weizmann Institute of Science, Rehovot, Israel

[173] Department of Physics, University of Wisconsin, Madison WI, United States of America

[174] Fakultät für Physik und Astronomie, Julius-Maximilians-Universität, Würzburg, Germany

[175] Fachbereich C Physik, Bergische Universität Wuppertal, Wuppertal, Germany

[176] Department of Physics, Yale University, New Haven CT, United States of America

[177] Yerevan Physics Institute, Yerevan, Armenia

[178] Centre de Calcul de l'Institut National de Physique Nucléaire et de Physique des Particules (IN2P3), Villeurbanne, France

[a] Also at Department of Physics, King's College London, London, United Kingdom

[b] Also at Laboratorio de Instrumentacao e Fisica Experimental de Particulas - LIP, Lisboa, Portugal

[c] Also at Faculdade de Ciencias and CFNUL, Universidade de Lisboa, Lisboa, Portugal

[d] Also at Particle Physics Department, Rutherford Appleton Laboratory, Didcot, United Kingdom

[e] Also at TRIUMF, Vancouver BC, Canada

[f] Also at Department of Physics, California State University, Fresno CA, United States of America

[g] Also at Novosibirsk State University, Novosibirsk, Russia

[h] Also at Department of Physics, University of Coimbra, Coimbra, Portugal

[i] Also at Università di Napoli Parthenope, Napoli, Italy

[j] Also at Institute of Particle Physics (IPP), Canada

[k] Also at Department of Physics, Middle East Technical University, Ankara, Turkey

[l] Also at Louisiana Tech University, Ruston LA, United States of America

[m] Also at Dep Fisica and CEFITEC of Faculdade de Ciencias e Tecnologia, Universidade Nova de Lisboa, Caparica, Portugal

[n] Also at Department of Physics and Astronomy, Michigan State University, East Lansing MI, United States of America

[o] Also at Department of Physics, University of Cape Town, Cape Town, South Africa

[p] Also at Institute of Physics, Azerbaijan Academy of Sciences, Baku, Azerbaijan

[q] Also at Institut für Experimentalphysik, Universität Hamburg, Hamburg, Germany

[r] Also at Manhattan College, New York NY, United States of America

[s] Also at CPPM, Aix-Marseille Université and CNRS/IN2P3, Marseille, France

[t] Also at School of Physics and Engineering, Sun Yat-sen University, Guanzhou, China

[u] Also at Academia Sinica Grid Computing, Institute of Physics, Academia Sinica, Taipei, Taiwan

[v] Also at Laboratoire de Physique Nucléaire et de Hautes Energies, UPMC and Université Paris-Diderot and CNRS/IN2P3, Paris, France

[w] Also at School of Physical Sciences, National Institute of Science Education and Research, Bhubaneswar, India

[x] Also at Dipartimento di Fisica, Università La Sapienza, Roma, Italy

[y] Also at DSM/IRFU (Institut de Recherches sur les Lois Fondamentales de l'Univers), CEA Saclay (Commissariat à l'Energie Atomique et aux Energies Alternatives), Gif-sur-Yvette, France

[z] Also at Section de Physique, Université de Genève, Geneva, Switzerland

[aa] Also at Departamento de Fisica, Universidade de Minho, Braga, Portugal

[ab] Also at Department of Physics, The University of Texas at Austin, Austin TX, United States of America

[ac] Also at Department of Physics and Astronomy, University of South Carolina, Columbia SC, United States of America

[ad] Also at Institute for Particle and Nuclear Physics, Wigner Research Centre for Physics, Budapest, Hungary

[ae] Also at DESY, Hamburg and Zeuthen, Germany

[af] Also at International School for Advanced Studies (SISSA), Trieste, Italy

[ag] Also at LAL, Université Paris-Sud and CNRS/IN2P3, Orsay, France

[ah] Also at Faculty of Physics, M.V.Lomonosov Moscow State University, Moscow, Russia

[ai] Also at Nevis Laboratory, Columbia University, Irvington NY, United States of America

[aj] Also at Department of Physics, Oxford University, Oxford, United Kingdom

[ak] Also at Discipline of Physics, University of KwaZulu-Natal, Durban, South Africa

[*] Deceased